UNIVERSITY OF EDINBURGH

ABSTRACT OF THESIS (Regulation 7.9)

Name of Candidate DUNCAN JAMES MACKAY

Address [redacted]

Degree DOCTOR OF PHILOSOPHY *Date* OCTOBER 1985

Title of Thesis THE BEHAVIOUR OF RUTILE IN AQUEOUS AMINOALCOHOL SOLUTION

No. of words in the main text of Thesis approx. 80,000

Both the ease of dispersion and wet milling of rutile pigment, in aqueous solution, are improved through the addition of relatively small quantities of aminoalcohols. However, little work has previously been carried out to investigate these effects. The present work was performed to increase the understanding of the mode of interaction between rutile and such low molecular weight organic solutes. The behaviour of rutile in the presence of one example of the latter, namely monoisopropanolamine, was studied by a variety of techniques.

The isoelectric point of rutile shifted to a higher pH value by ca.2 unit in the presence of a 4×10^{-3} mol dm^{-3} MIPA solution. The electrophoretic mobility showed a maximum at a pH of ca.10.6.

The stability of rutile particles dispersed in MIPA solution was slightly lower than for the equivalent high pH distilled water dispersion. The decrease in particle number with time indicated that a certain degree of reversible aggregation was taking place. This effect was more pronounced in the case of rutile dispersed in MIPA solution.

Rutile dispersed in aqueous MIPA solution was found to settle to give a compact sediment which was very easy to redisperse. The equivalent high pH distilled water sol settled to give a sediment which was difficult to redisperse. The dispersing ability of MIPA was inhibited by the presence of electrolyte-the concentration and valency of the cation being the important factors. The rate of production of primary particles was significantly faster in the presence of MIPA, an increase in the ionic strength inhibiting the process.

The centrifugal force necessary to prevent the redispersion of rutile was found to be significantly higher for sols containing MIPA concentration greater than approx. 4×10^{-3} mol dm^{-3}. The presence of a similar ionic strength was found to be sufficient to significantly negate the effect of the aminoalcohol.

The study of the dynamic viscosity of aqueous MIPA solutions indicated that the amino group is the major contributor to the hydrogen-bonding properties of the organic molecule. The study also indicated that the MIPA-water interaction is affected by electrolyte-water interactions, and vice-versa.

The rheological behaviour of high solids content slurries showed that a 0.04%w/w MIPA content was sufficient to reduce the viscosity, at a given shear rate, by over an order of magnitude. The effect of relatively minute quantities of MIPA, less than 5μmol g^{-1}, on the flow properties was large.

Rutile was found to be able to photo-oxidise aqueous solutions of MIPA in the presence of diffuse daylight.

THE BEHAVIOUR OF RUTILE IN AQUEOUS AMINOALCOHOL SOLUTION

Duncan James Mackay

Part B

Submitted for the Degree of Doctor of Philosophy

of

The University of Edinburgh

Supervisor

Dr. W.D. Cooper

October 1985

APPENDIX A

POTENTIOMETRIC TITRATIONS OF MIPA SOLUTIONS

APPENDIX A. - Potentiometric Titration of MIPA Solutions

As mentioned in section 7.2.1.3 several variants of the titration of aqueous MIPA solutions were studied.

a) Titration against hydrochloric acid.

As a result of the relatively strong basicity of the amino group a direct titration agains hydrochloric acid gave a well-defined end point. The pH span at the equivalence point (about pH 5.5) was a function of MIPA content but for a sample containing greater than 30 micromoles of aminoalcohol was sufficiently large. Typically the span would be 4 units. For samples containing little aminoalcohol the quality of the end point was good if the concentration of the hydrochloric acid titrant was greater than 5 times that of the aminoalcohol. In this manner a 2 cm^3 sample of a nominal 0.002 mol dm^{-3} MIPA solution could be accurately analysed. However, in cases where the pH of the MIPA solution had been altered either by the addition of acid (to completely or partially neutralise the amino groups) or alkali this direct titration against standard acid is obviously of no practical use - the method can only give the total titratable base content of a sample. Therefore a more general titration technique was required. Such a technique would of necessity involve adding excess alkali or acid and backtitrating with acid or alkali. Both possibilities were investigated at length.

b) Addition of excess alkali and backtitration against standard acid.

The addition of excess sodium hydroxide to a sample of MIPA and titrating against standard HCL produced a titration curve consisting of two equivalence points. The first point was rather ill-defined and occurred at a pH of about 10.5, but the second was very sharp at a pH of about 6.0. The former was assigned to the sodium hydroxide neutralisation and the latter to the MIPA. This assignment was based both on the fact that the stronger base would be titrated first and because the calculated values of alkali and MIPA concentrations agreed with those expected. The separation of the two points could be increased through the use of a more dilute titrant but the quality of the equivalence regions suffered. Acceptable titrations could be obtained

down to about 60 micromoles of MIPA giving an accuracy of better than 4%.

A comparison between the direct titration against acid and the addition of excess alkali prior to titration against acid for samples of MIPA solution, under equilibrium pH conditions, indicated that agreement was acceptable.

NOMINAL MIPA CONCENTRATION /mol dm^{-3}	TITRATION VALUE	
	Against HCL /mol dm^{-3}	Backtitration /mol dm^{-3}
0.103	0.103-0.105	0.101-0.108
0.0207	0.0202-0.0208	0.0206
0.0103	0.0104	0.0108

c) Addition of excess acid and backtitration against standard alkali.

The addition of excess hydrochloric acid to a MIPA sample and titrating against standard sodium hydroxide also gave a curve consisting of two equivalence points. The first point was sharp whereas the second was less well defined. The first occurred at a pH of about 6.5 and was due to the neutralisation of the excess strong acid. The other at a pH of about 10.5 was due to neutralisation of the relatively weak conjugate acid of the amino group. The limitation of this method was, as with the previous one, the gradual erosion of the definition of the high pH end point with a reduction in the amount of MIPA present.

d) Performing titrations in electrolyte solution.

It was found that by carrying out the titrations in 0.1 mol dm^{-3} potassium chloride solution the range of titrant volume over which the equivalence zones extended was decreased. However, the increase in precision was not sufficient.

e) Performing titrations in the presence of formaldehyde.

Formaldehyde reacts with the amino group of organic compounds containing that functional group to give an adduct. In forming this complex the formaldehyde is able to displace, stoichiometrically, the hydrogen ion from a protonated amino group. The effect of the addition of small quantities of a 37% v/v formaldehyde solution on the acid base titration was studied.

The addition of 0.1-0.2 cm^3 formaldehyde solution to the mixture prior to titration was found to significantly improve the quality of the less clearly defined end-point in each of the titration methods b) and c). The quality of the well defined end-points tended to suffer slightly, however. The precision of the analysis was increased to about 1.5%.

It was discovered, in the titration against acid in the presence of excess alkali and formaldehyde, that consistently larger values for the MIPA concentration were determined that were measured by direct titration against acid (for MIPA solutions at equilibrium pH). The discrepancy was about 5% and was a systematic error. The range of formaldehyde volumes used was found to have no effect on the strong acid-strong alkali titration nor any measureable effect on the total volume of acid required to titrate the base content of a MIPA sample plus excess alkali. However, increasing the formaldehyde volume was found to produce a decrease in the total volume of acid required to achieve complete neutralisation - the addition of 2 cm^3 formaldehyde solution lowered the volume of acid required by about 4%.

A further increase in the formaldehyde addition led to the disappearance of the end-point assigned to the neutralisation of MIPA. A similar quantity of formaldehyde also made the equivalence point in the direct titration of MIPA against acid significantly less well defined.

Similar volumes of the aldehyde were found to influence the result of the titration between hydrochloric acid and sodium hydroxide. Tests indicated that increasing the ratio of formaldehyde to acid, or alkali, decreased the apparent concentration of the alkali. It was concluded

that the formaldehyde solution contained a small amount of titratable acid. Based on the reported impurity content of the formaldehyde it was possible to calculate that the equivalent of about 0.033 mol dm^{-3} formate ions was present. Direct titration gave a value of 0.0063 ±0.0004 mol dm^{-3} for the titratable acid content of the formaldehyde solution. The shape of the curve indicated that the formaldehyde was partially neutralised since no sign of the rather shallow plateau region associated with the titration of a weak organic acid was apparent.

The presence of both formic acid and formate in the aliquots of formaldehyde explains the discrepancies found in the titrations of MIPA samples. When titrating MIPA in the presence of excess acid against alkali the formate ion content of the added formaldehyde would be converted to the weak organic acid. Subsequent neutralisation by the alkali would involve titrating 3 acids: hydrochloric acid, formic acid, and the conjugate acid form of MIPA. Calculation of the MIPA concentration would consequently be affected by the volume of alkali required to neutralise the two weak organic acids and by the amount of strong acid required to protonate all the formate ions. When titrating MIPA in the presence of excess alkali against acid the formic acid plus formate content of the added formaldehyde affects the total quantity of titratable base. After neutralisation of the strong base the sample would contain a mixture of formate ions and neutral MIPA, the former of which hydrolyse to release hydroxide ions. The calculated MIPA concentration would be too high by the equivalent of the formate ion content. Allowance for the total formate content of the added aliquots of formaldehyde was found to bring the results of the titration into good agreement with the direct titration of MIPA against hydrochloric cid.

The hydrolysis of the formate ions explained the observation that, after neutralisation of the strong base, a gradual rise in pH was observed between subsequent additions of strong acid.

APPENDIX B

EXPERIMENTAL DATA

APPENDIX B - Experimental Data

The results of the relevant experiments are presented in the following tables. The symbols have the meaning:

Tables B.1

μ_{EP}	electrophoretic mobility
μ_{EO}	electro-osmotic mobility

Tables B.2

k	coagulation rate constant
N_o	initial number of primary particles
W	stability ratio

Tables B.3

$[MIPA]_o$	initial concentration of MIPA
$[MIPA]_F$	final concentration of MIPA
$[MIPA^+]_o$	initial concentration of the conjugate acid form of MIPA
$[MIPA^+]_F$	final concentration of the conjugate acid form of MIPA

Tables B.4

NUM	number of primary particles per gram rutile
R	ratio of number g MIPA to number g rutile
NI	number of inversions of the dispersion

Tables B.5

c	concentration in g per 100 cm^3
η_r	relative viscosity
η_{SP}	specific viscosity
η	viscosity

Tables B.6

τ	shear stress
γ	shear rate

Tables B.7

C_o	initial number of primary particles
c	final number of primary particles
F	$= C/C_o$
ω	centrifuge bowl rotational speed
t_c	time of centrifugation

Adsorption isotherms

The decrease in the bulk solution MIPA concentration, as the result of adsorption at the rutile particle surface and subsequent oxidation, was studied in the presence of light.

The results for the adsorption isotherms carried out are given in tables B.3.1-B.3.34. Each table describes the conditions under which the isotherm was measured. The time factor refers to the period between initially dispersing the rutile in the MIPA solution and separating the solids from the solution by centrifugation. The agitation factor refers to the rotational speed of the end-over-end (EOE) apparatus. The pH_0 factor is the measured pH, at ambient temperature, of the MIPA before contact with the rutile. $[MIPA]_0$ and $[MIPA]_F$ refer to the solution MIPA concentrations before and after contact with the dispersed rutile, respectively. What would normally be termed "solute adsorbed" is in fact called "amino loss", since, as will become apparent later, not all the experimentally measured decrease in solution MIPA content can be ascribed to adsorption at the rutile-solution interface. For the purposes of the appropriate graphs the figures are identified by AI numbers which refer to the relevant adsorption isotherm.

The numerous isotherms studied can be classified into general types

i) constant [MIPA], variable pH

ii) constant [MIPA], variable ionic strength

iii) constant pH and IS, variable [MIPA]

iv) variable time of equilibration.

Constant MIPA Concentration-Variable pH

The results for AI 4 are given in table B.3.4 and plotted in figure B.3.1. For this particular isotherm the ionic strength was not held constant as the pH was varied - the ionic strength being due to the conjugate acid form of MIPA. The numbers by the points represent the appropriate ionic strength (in millimolar) of the solution. In spite of the increase in ionic strength as the pH decreases there is a maximum in the amount of amino loss in the region of pH 9.

Table B.3.9 and figure B.3.2 show the results for AI 9 for which the ionic strength was held constant at 0.1 mol dm^{-3} by using KNO_3 as the backing electrolyte. There appears to be no identifiable maximum for this isotherm, although it is clear that at low pH there is negligible loss of amino group. The time of equilibration for this isotherm was ca. twice as long as for the previous one but the amounts of amino loss are a factor of 2 lower. There is, therefore, an effect of ionic strength on the degree of amino loss. The values in table B.3.9 indicate that there is an increase in the $[MIPA^+]$ during the time of equilibration for all but the samples at pH 8.76 and 7.85 which give a decrease.

The results for AI 13 (table B.3.13 and figure B.3.3) are for a lower total ionic strength and a smaller range of pH. There is a maximum in the isotherm, pH 10.6-10.8, with a definite drop in amino loss at both lower and higher pH. The concentration of the conjugate acid form once again increases during the timescale of the isotherm. This effect could be due to one or more of the following reasons

i) partial neutralisation by carbon dioxide;

ii) partial neutralisation by hydrogen ions desorbing from the rutile surface;

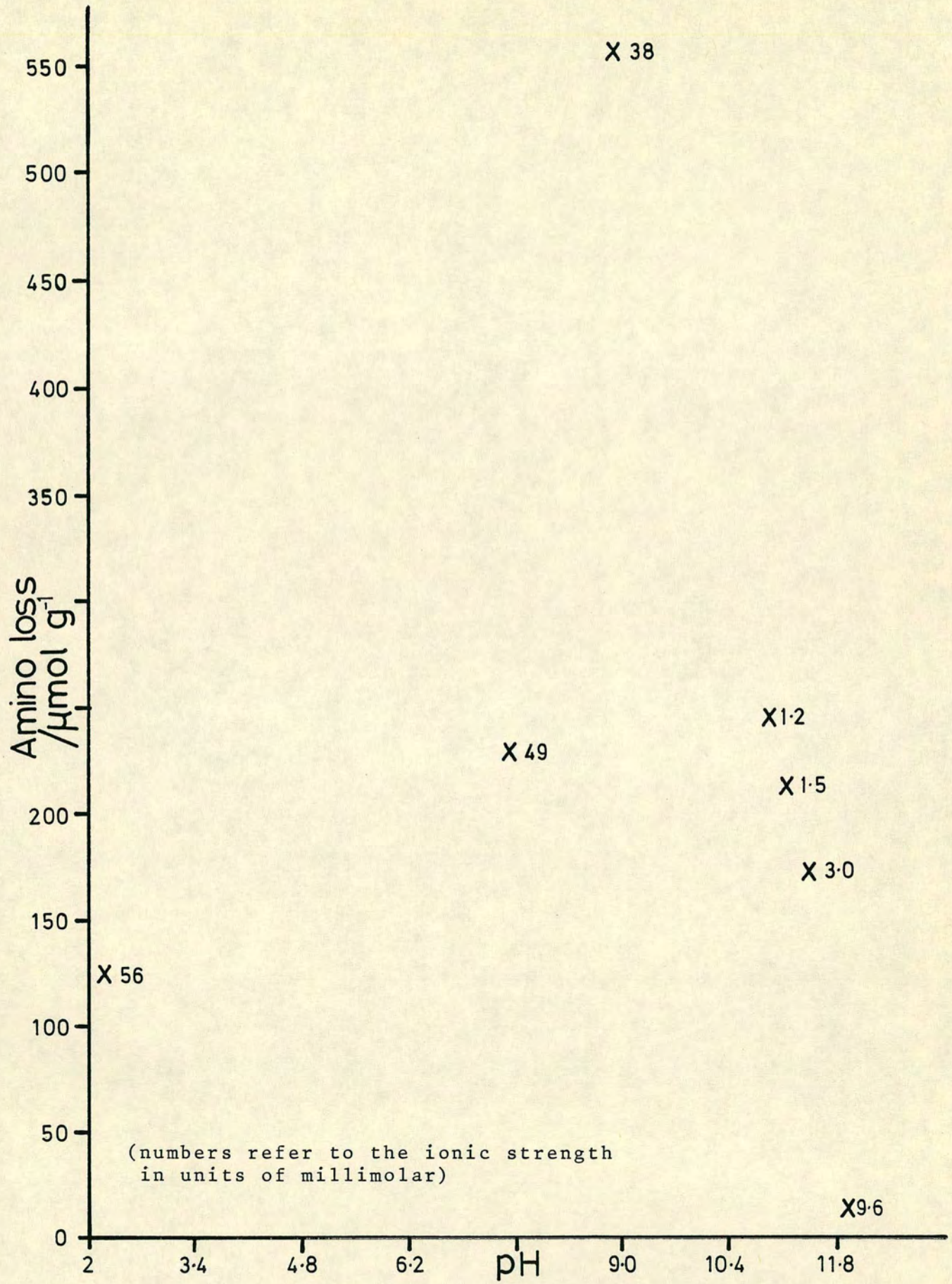

FIGURE B.3.1 AI 4

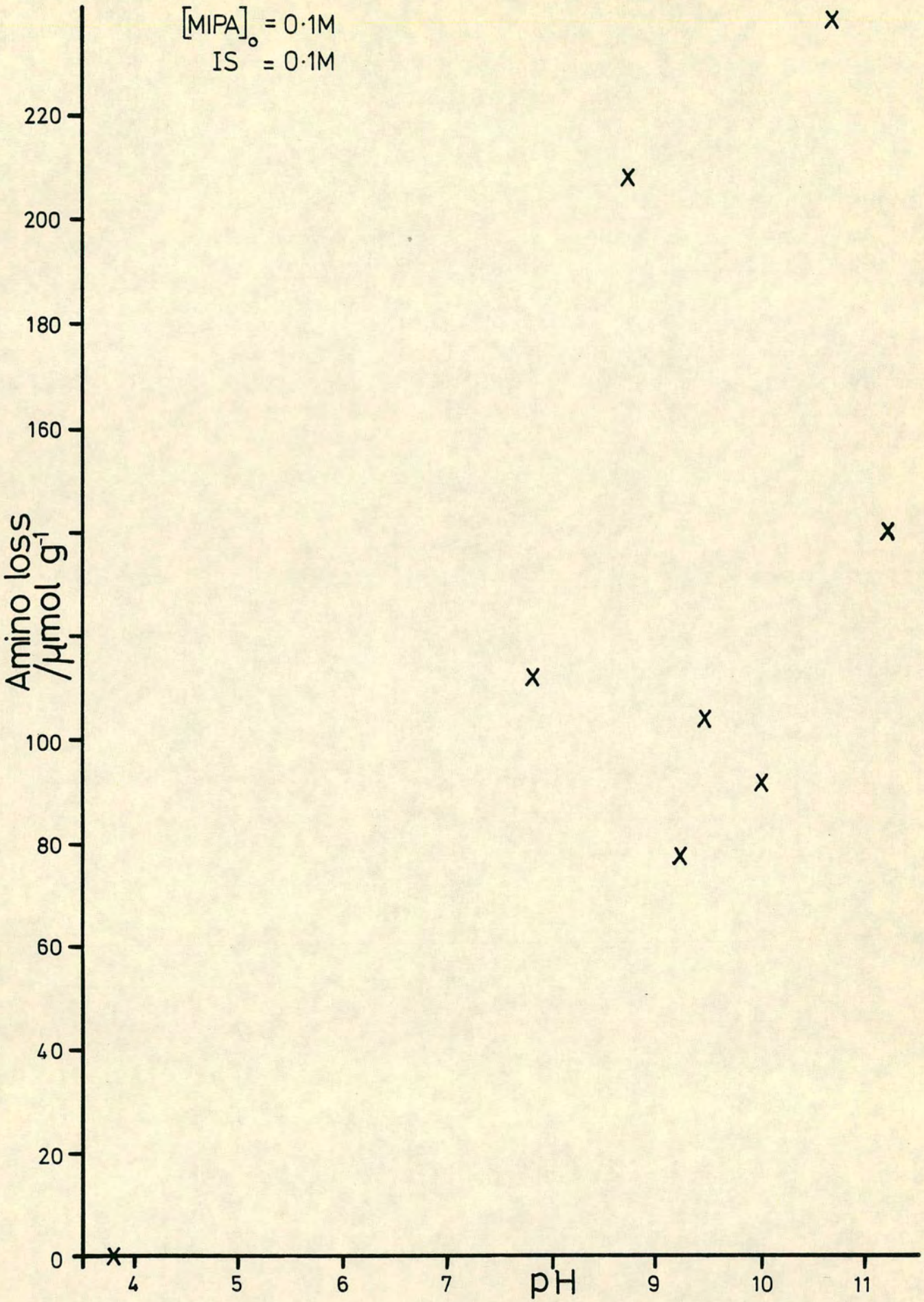

FIGURE B.3.2 AI 9

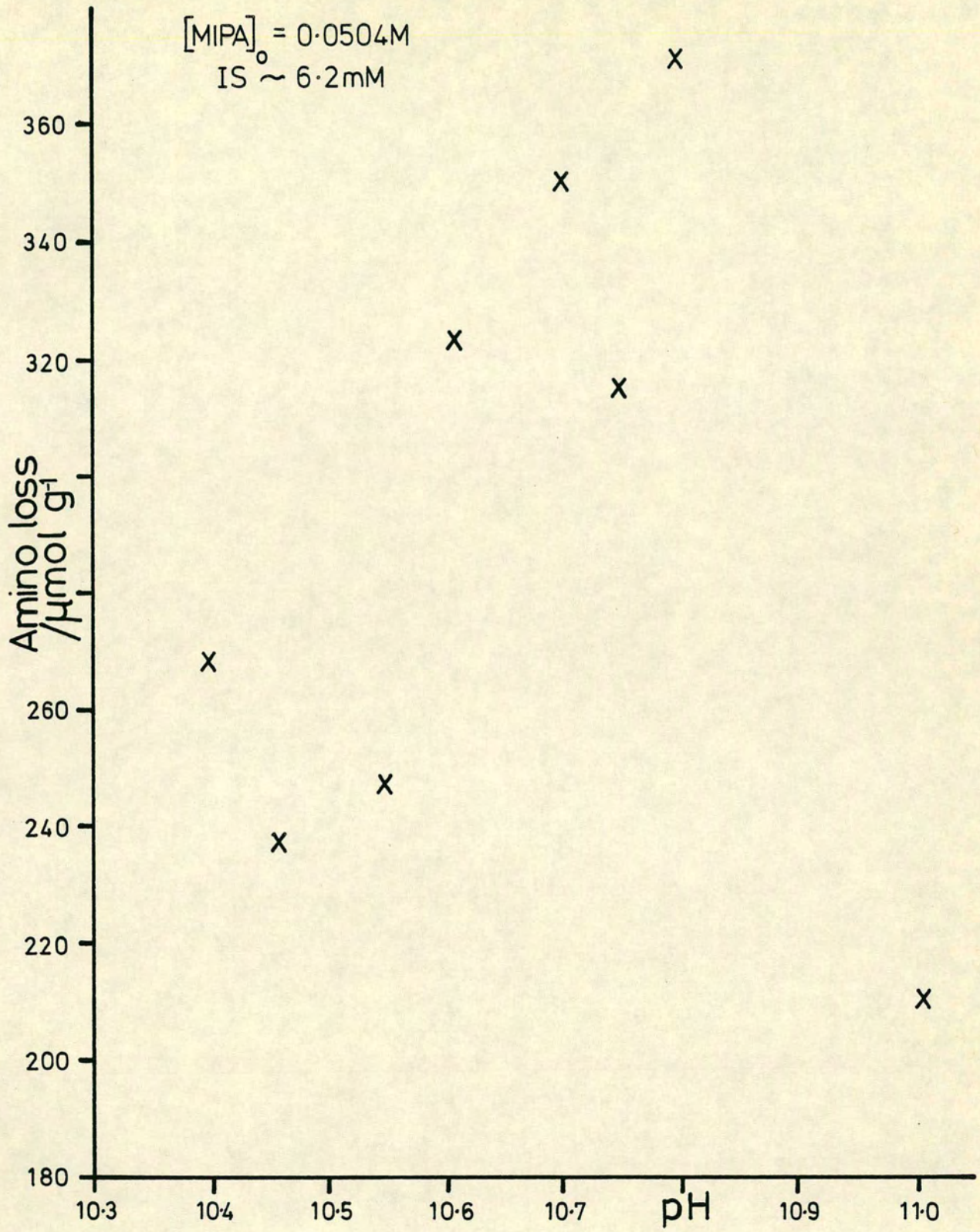

FIGURE B.3.3 AI 13

iii) adsorption of the charged MIPA molecules at the rutile surface with a resultant increase in the dissociation of the uncharged MIPA molecules to reattain equilibrium;

iv) photocatalytic oxidation of MIPA to produce a species possessing an amino group with a higher basicity and hence increased conjugate acid content.

In fact iii) will show up as an increase in the value of the ratio $[MIPA^+]/[MIPA]$. Both AI 9 and AI 13 give such an effect.

Partial neutralisation by CO_2 absorption during equilibration may not be a significant factor since the quantity of air enclosed with the dispersion in the test-tube was quite small, ca. 3 cm^3.

AI 16 shows that little or no amino loss was detected for a 2 mM MIPA solution at a total ionic strength of 5-6 mM. However, it is very likely that the product of the oxidation of the MIPA molecules possesses an amino group which has a different (in fact higher) extinction coefficient for the product of the reaction with ninhydrin; so the analysis, which of necessity is calibrated for MIPA, will give rise to an apparently high final MIPA concentration. The rather high final MIPA concentrations support this view.

Constant Conjugate Acid Concentration

Table B.3.21 and figure B.3.4 show the results for AI 19 which investigated how the amino loss was affected by the variation in solution pH produced by a variation in MIPA concentration at a constant conjugate acid concentration. The ionic strength was approximately fixed over the pH range studied. The graph suggests that there is a maximum in the amino loss at a pH ~10.1 where the initial ratio of conjugate acid to total MIPA concentration was 0.28. The $[MIPA^+]$ was found to remain roughly constant over the period of the isotherm whereas, obviously, the total MIPA concentration decreased. Thus it would be expected that the pH of the dispersion medium decreased during the time of equilibration. (The sample at $[MIPA]_0$ = 0.1 M in fact had been adjusted to pH 10.22 with

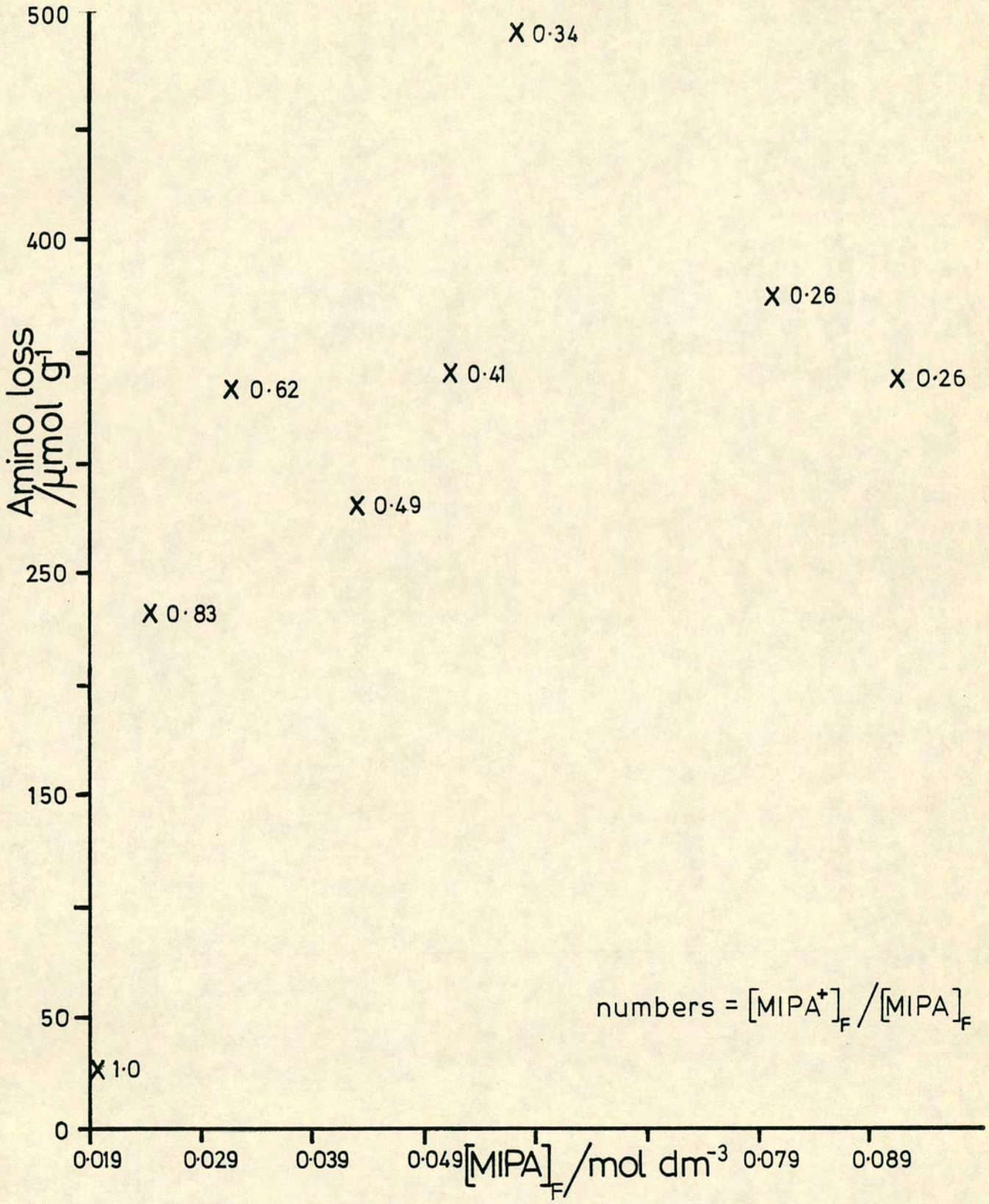

FIGURE B.3.4 AI 19

HNO_3 whereas all the other samples had the equivalent of 0.0193 mol dm^{-3} HNO_3 added. The tabulated value for $[MIPA^+]_0$ for this sample refers to the stock solution and not to the appropriate value for the isotherm aliquot. Calculation gives a value of 0.0252 mol dm^{-3} for $[MIPA^+]_0$ for this sample.)

Variable MIPA Concentration-Constant pH

Table B.3.6 and figure B.3.5 give the results for AI 6 which was carried out at pH ~9.5 and ionic strength ~0.5 mol dm^{-3}. An increase in the MIPA concentration is associated with an increase in the amino loss. The ratio of conjugate acid to total MIPA concentration was found to increase after equilibration for all samples. Therefore the bulk solution pH decreased.

AI 10 (table B.3.10 and figure B.3.6) was carried out at a fixed pH of 11.3, the ionic strength being similarly fixed at $2x10^{-3}$ mol dm^{-3}. The shape of the isotherm conforms more closely to the class L described by Giles et al. A plateau can be defined at an amino loss of ca. 310 μmol g^{-1} with indications of an increase in the amino loss at higher MIPA concentrations.

AI 14 (table B.3.14 and figure B.3.7) represents the equivalent isotherm but at an ionic strength of 0.1 mol dm^{-3}. The shape of the isotherm is completely different - there is an enhanced amino loss starting at ca. 0.060 mol dm^{-3}. Below this equilibrium MIPA concentration the appropriate amino loss is lower than for AI 10 but above this concentration the amino loss associated with the high ionic strength solutions approaches and exceeds that of the low ionic strength samples.

Table B.3.22 and figure B.3.8 show the results for AI 20 which was carried out under conditions of pH and ionic strength controlled by the dissociation of the MIPA. The isotherm possesses a similar shape to that of AI 10 with similar values of amino loss, although the curve has levelled off at the higher MIPA concentrations. Plotted on the same figure are the results for AI 21 (table B.3.23) which was performed at a constant pH of 11.0. The isotherm shows a plateau at an amino loss of

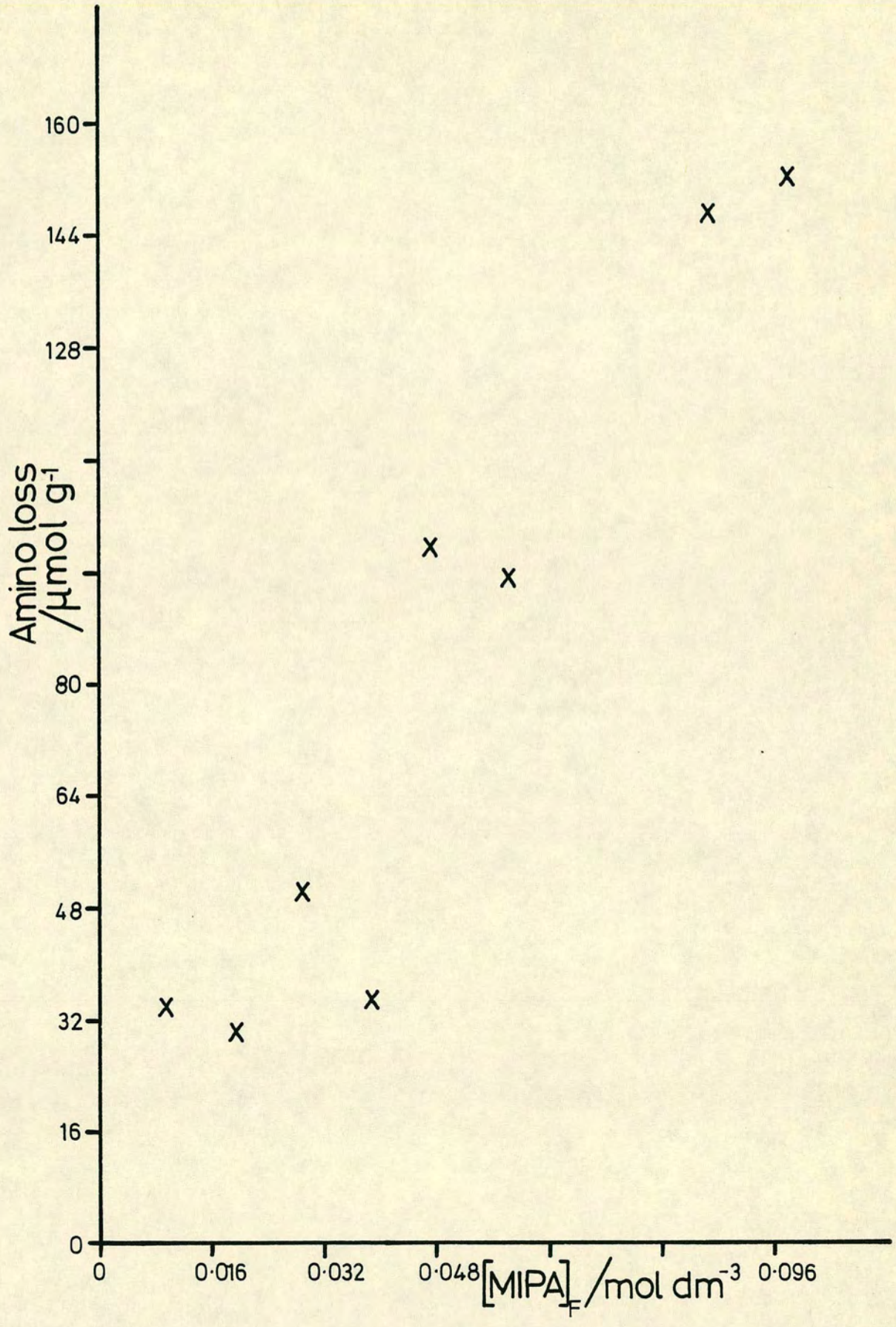

FIGURE B.3.5 AI 6

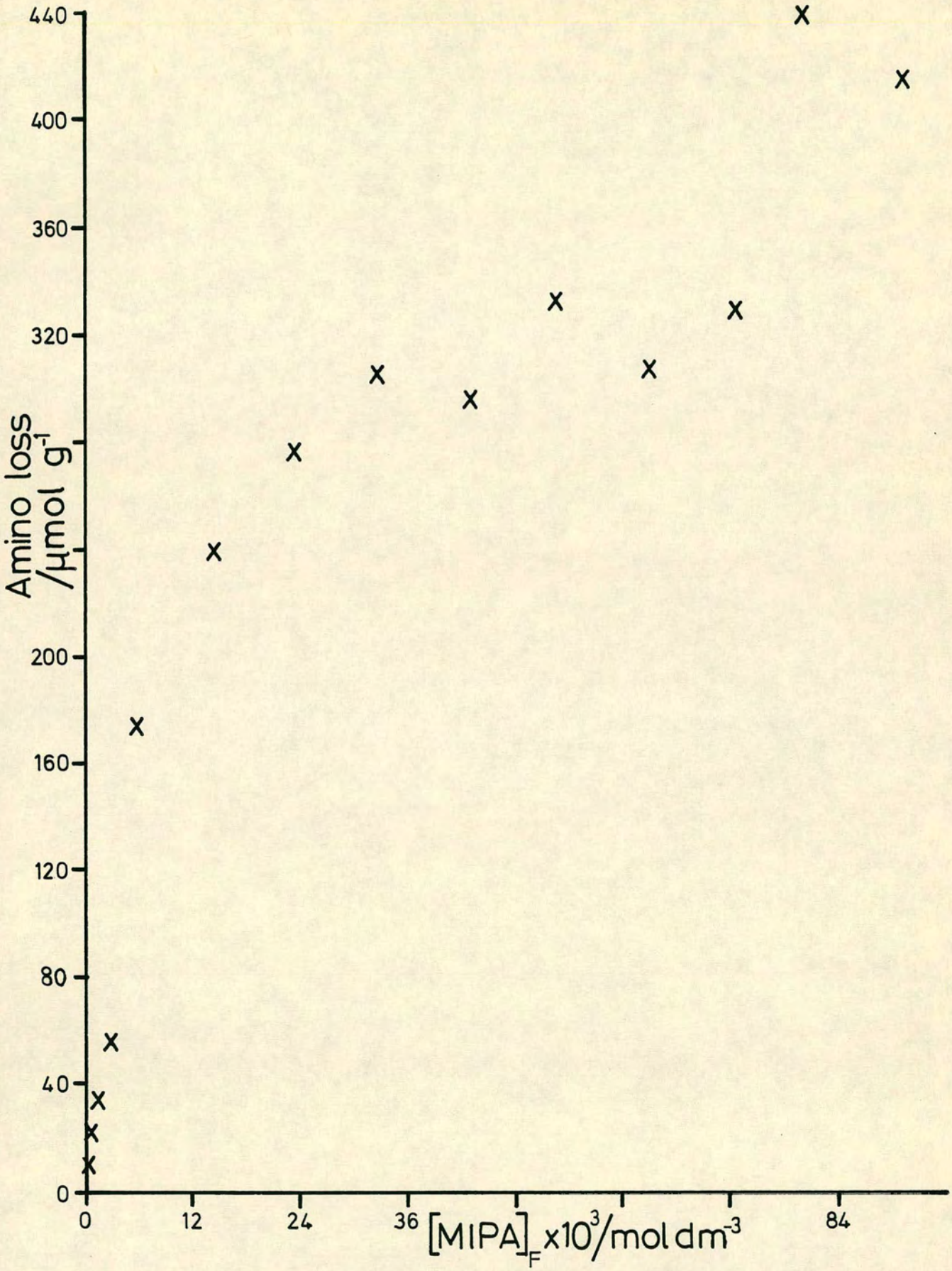

FIGURE B.3.6 AI 10

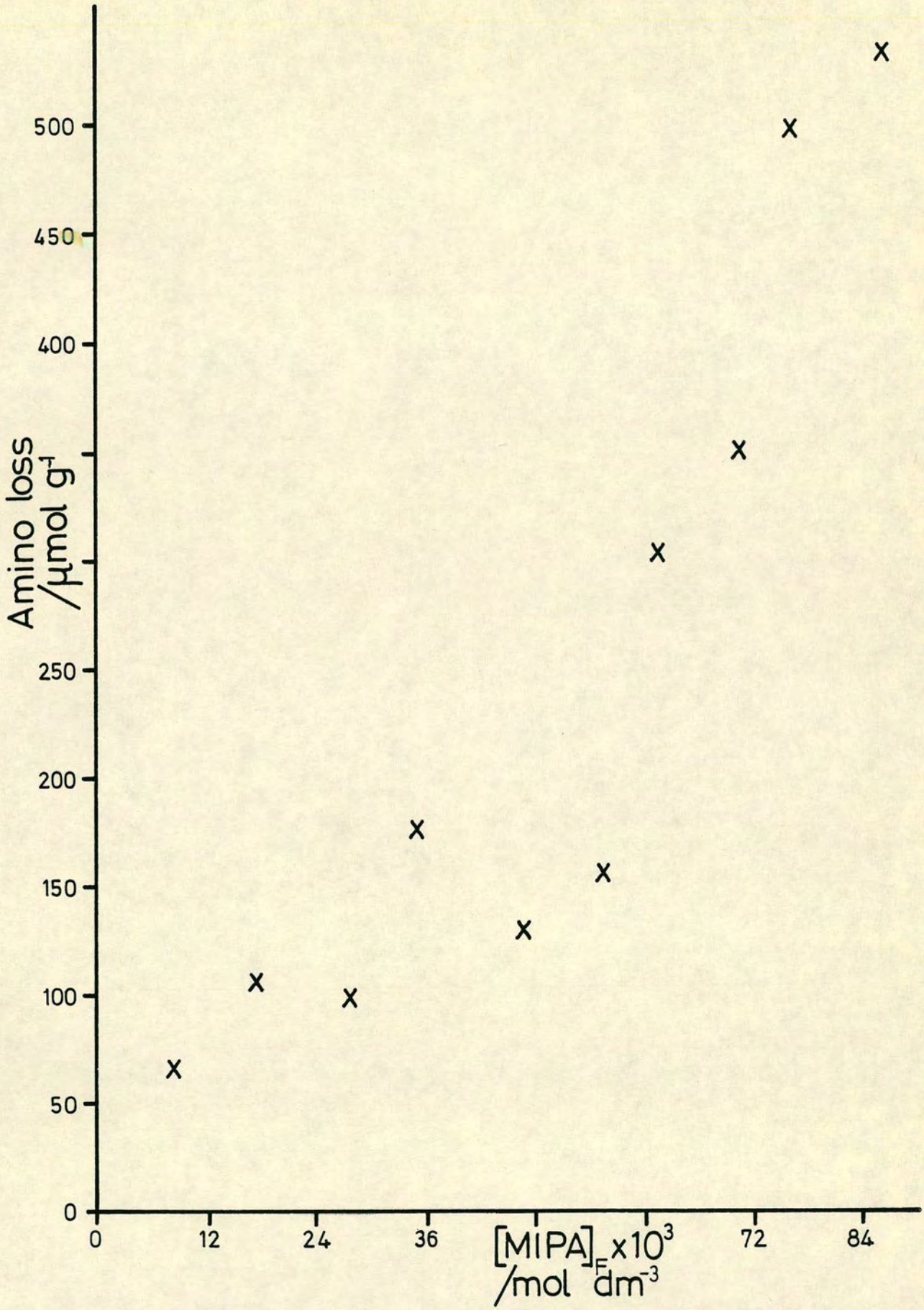

FIGURE B.3.7 AI 14

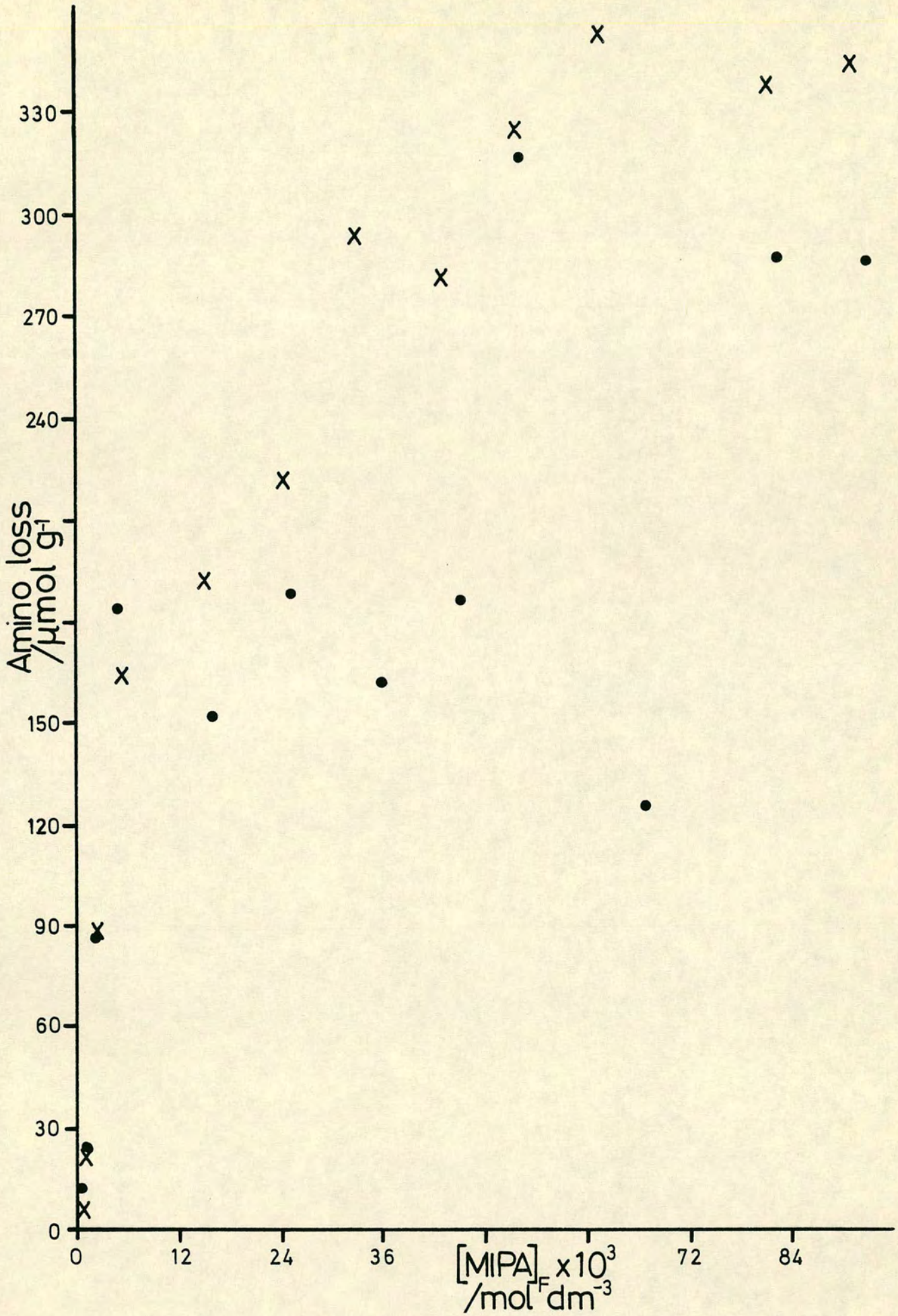

FIGURE B.3.8 AI 20(crosses),AI 21(dots)

ca. 180 μmol g^{-1}, although the higher MIPA concentrations increase the amino loss.

AI 5 was carried out at an ionic strength of 0.1 mol dm^{-3}, the pH being determined by the MIPA concentration (table B.3.5 and figure B.3.9). Equivalent equilibrium MIPA concentrations give similar amino losses to those for AI 20, although the period of equilibration for AI 5 was 25% longer for AI 5. The amino loss for the two highest MIPA concentrations indicates enhanced adsorption. Table B.3.7 contains the results of AI 7 which was the corresponding isotherm to AI 21 at high ionic strength. However, the period of equilibration was rather shorter (2.5 days). The results suggest that either little or no amino loss took place.

Variable Time of Equilibration

The effect of a variation in the period of contact between the rutile and MIPA solution was investigated for different MIPA solutions.

Tables B.3.8 and B.3.12 show the effect of a variation in the ionic strength (AI 8 and 12). The resulting curves, figure B.3.10, show no sign of reaching a limiting value for the amino loss. But it would appear that the higher ionic strength samples (filled circles) reach a more well defined asymptote within 800 hours. It should be noted that adsorption of even long chain molecules, such as polymers, does not take as long as this to reach an equilibrium value. So the decrease in MIPA concentration is not solely due to adsorption.

Figure B.3.11 shows the variable time study for 2×10^{-3} mol dm^{-3} MIPA (AI 15). For this case the curve does appear to reach a plateau (ca. 24 μmolg g^{-1}), however two points can be made which once again indicate that the amino loss cannot be taken as solely the result of adsorption. Firstly, the plateau appears after ca. 60 hours which is rather excessive for the adsorption of a low molecular weight species. Secondly, the isotherm exhibits a maximum with the measured amino loss decreasing at longer times which could be explained by the presence of a second species possessing an amino functional group whose adduct with ninhydrin has a

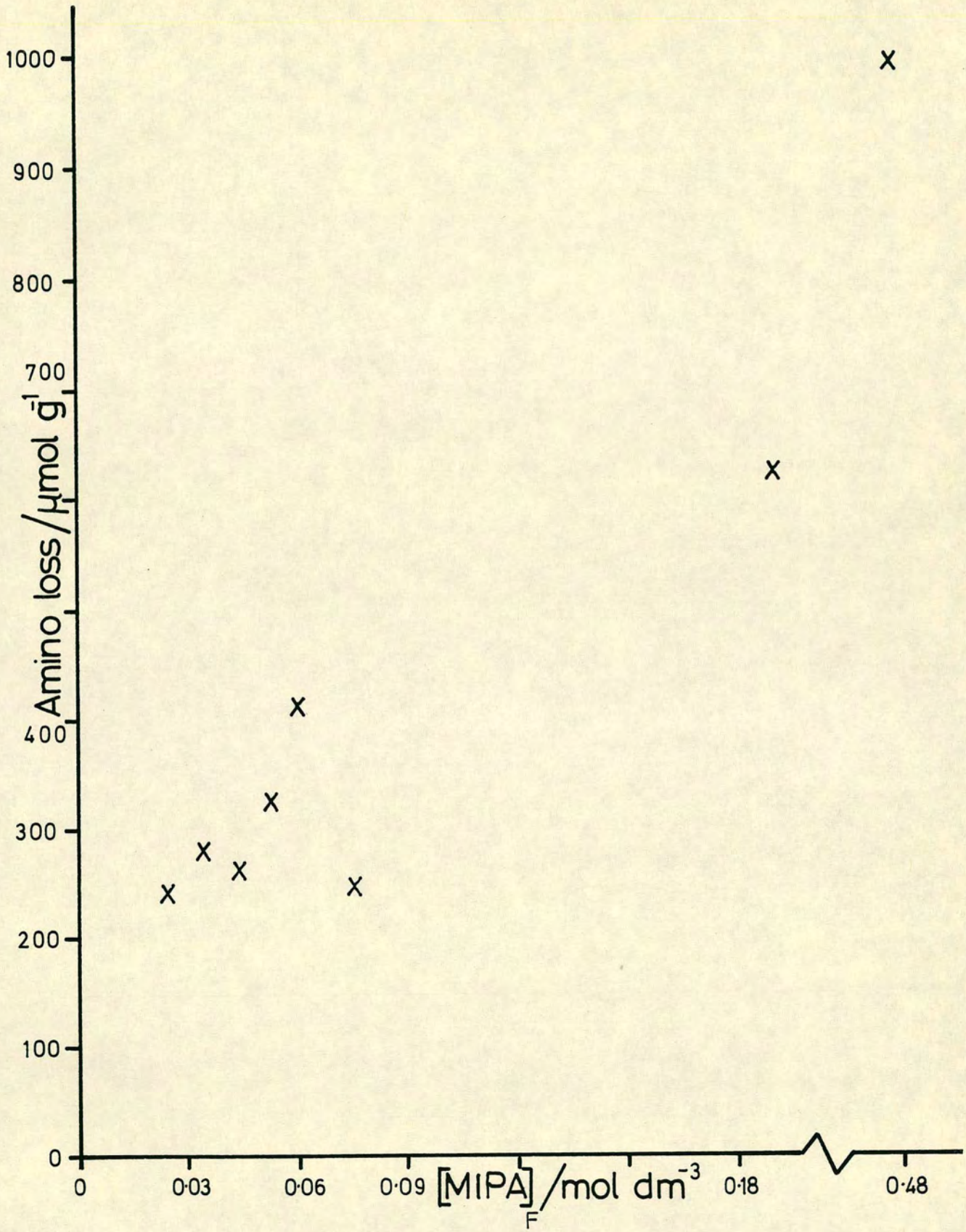

FIGURE B.3.9 AI 5

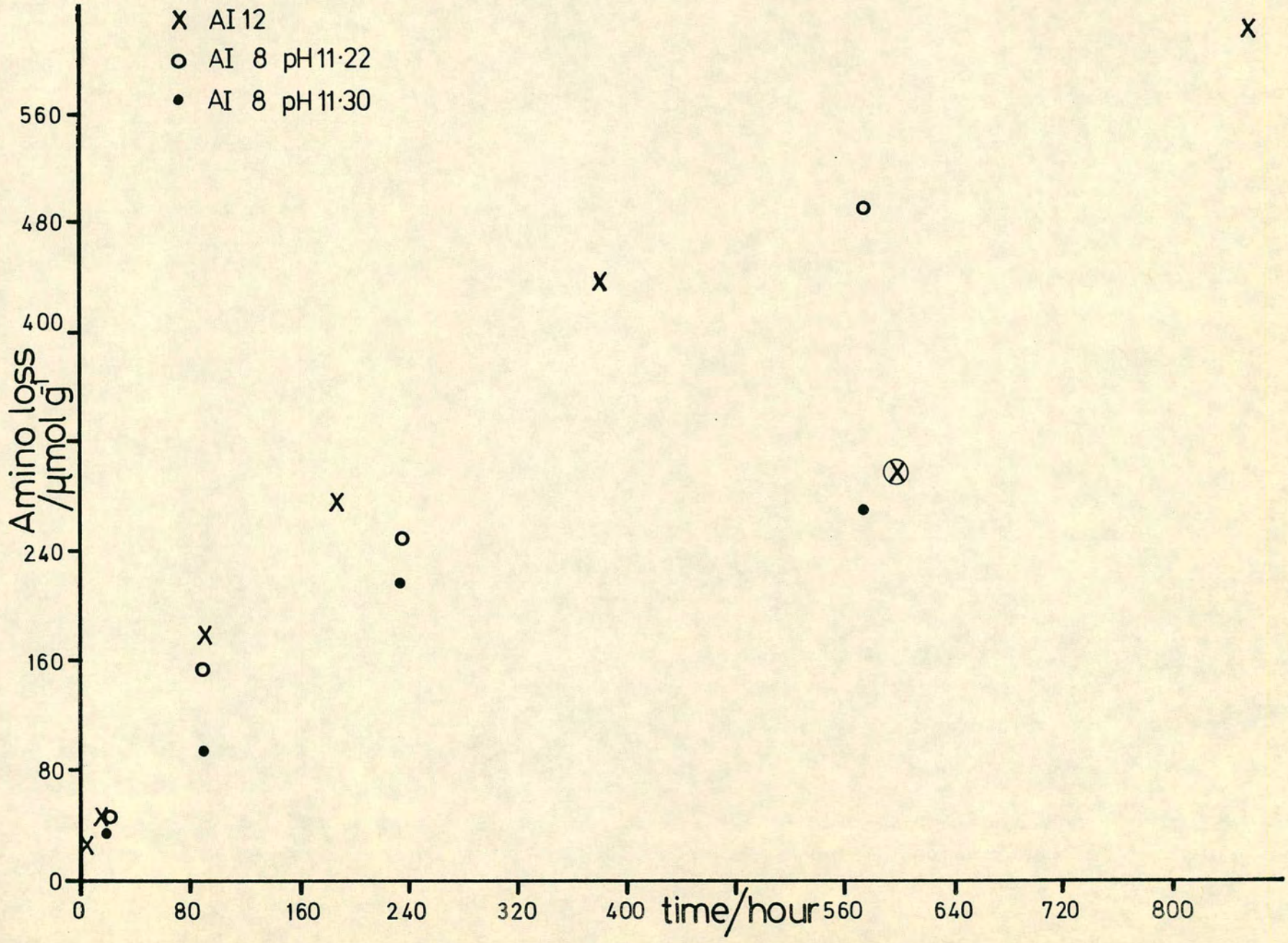

FIGURE B.3.10 AI 8,12 conc. $MIPA_o$=0.1M

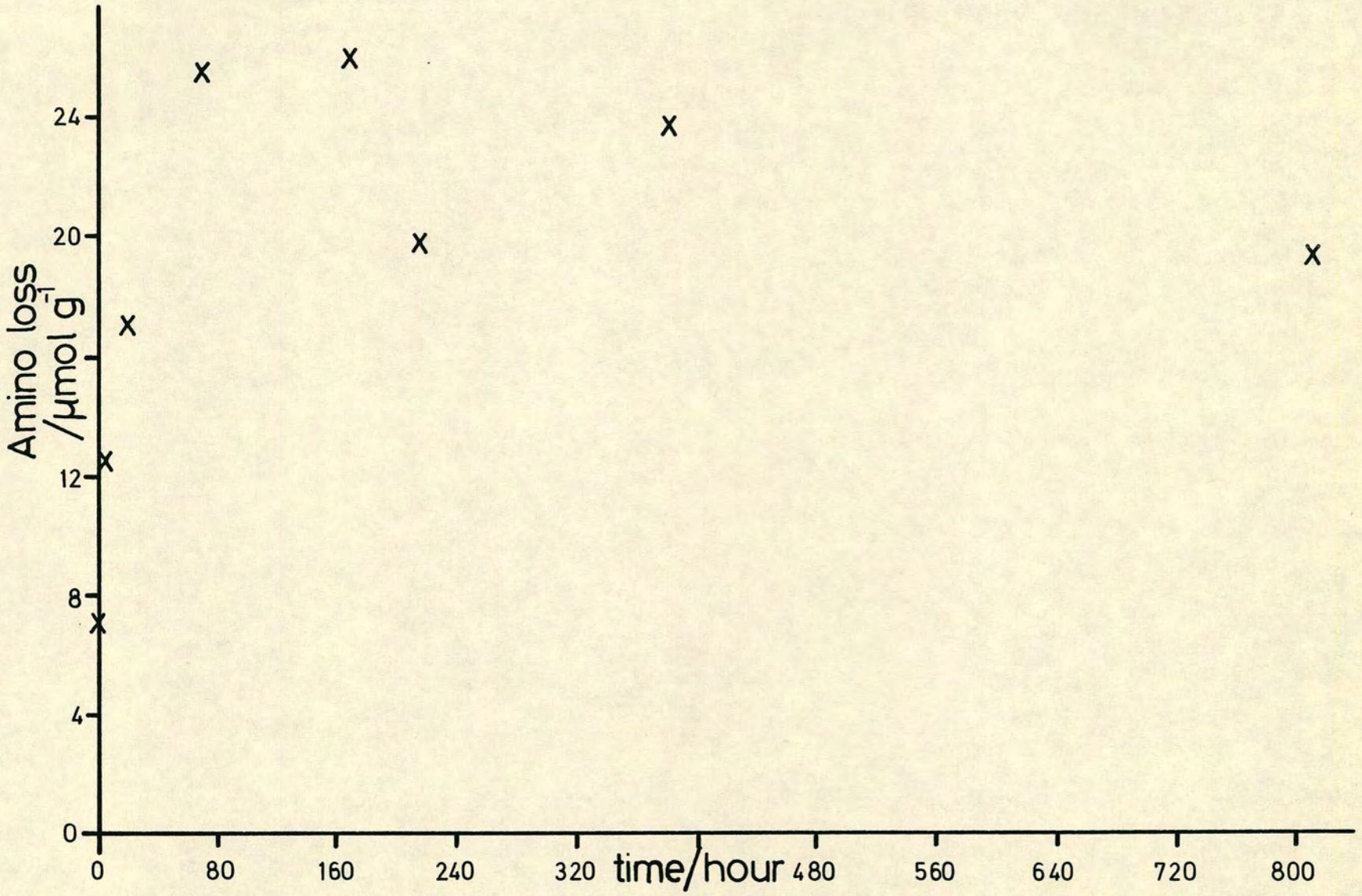

FIGURE B.3.11 AI 15

higher extinction coefficient at the wavelength of light used for the analysis.

The results for AI 18 (table B.3.20) support this conclusion. In addition, it was observed that the quality of a given dispersion became poorer as the time of equilibration, in the presence of daylight, increased.

AI 23 was performed under conditions such that the dispersions were constantly illuminated by a standard 60 watt light bulb. The curve for the 0.1 mol dm^{-3} MIPA is similar to that found for AI 12 (figure B.3.12). The results for the 0.05 mol dm^{-3} MIPA samples fall below those for the higher concentration as would be expected.

Variable Ionic Strength-Constant [MIPA]

Isotherms AI 11, 17 and 24 were performed to assess the effect of the solution ionic strength on the amount of amino loss from a 0.1 mol dm^{-3} MIPA solution. Potassium nitrate was used as the backing electrolyte. The results are rather scattered, although for a given isotherm the highest ionic strengths give the lowest amino loss. The quality of the initial dispersion is obviously an important factor in determining the amino loss because the better the dispersion the greater the effective rutile surface area available for interaction with the solution. All six samples for AI 24 formed good dispersions as was indicated by the uniform, milky appearance. After the period of equilibration the highest ionic strength dispersion was found to have coarsened.

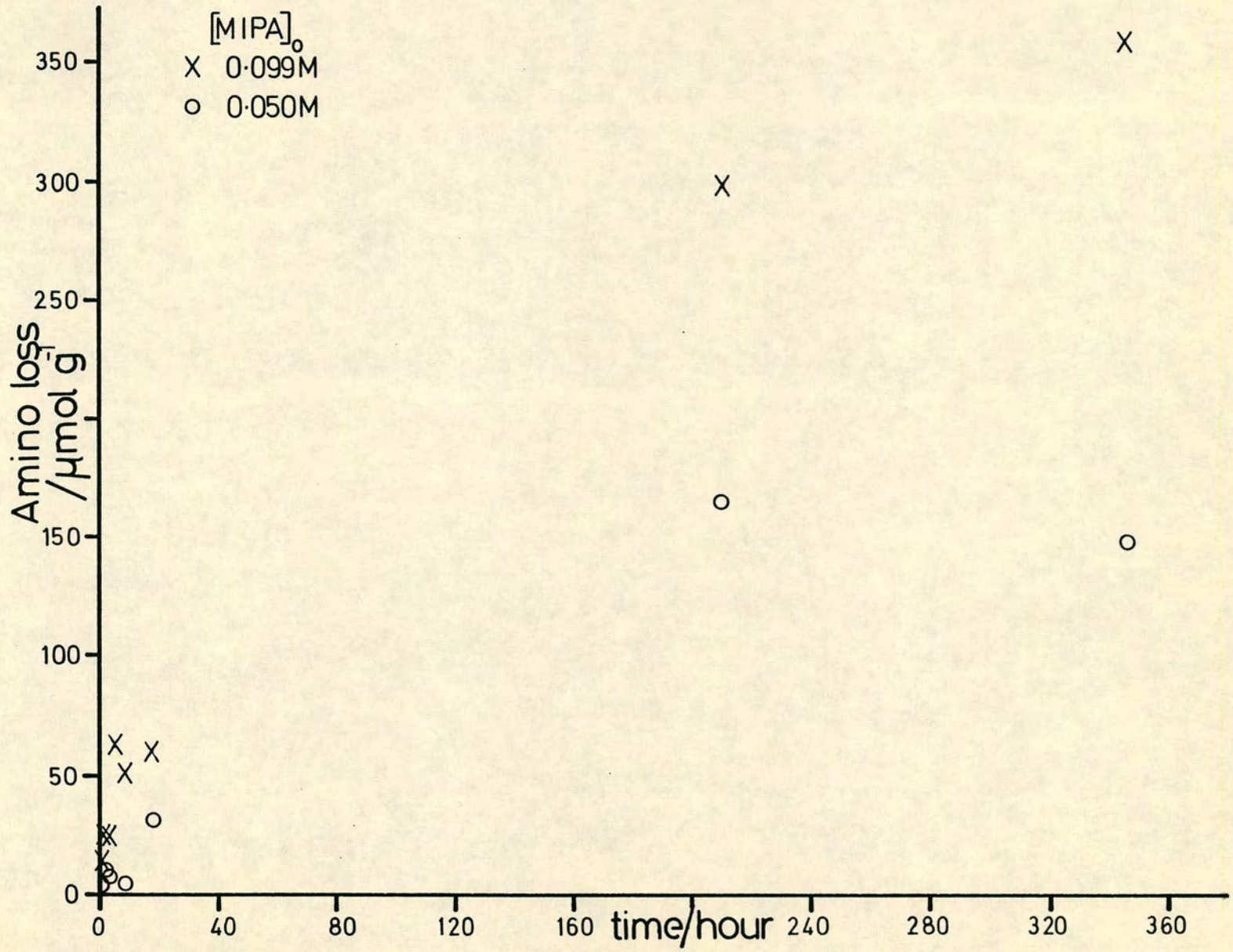

FIGURE B.3.12 AI 23

FIGURE B.3.13 AI 24(crosses),11(circles),17(dots)

TABLE B.1.1. Electrophoresis data for the unwashed rutile pigment

Run	Solution	pH	Ionic Strength/ mol dm^{-3}	Kappa $x10^{-8}$/ m^{-1}	$\mu_{EP} x10^8$/ $m^2\ V^{-1}\ s^{-1}$	$\mu_{EO} x10^8$/ $m^2\ V^{-1}\ s^{-1}$
EP2	3.1mM HNO_3	2.58	$3.1x10^{-3}$	1.83	1.920±0.345	3.575±0.264
EP4	1mM KNO_3	3.63	$1.2x10^{-3}$	1.14	-0.397±0.113	4.583±0.200
EP6	1mM KNO_3	4.04	$1.1x10^{-3}$	1.09	-0.377±0.239	4.349±0.231
EP1	1mM KNO_3	6.10	$1.0x10^{-3}$	1.04	-3.677±0.197	8.294±0.348
EP3	1mM KNO_3	9.5	$1.0x10^{-3}$	1.04	-3.748±0.323	9.533±0.429
EP5	0.5mM KNO_3	10.53	$0.8x10^{-3}$	0.931	-3.529±0.185	7.185±0.303

TABLE B.1.2. Electrophoresis data for the Soxhlet washed rutile (low pH)

Run	Solution	pH	Ionic Strength/ mol dm^{-3}	Kappa 10^{-8}/ m^{-1}	$\mu_{EP} x10^8$/ $m^2\ V^{-1}\ s^{-1}$	$\mu_{EO} x10^8$/ $m^2\ V^{-1}\ s^{-1}$
EP16	0.1M KNO_3	2.31	0.105	10.7	1.047±0.096	0.590±0.061
EP9	3mM HNO_3	2.98	$3x10^{-3}$	1.80	1.265±0.195	4.528±0.218
EP24	1mM KNO_3	3.14	$1.7x10^{-3}$	1.36	1.799±0.423	3.710±0.300
EP29	1mM KNO_3	4.05	$1.1x10^{-3}$	1.09	1.757±0.191	4.207±0.204
EP61	4mM KNO_3	3.72	$4.2x10^{-3}$	2.13	1.424±0.402	4.543±0.294
EP11	1mM KNO_3	4.2	$1.1x10^{-3}$	1.09	0.244±0.234	4.985±0.251
EP28	1mM KNO_3	4.95	$1x10^{-3}$	1.04	1.222±0.238	4.996±0.248
EP14	0.1M KNO_3	5.5	0.10	10.4	1.016±0.168	1.154±0.098
EP22	1mM KNO_3	5.65	$1x10^{-3}$	1.04	0.179±0.215	6.286±0.288
EP7	1mM KNO_3	5.73	$1x10^{-3}$	1.04	-1.248±0.260	6.747±0.320
EP12	1mM KNO_3	6.46	$1x10^{-3}$	1.04	-2.505±0.155	8.545±0.356
EP57	4mM KNO_3	6.78	$4x10^{-3}$	2.08	-1.676±0.216	6.869±0.285
EP27	1mM KNO_3	7.05	$1x10^{-3}$	1.04	-1.611±0.357	8.401±0.406
EP13	1mM KNO_3	7.1	$1x10^{-3}$	1.04	-3.035±0.189	8.779±0.369

TABLE B.1.3. Electrophoresis data for the Soxhlet washed rutile (high pH)

Run	Solution	pH	Ionic Strength/ mol dm^{-3}	Kappa 10^{-8}/ m^{-1}	$\mu_{EP} \times 10^8$/ $m^2\ V^{-1}\ s^{-1}$	$\mu_{EO} \times 10^8$/ $m^2\ V^{-1}\ s^{-1}$
EP26	1mM KNO_3	9.15	1×10^{-3}	1.04	-3.758±0.242	10.459±0.443
EP56	2mM KNO_3	9.54	2×10^{-3}	1.47	-3.616±0.207	8.632±0.332
EP8	1mM KNO_3	9.85	1.07×10^{-3}	1.08	-3.913±0.204	10.053±0.418
EP10	1mM KNO_3	10.18	1.6×10^{-3}	1.32	-3.763±0.209	9.737±0.407
EP25	1mM KNO_3	10.2	1.2×10^{-3}	1.14	-3.705±0.222	10.576±0.443
EP59	1mM KNO_3	10.35	1.2×10^{-3}	1.14	-4.482±0.214	10.269±0.386
EP15	0.10M KNO_3	10.47	0.100	10.4	-2.169±0.143	3.193±0.151
EP23	1mM KNO_3	10.7	1.5×10^{-3}	1.27	-3.911±0.179	9.967±0.409
EP54	water	10.71	0.5×10^{-3}	0.736	-4.145±0.217	11.732±0.441
EP39	water	11.39	2.45×10^{-3}	1.63	-3.377±0.372	10.063±0.432
EP55	water	11.4	2.51×10^{-3}	1.65	-3.829±0.223	10.224±0.391
EP70	2mM KNO_3	11.32	4.09×10^{-3}	2.10	-3.314±0.181	9.026±0.342
EP71	3mM KNO_3	11.32	5.09×10^{-3}	2.35	-3.295±0.156	8.727±0.326
EP72	4mM KNO_3	11.36	6.29×10^{-3}	2.61	-3.505±0.162	8.437±0.316
EP73	10mM KNO_3	11.33	12.1×10^{-3}	3.62	-2.604±0.129	7.077±0.265
EP79	3.9mM LiCl	11.29	5.87×10^{-3}	2.52	-3.329±0.215	8.576±0.335

TABLE B.1.4. Electrophoresis data for the washed rutile in aqueous MIPA solution

Run	Solution	pH	Ionic Strength/ mol dm^{-3}	Kappa 10^{-8}/ m^{-1}	$\mu_{EP} \times 10^8$/ $m^2\ V^{-1}\ s^{-1}$	$\mu_{EO} \times 10^8$/ $m^2\ V^{-1}\ s^{-1}$
EP18	0.16mM MIPA	10.2	0.16×10^{-3}	0.416	-3.941±0.208	11.590±0.480
EP17	4.4mM MIPA	10.2	1×10^{-3}	1.04	-4.756±0.341	10.826±0.476
EP33	0.01M MIPA	10.81	0.65×10^{-3}	0.839	-2.261±0.157	7.817±0.329
EP31	0.05M MIPA	11.12	1.3×10^{-3}	1.19	-3.834±0.345	8.619±0.403
EP34	0.06M MIPA	11.18	1.5×10^{-3}	1.27	-2.419±0.138	6.111±0.256
EP32	0.09M MIPA	11.21	1.6×10^{-3}	1.32	-5.072±0.424	8.607±0.427
EP46	0.5mM MIPA	11.30	2×10^{-3}	1.47	-3.059±0.263	10.432±0.412
EP40	0.99mM MIPA	11.33	2.1×10^{-3}	1.51	-2.129±0.342	10.021±0.424
EP43	1.98mM MIPA	11.32	2.1×10^{-3}	1.51	-2.890±0.229	10.432±0.403
EP44	3.96mM MIPA	11.31	2×10^{-3}	1.47	-3.057±0.202	10.174±0.388
EP45	19.8mM MIPA	11.34	2.2×10^{-3}	1.54	-2.790±0.331	9.880±0.415
EP41	9.9mM MIPA	11.31	2×10^{-3}	1.47	-2.804±0.124	9.917±0.366
EP42	0.099M MIPA	11.41	2.6×10^{-3}	1.68	-3.816±0.269	9.731±0.385
EP58	4mM MIPA	11.37	2.3×10^{-3}	1.58	-4.754±0.222	10.217±0.384
EP66	4mM MIPA 1mM KNO_3	11.33	3.1×10^{-3}	1.83	-3.942±0.225	9.448±0.364
EP67	4mM MIPA 2mM KNO_3	11.32	4.1×10^{-3}	2.11	-3.580±0.200	9.176±0.350
EP68	4mM MIPA 3mM KNO_3	11.32	5.1×10^{-3}	2.35	-3.280±0.171	8.515±0.321
EP69	4mM MIPA 4mM KNO_3	11.33	6.1×10^{-3}	2.57	-3.141±0.149	8.134±0.304

TABLE B.1.5. Electrophoresis data for the washed rutile in aqueous MIPA solution

Run	Solution	pH	Ionic Strength/ mol dm^{-3}	Kappa 10^{-8}/ m^{-1}	$\mu_{EP} \times 10^8$/ $m^2\ V^{-1}\ s^{-1}$	$\mu_{EO} \times 10^8$/ $m^2\ V^{-1}\ s^{-1}$
EP60	4mM MIPA	3.62	4.2×10^{-3}	2.13	-1.708±0.188	4.097±0.193
EP77	4mM MIPA	3.70	4.2×10^{-3}	2.13	0.770±0.502	3.790±0.337
EP75	4mM MIPA	4.27	4×10^{-3}	2.08	0.915±0.180	4.530±0.200
EP76	4mM MIPA	5.47	4×10^{-3}	2.08	0.677±0.440	5.684±0.342
EP48	4mM MIPA	6.91	3.8×10^{-3}	2.03	0.307±0.424	7.005±0.368
EP74	4mM MIPA	7.74	3.9×10^{-3}	2.06	-1.943±0.155	7.544±0.289
EP65	4mM MIPA	7.78	3.9×10^{-3}	2.06	-2.060±0.237	7.311±0.305
EP50	4mM MIPA	9.20	2.6×10^{-3}	1.68	-3.308±0.181	8.537±0.324
EP47	4mM MIPA	9.7	1.4×10^{-3}	1.23	-3.842±0.204	9.251±0.352
EP80	4mM MIPA	9.94	0.98×10^{-3}	1.03	-3.872±0.204	9.900±0.381
EP49	4mM MIPA	10.10	0.73×10^{-3}	0.889	-4.240±0.239	10.493±0.401
EP51	4mM MIPA	10.30	0.50×10^{-3}	0.736	-4.348±0.188	10.376±0.385
EP52	4mM MIPA	10.50	0.33×10^{-3}	0.598	-4.802±0.265	11.603±0.443
EP53	4mM MIPA	10.55	0.35×10^{-3}	0.616	-4.996±0.331	11.905±0.470
EP62	4mM MIPA	10.62	0.42×10^{-3}	0.674	-5.473±0.349	11.583±0.461
EP63	4mM MIPA	11.02	1.05×10^{-3}	1.07	-5.048±0.365	10.869±0.445
EP64	4mM MIPA	11.22	1.67×10^{-3}	1.34	-4.550±0.318	10.456±0.420

TABLE B.1.6. Electrophoresis data for the washed rutile in aqueous MIPA solution

Run	Solution	pH	Ionic Strength/ mol dm^{-3}	Kappa 10^{-8}/ m^{-1}	$\mu_{EP} \times 10^8$/ $m^2\ V^{-1}\ s^{-1}$	$\mu_{EO} \times 10^8$/ $m^2\ V^{-1}\ s^{-1}$
EP82	0.5mM MIPA	10.62	0.42×10^{-3}	0.674	-4.110±0.178	11.942±0.443
EP84	1mM MIPA	10.55	0.35×10^{-3}	0.616	-4.686±0.235	12.063±0.459
EP81	10mM MIPA	10.52	0.85×10^{-3}	0.959	-4.509±0.272	10.164±0.407
EP83	0.1M MIPA	10.57	7.1×10^{-3}	2.76	-3.662±0.181	6.723±0.264
EP89	4mM MIPA 1mM LiCL	10.30	1.6×10^{-3}	1.32	-4.677±0.293	10.185±0.402
EP50	4mM MIPA 4mM LiCL	10.48	4.4×10^{-3}	2.18	-4.232±0.245	9.004±0.351
EP91	4mM MIPA 4mM KNO_3	10.48	4.4×10^{-3}	2.18	-3.614±0.239	8.295±0.330
EP92	4mM MIPA 4.2mM KCL	10.50	4.56×10^{-3}	2.22	-3.929±0.228	8.390±0.327
EP93	4mM MIPA 4.4mM NaF	10.40	4.85×10^{-3}	2.294	-4.348±0.245	8.459±0.333
EP94	1mM MIPA 4mM LiCL	11.10	5.26×10^{-3}	1.17	-4.004±0.198	8.951±0.339
EP95	4mM MIPA 4mM LiCL	11.09	5.23×10^{-3}	1.15	-3.796±0.215	8.649±0.333
EP78	4mM MIPA 3.92mM LiCL	11.31	5.96×10^{-3}	2.54	-3.600±0.342	8.061±0.358
EP85	0.5mM MIPA 4mM KNO_3	11.08	5.20×10^{-3}	1.14	-3.601±0.210	8.615±0.332
EP86	2mM MIPA 4mM KNO_3	11.10	5.26×10^{-3}	1.17	-3.588±0.207	8.554±0.330
EP87	4mM MIPA 4mM KNO_3	11.11	5.29×10^{-3}	1.18	-3.578±0.197	8.463±0.324
EP88	8mM MIPA 4mM KNO_3	11.05	5.12×10^{-3}	1.10	-3.646±0.196	8.242±0.315

TABLE B.1.7. Electrophoretic mobilities of rutile particles subjected to a period of equilibration with MIPA solution

Run	Solution	pH	Ionic Strength/ mol dm^{-3}	Kappa 10^{-8}/ m^{-1}	$\mu_{EP} \times 10^8$/ $m^2\ V^{-1}\ s^{-1}$	$\mu_{EO} \times 10^8$/ $m^2\ V^{-1}\ s^{-1}$
EP35	15mM MIPA	11	1.0×10^{-3}	1.04	-5.331±0.447	10.934±0.477
EP38	25mM MIPA	11	1.0×10^{-3}	1.04	-4.197±0.225	10.557±0.400
EP37	52mM MIPA	11.1	1.26×10^{-3}	1.17	-3.660±0.229	9.355±0.363
EP36	0.091M MIPA	11.2	1.58×10^{-3}	1.31	-3.950±0.243	8.385±0.332

Rutile particles equilibrated (20 days) in aqueous MIPA solution. Mobility measurement carried out in the appropriate equilibrium MIPA solution.

	Amino loss/ μmol g^{-1}
EP35	197
EP36	347
EP37	328
EP38	225

TABLE B.2.1. Rapid coagulation rates for the washed rutile in aqueous solution (25°C)

Run	Solution	pH	Ionic Strength/ mol dm^{-3}	$kx10^{18}$/ m^3 s^{-1}	N_0x10^{-14}/ m^{-3}
PC6	KNO_3	5.80	0.100	4.80±0.93	1.84
PC22	KNO_3	5.5	0.100	7.58±1.16	5.64
PC23	KNO_3	5.5	0.100	5.18±1.02	4.70
PC24	KNO_3	5.5	0.100	4.61±0.27	3.49
PC25	KNO_3	5.5	0.100	5.55±0.34	4.31
PC27	KNO_3	5.7	0.100	5.62±0.71	5.16
PC28	KNO_3	5.7	0.100	6.27±0.32	6.38
PC32	KNO_3	5.6	0.100	7.16±0.43	3.63
PC33	KNO_3	5.6	0.100	7.02±0.43	3.07
PC17	KNO_3	5.7	0.100	5.57±0.34	4.73
PC18	KNO_3	5.7	0.100	5.57±0.45	7.36
PC19	KNO_3	5.7	0.100	5.77±0.41	6.66
PC20	KNO_3	5.7	0.100	6.59±0.48	8.27
PC21	KNO_3	5.7	0.100	6.48±0.95	4.10
PC26	KNO_3	5.7	0.100	6.21±0.68	6.49

TABLE B.2.2. Coagulation rate constants for the washed rutile in aqueous solution (25°C)

Run	Solution	pH	Ionic Strength/ mol dm^{-3}	$kx10^{18}$/ m^3 s^{-1}	N_0x10^{-14}/ m^{-3}	W
PC34	10^{-5}M KNO_3	6.0	$1.1x10^{-5}$	0.589±0.041	3.33	10.3
PC37	10^{-5}M KNO_3	6.04	$1.1x10^{-5}$	0.291±0.011	3.76	20.9
PC45	10^{-5}M KNO_3	6.00	$1.1x10^{-5}$	0.730±0.086	3.22	8.33
PC48	10^{-5}M KNO_3	6.16	$1.1x10^{-5}$	0.468±0.039	3.67	13.0
PC51	10^{-5}M KNO_3	5.85	$1.1x10^{-5}$	0.348±0.039	3.86	17.5
PC40	$5x10^{-5}$M KNO_3	5.90	$5.1x10^{-5}$	0.571±0.016	3.47	10.6
PC43	$5x10^{-5}$M KNO_3	6.05	$5.1x10^{-5}$	0.584±0.100	4.44	10.4
PC35	10^{-4}M KNO_3	5.96	$1x10^{-4}$	0.537±0.030	3.20	11.3
PC38	10^{-4}M KNO_3	6.03	$1x10^{-4}$	0.650±0.080	3.96	9.35
PC46	10^{-4}M KNO_3	5.92	$1x10^{-4}$	0.766±0.145	2.75	7.94
PC49	10^{-4}M KNO_3	5.97	$1x10^{-4}$	0.541±0.030	3.72	11.2
PC52	10^{-4}M KNO_3	5.71	$1x10^{-4}$	0.348±0.018	3.05	15.8
PC53	10^{-4}M KNO_3	5.72	$1x10^{-4}$	0.411±0.020	4.44	14.8
PC67	10^{-4}M KNO_3	5.96	$1x10^{-4}$	0.379±0.029	4.79	16.0
PC41	$5x10^{-4}$M KNO_3	5.85	$5x10^{-4}$	0.634±0.046	3.39	9.59
PC50	$5x10^{-4}$M KNO_3	5.80	$5x10^{-4}$	0.677±0.086	3.29	8.98
PC75	$5x10^{-4}$M KNO_3	5.8	$5x10^{-4}$	1.34±0.25	3.86	4.54
PC80	$5x10^{-4}$M KNO_3	5.8	$5x10^{-4}$	1.12±0.07	3.32	5.43

TABLE B.2.3. Coagulation rate constants for the washed rutile in aqueous solution (25°C)

Run	Solution	pH	Ionic Strength/ mol dm^{-3}	$kx10^{18}$/ m^3 s^{-1}	N_0x10^{-14}/ m^{-3}	W
PC81	$5x10^{-4}$M KNO_3	5.7	$5x10^{-4}$	1.84±0.04	4.07	3.30
PC82	$5x10^{-4}$M KNO_3	5.7	$5x10^{-4}$	1.60±0.13	4.10	3.80
PC71	$5x10^{-4}$M KNO_3	5.7	$5x10^{-4}$	2.14±0.13	3.30	2.84
PC72	$5x10^{-4}$M KNO_3	5.7	$5x10^{-4}$	1.25±0.22	3.51	4.86
PC73	$5x10^{-4}$M KNO_3	5.7	$5x10^{-4}$	0.966±0.041	3.86	6.29
PC76	$5x10^{-4}$M KNO_3	5.7	$5x10^{-4}$	1.59±0.04	3.41	3.82
PC77	$5x10^{-4}$M KNO_3	5.7	$5x10^{-4}$	1.88±0.20	4.26	3.23
PC78	$5x10^{-4}$M KNO_3	5.7	$5x10^{-4}$	1.67±0.03	4.21	3.64
PC79	$5x10^{-4}$M KNO_3	5.7	$5x10^{-4}$	1.25±0.08	4.42	4.86
PC9	$5x10^{-3}$M KNO_3	5.65	$5.1x10^{-3}$	5.48±1.18	4.31	1.11
PC42	$5x10^{-3}$M KNO_3	5.65	$5x10^{-3}$	6.41±0.09	3.17	0.95
PC5	$1x10^{-2}$M KNO_3	5.90	$1x10^{-2}$	3.50±0.39	2.96	1.74
PC7	$1x10^{-2}$M KNO_3	5.70	$1x10^{-2}$	7.96±0.23	4.47	0.76
PC3	water	2.60	$2.5x10^{-3}$	1.84±0.07	2.98	3.30
PC2	$1x10^{-3}$M KNO_3	3.26	$1.5x10^{-3}$	2.68±0.14	4.90	2.27
PC12	$1x10^{-2}$M KNO_3	9.69	$1x10^{-2}$	1.45±0.02	3.94	4.19
PC121	water	11.12	$1.3x10^{-3}$	1.29±0.24	3.30	4.71

TABLE B.2.4. Coagulation rate constants as a function of ionic strength at high pH

Run	Solution	pH	Ionic Strength/ mol dm^{-3}	$kx10^{18}$/ m^3 s^{-1}	N_0x10^{-14}/ m^{-3}	W
PC121	water	11.12	$1.3x10^{-3}$	1.29±0.24	3.30	4.71
PC122	5mM KNO_3	11.14	$6.3x10^{-3}$	1.40±0.11	3.41	4.34
PC123	10.3mM KNO_3	11.08	$1.15x10^{-2}$	1.40±0.10	3.47	4.34
PC126	11.5mM KNO_3	11.16	$1.29x10^{-2}$	1.73±0.19	3.67	3.51
PC125	15mM KNO_3	11.10	$1.63x10^{-2}$	2.13±0.03	3.72	2.85
PC127	16.5mM KNO_3	11.22	$1.82x10^{-2}$	2.55±0.02	3.46	2.38
PC124	20.8mM KNO_3	11.18	$2.23x10^{-2}$	3.71±0.09	3.65	1.64
PC141	1.24mM $Ba(NO_3)_2$	11.29	$5.67x10^{-3}$	4.55±0.23	3.38	1.34

TABLE B.2.5. Coagulation rate constants in aqueous MIPA solution (25°C)

Run	[MIPA]/ mol dm^{-3}	pH	Ionic Strength/ mol dm^{-3}	$kx10^{19}$/ m^3 s^{-1}	N_0x10^{-14}/ m^{-3}	W
PC60	0.018	10.81	$0.75x10^{-3}$	3.05±0.09	3.47	19.9
PC54	0.020	10.62	$1.27x10^{-3}$	8.09±0.61	4.89	7.52
PC61	0.036	10.95	$1.10x10^{-3}$	4.11±0.20	3.96	14.8
PC62	0.045	11.00	$1.23x10^{-3}$	5.64±0.43	3.94	10.8
PC55	0.050	11.00	$1.37x10^{-3}$	3.52±0.36	2.81	17.3
PC63	0.054	11.01	$1.48x10^{-3}$	2.82±0.25	2.97	21.6
PC56	0.060	11.00	$1.64x10^{-3}$	1.58±0.06	3.44	38.5
PC64	0.072	11.10	$1.58x10^{-3}$	5.46±0.25	3.72	11.1
PC57	0.080	11.09	$1.79x10^{-3}$	3.32±0.20	2.75	18.3
PC65	0.090	11.13	$1.84x10^{-3}$	7.51±0.34	4.03	8.10
PC58	0.10	11.18	$1.83x10^{-3}$	3.02±0.14	3.43	20.1
PC59	0.20	11.30	$2.79x10^{-3}$	3.30±0.09	3.90	18.4
PC31	0.50	11.5	$4.42x10^{-3}$	4.09±0.02	5.82	14.9
PC66	0.09	11.39	$2.45x10^{-3}$	5.25±0.20	4.26	11.6

TABLE B.2.6. Coagulation rate constants for rutile dispersed in aqueous MIPA solution as a function of ionic strength

Run	Solution	pH	Ionic Strength/ mol dm^{-3}	$kx10^{18}$/ m^3 s^{-1}	N_0x10^{-14}/ m^{-3}	W
PC112	0.1M MIPA	11.2	$1.58x10^{-3}$	1.28±0.07	3.70	4.75
PC113	0.1M MIPA 0.9mM KNO_3	11.2	$2.48x10^{-3}$	1.58±0.07	4.31	3.85
PC117	0.1M MIPA 2.9mM KNO_3	11.2	$4.48x10^{-3}$	1.46±0.06	4.05	4.16
PC114	0.1M MIPA 5.4mM KNO_3	11.2	$6.98x10^{-3}$	1.80±0.14	3.51	3.38
PC115	0.1M MIPA 9.8mM KNO_3	11.2	$1.14x10^{-2}$	1.94±0.23	4.47	3.13
PC116	0.1M MIPA 13.2mM KNO_3	11.2	$1.48x10^{-2}$	3.16±0.29	3.74	1.92
PC118	0.1M MIPA 16.5mM KNO_3	11.2	$1.81x10^{-2}$	6.23±0.20	3.29	0.98
PC119	0.1M MIPA 19.2mM KNO_3	11.2	$2.08x10^{-2}$	3.68±0.20	5.02	1.65
PC135	0.1M MIPA	11.2	$1.58x10^{-3}$	2.19±0.29	3.36	2.78
PC140	0.1M MIPA 1.09mM $Ba(NO_3)_2$	11.2	$4.85x10^{-3}$	7.75±0.52	3.27	0.78
PC128	1mM MIPA	10.2	$0.16x10^{-3}$	1.65±0.15	3.58	3.68
PC133	1mM MIPA 2.3mM KNO_3	10.2	$2.46x10^{-3}$	2.57±0.02	4.10	2.37
PC134	1mM MIPA 3.8mM KNO_3	10.2	$3.96x10^{-3}$	2.16±0.20	3.94	2.81
PC132	1mM MIPA 5.9mM KNO_3	10.2	$6.06x10^{-3}$	2.48±0.14	3.63	2.45
PC129	1mM MIPA 9.2mM KNO_3	10.2	$9.36x10^{-3}$	2.34±0.09	3.90	2.60
PC131	1mM MIPA 11.6mM KNO_3	10.2	$1.18x10^{-2}$	1.92±0.12	4.53	3.17
PC130	1mM MIPA 15.5mM KNO_3	10.2	$1.57x10^{-2}$	5.07±0.10	3.76	1.20

TABLE B.2.7. Coagulation rate constants for rutile dispersed in aqueous MIPA solution (25°C)

Run	Solution	pH	Ionic Strength/ mol dm^{-3}	$kx10^{18}$/ m^3 s^{-1}	N_0x10^{-14}/ m^{-3}	W
PC153	0.02M MIPA	11.29	$1.95x10^{-3}$	0.748±0.164	3.59	8.13
PC154	4mM MIPA	11.28	$1.95x10^{-3}$	0.998±0.191	3.51	6.09
PC155	1mM MIPA	11.28	$1.95x10^{-3}$	0.850±0.098	3.70	7.15
PC156	0.4mM MIPA	11.28	$1.95x10^{-3}$	1.28±0.13	3.52	4.75
PC136	0.02M MIPA 0.96mM NH_3^+	10.8	$1.71x10^{-3}$	1.43±0.06	3.33	4.25
PC139	0.02M MIPA 1.9mM NH_3^+	10.6	$1.9x10^{-3}$	1.30±0.08	3.72	4.68
PC138	0.02M MIPA 7.7mM NH_3^+	9.86	$7.7x10^{-3}$	1.39±0.08	3.27	4.37
PC137	0.02M MIPA 20mM NH_3^+	2.55	$2.3x10^{-2}$	6.77±0.93	4.07	0.90
PC144	0.02M MIPA	10.96	$0.91x10^{-3}$	0.955±0.125	3.68	6.37
PC162	0.0102M MIPA 10mM KNO_3	10.7	$1x10^{-2}$	1.13±0.05	4.10	5.38
PC163	0.0102M MIPA 3.84mM NH_3^+ 6.15mM KNO_3	9.6	$1x10^{-2}$	1.89±0.11	3.94	3.22
PC164	0.0102M MIPA 5.76mM NH_3^+ 4.23mM KNO_3	9.3	$1x10^{-2}$	0.988±0.025	3.68	6.15
PC165	0.0102M MIPA 8.26mM NH_3^+ 1.73mM KNO_3	9.0	$1x10^{-2}$	1.45±0.12	3.78	4.19
PC166	0.0102M MIPA 0.010M NH_3^+	7.4	$1x10^{-2}$	0.823±0.130	3.70	7.39

TABLE B.2.8. Coagulation rate constants for rutile in aqueous solution (25°C)

Run	Solution	pH	Ionic Strength/ mol dm^{-3}	$kx10^{18}$/ m^3 s^{-1}	$N_0 x10^{-14}$/ m^{-3}	W
PC144	0.02M MIPA	10.96	$0.91x10^{-3}$	0.955±0.125	3.68	6.37
PC146	water	10.95	$0.89x10^{-3}$	0.593±0.036	3.92	10.3
PC145	0.02M MIPA 0.025M KNO_3	10.9	$2.60x10^{-2}$	5.62±0.07	5.51	1.08
PC147	0.02M MIPA 3.8mM NH_3^+	10.28	$4.55x10^{-3}$	1.42±0.17	3.59	4.28
PC148	3.68mM KNO_3	10.29	$3.68x10^{-3}$	1.25±0.11	3.54	4.86
PC149	0.02M MIPA 9.46mM NH_3^+	9.72	$1.02x10^{-2}$	1.15±0.15	3.36	5.29
PC150	9.65mM KNO_3	9.70	$9.65x10^{-3}$	1.30±0.12	3.92	4.68
PC151	0.02M MIPA 13.2mM NH_3^+	9.39	$1.40x10^{-2}$	0.891±0.125	3.41	6.82
PC152	13.4mM KNO_3	9.38	$1.34x10^{-2}$	2.59±0.43	2.81	2.35

TABLE B.2.9. Coagulation rate constants for rutile in aqueous solution

Run	Solution	pH	Ionic Strength/ mol dm^{-3}	T/ °C	$kx10^{19}$/ m^3 s^{-1}	$N_0 x10^{-14}$/ m^{-3}	W
PC157	10mM MIPA	10.9	$0.79x10^{-3}$	55.6	3.64±0.46	3.54	16.7
PC159	10mM MIPA	10.9	$0.79x10^{-3}$	55.6	2.68±0.36	2.76	22.7
PC158	water	11.0	$1x10^{-3}$	55.6	3.07±0.14	3.26	19.8
PC160	10mM MIPA	10.85	$0.72x10^{-3}$	37.4	9.51±1.98	3.43	6.39
PC161	water	10.86	$0.72x10^{-3}$	37.4	13.0±2.3	3.35	4.68

TABLE B.2.10. Coagulation rate constants for rutile particles redispersed in the equilibrium adsorption isotherm solution

Run	Solution	pH	Amino Loss/ $\mu mol\ g^{-1}$	Ionic Strength/ $mol\ dm^{-3}$	$kx10^{18}$/ $m^3\ s^{-1}$	N_0x10^{-14}/ m^{-3}	W
PC68	2mM MIPA	10.4	8	$0.24x10^{-3}$	1.56±0.10	4.89	3.90
PC70	2mM MIPA	10.4	8	$0.24x10^{-3}$	1.17±0.08	3.41	5.20
PC69	2mM MIPA	10.4	24	$0.24x10^{-3}$	1.20±0.06	3.96	5.07
PC85	0.0439M MIPA	11.0	238	$1.20x10^{-3}$	0.471±0.057	3.51	12.9
PC86	0.0439M MIPA	11.0	238	$1.20x10^{-3}$	0.687±0.030	2.71	8.85
PC87	0.0439M MIPA	11.0	238	$1.20x10^{-3}$	0.730±0.066	3.59	8.33
PC88	0.0495M MIPA	11.07	12*	$1.2x10^{-3}$	1.34±0.02	3.23	4.54
PC83	0.090M MIPA	11.2	400	$1.6x10^{-3}$	0.0948±0.0034	4.19	64.1
PC84	0.0986M MIPA	11.22	40*	$1.7x10^{-3}$	0.105±0.005	3.13	57.9
PC90	0.0986M MIPA	11.22	40*	$1.7x10^{-3}$	0.103±0.006	5.02	59.0
PC89	0.10M MIPA	11.22	238	$1.7x10^{-3}$	1.14±0.14	3.36	5.33
PC120	0.10M MIPA	11.22	36*	$1.7x10^{-3}$	1.35±0.06	3.63	4.50
PC91	0.081M MIPA 0.019M NH_3^+	10.2	380	$2.08x10^{-2}$	4.50±0.14	4.26	1.35
PC92	0.058M MIPA 0.019M NH_3^+	10.0	490	$2.06x10^{-2}$	4.25±0.54	3.43	1.43
PC93	0.043M MIPA 0.019M NH_3^+	9.9	285	$2.04x10^{-2}$	4.39±0.23	5.06	1.38

* Rutile equilibrated with aqueous MIPA solution in the absence of light.

TABLE B.2.11. Coagulation rate constants for rutile particles redispersed in the equilibrium adsorption solution (25°C)

Run	Solution	pH	Amino Loss/ μmol g^{-1}	Ionic Strength/ mol dm^{-3}	$kx10^{18}$/ m^3 s^{-1}	N_0x10^{-14}/ m^{-3}	W
PC95	0.015M MIPA	10.8	197	$0.65x10^{-3}$	0.739±0.052	3.68	8.23
PC96	0.025M MIPA	10.9	225	$0.84x10^{-3}$	0.950±0.098	3.86	6.40
PC97	0.033M MIPA	11.0	290	$0.96x10^{-3}$	1.35±0.29	3.07	4.50
PC98	0.043M MIPA	11.1	280	$1.1x10^{-3}$	0.928±0.105	3.23	6.55
PC99	0.052M MIPA	11.1	328	$1.2x10^{-3}$	2.21±0.29	3.54	2.75
PC100	0.052M MIPA	11.1	328	$1.2x10^{-3}$	2.24±0.51	3.23	2.71
PC101	0.061M MIPA	11.1	356	$1.3x10^{-3}$	2.77±0.16	3.09	2.19
PC102	0.082M MIPA	11.2	330	$1.5x10^{-3}$	2.18±0.17	4.12	2.79
PC103	0.082M MIPA	11.2	330	$1.5x10^{-3}$	2.66±0.30	4.24	2.29
PC104	0.091M MIPA	11.2	347	$1.6x10^{-3}$	1.40±0.13	3.20	4.34
PC105	0.10M MIPA	11.22	330	$1.6x10^{-3}$	2.13±0.25	3.16	2.85
PC106	0.10M MIPA	11.22	330	$1.6x10^{-3}$	1.70±0.15	2.96	3.58
PC107	0.0164M MIPA	11.0	150	$1.0x10^{-3}$	2.43±0.18	3.80	2.50
PC109	0.0524M MIPA	11.0	310	$1.48x10^{-3}$	2.50±0.02	3.27	2.43
PC110	0.067M MIPA	10.9	133	$2.38x10^{-3}$	2.93±0.02	3.46	2.08
PC108	0.093M MIPA	11.0	285	$2.55x10^{-3}$	2.48±0.16	3.43	2.45
PC111	0.09M MIPA	11.2	365	$1.59x10^{-3}$	0.539±0.032	3.51	11.3

TABLE B.3.1. Adsorption isotherm 1 - variable MIPA concentration, equilibrium pH

TIME = 162 hrs T = 25°C AGITATION = 34 rpm

$[MIPA]_0$/ mol dm^{-3}	pH_0	Ionic Strength/ mol dm^{-3}	[MIPA]/ mol dm^{-3}	Amino Loss/ μmol g^{-1}
0.00517	10.44	0.38×10^{-3}	0.00264	202
0.0103	10.62	0.54×10^{-3}	0.00568	441
0.0207	10.77	0.76×10^{-3}	0.0162	466
0.103	11.17	1.70×10^{-3}	0.0943	887

TABLE B.3.2. Adsorption isotherm 2 - time of adsorption variation

T = 25°C AGITATION = 104 rpm

$[MIPA]_0$/ mol dm^{-3}	pH_0	Ionic Strength/ mol dm^{-3}	Time Eqm/ hour	[MIPA]/ mol dm^{-3}	Amino Loss/ μmol g^{-1}
0.0507	11.07	1.20×10^{-3}	19	0.0455	262
0.0507	11.07	1.20×10^{-3}	87	0.0447	301
0.0507	11.07	1.20×10^{-3}	182	0.0435	404
0.0507	11.07	1.20×10^{-3}	255	0.0438	405

TABLE B.3.3. Adsorption isotherm 3 - variable MIPA concentration, equilibrium pH

TIME = 6.5 days T = 25°C AGITATION = 110 rpm

$[MIPA]_0$/ mol dm^{-3}		pH_0	Ionic Strength/ mol dm^{-3}	$[MIPA]_F$/ mol dm^{-3}		Amino Loss/ μmol g^{-1}	
HCL	HCHO			HCL	HCHO	HCL	HCHO
0.0297	0.0302	10.92	0.92×10^{-3}	0.0232	0.0265	319	181
0.0397	0.0402	11.01	1.06×10^{-3}	0.0323	0.0359	399	232
0.0501	0.0498	11.10	1.19×10^{-3}	0.0402	0.0436	499	313
0.0599	0.0601	11.10	1.30×10^{-3}	0.0530	0.0557	358	228
0.0700	0.0702	11.18	1.40×10^{-3}	0.0595	0.0633	506	333
0.0789	0.0790	11.18	1.49×10^{-3}	0.0692	0.0737	461	252
0.200	0.201	11.40	2.37×10^{-3}	0.188	0.192	581	436
0.503	0.505	11.61	3.77×10^{-3}	0.478	0.500	1160	232

TABLE B.3.4. Adsorption isotherm 4 - constant MIPA concentration variable pH

TIME = 5.5 days T = 25°C AGITATION = 110 rpm
$[MIPA]_0$ = 0.0500 mol dm^{-3}

Ionic Strength/ mol dm^{-3}	pH_0	$[MIPA]_F$/ mol dm^{-3}	Amino Loss/ μmol g^{-1}
9.55×10^{-3}	11.98	0.0497	15
2.95×10^{-3}	11.47	0.0467	173
1.51×10^{-3}	11.18	0.0457	214
1.19×10^{-3}	10.96	0.0451	245
3.82×10^{-2}	8.94	0.0392	557
4.94×10^{-2}	7.54	0.0451	229
5.6×10^{-2}	2.22	0.0475	125

TABLE B.3.5. Adsorption isotherm 5 - variable MIPA concentration, 0.1 mol dm^{-3} electrolyte

$[KNO_3]$ = 0.100 mol dm^{-3} TIME = 24.5 days T = 25°C
AGITATION = 110 rpm

$[MIPA]_0$/ mol dm^{-3}	pH	$[MIPA]_F$/ mol dm^{-3}	Amino Loss/ μmol g^{-1}
0.0296	10.91	0.0249	242
0.0407	10.99	0.0351	281
0.0499	11.02	0.0449	263
0.0606	11.09	0.0537	324
0.0693	11.11	0.0609	412
0.0812	11.14	0.0764	245
0.203	11.33	0.191	625
0.498	11.55	0.478	994

TABLE B.3.6. Adsorption isotherm 6 - variable MIPA concentration, 0.48 mol dm^{-3} electrolyte

$[KNO_3]$ = 0.48 mol dm^{-3} TIME = 4.5 days T = 25°C
AGITATION = 34 rpm

a $[MIPA]_0$/ mol dm^{-3}	b $[MIPA^+]_0$/ mol dm^{-3}	pH_0	Ratio b/a	c $[MIPA]_F$/ mol dm^{-3}	d $[MIPA^+]_F$/ mol dm^{-3}	Ratio d/c	Amino Loss/ μmol g^{-1}
0.0105	0.0051	9.48	0.49	0.00984	0.00754	0.77	33.8
0.0203	0.0094	9.52	0.46	0.0197	0.0134	0.68	30.7
0.0302	0.0121	9.50	0.40	0.0292	0.0205	0.70	50.5
0.0399	0.0166	9.49	0.42	0.0392	0.0270	0.69	35.1
0.0496	0.0234	9.47	0.47	0.0476	0.0330	0.69	99.4
0.0606	0.0257	9.49	0.42	0.0587	0.0393	0.67	95.1
0.0899	0.0332	9.51	0.37	0.0870	0.0575	0.66	147
0.101	0.0317	9.50	0.31	0.0980	0.0631	0.64	152

TABLE B.3.7. Adsorption isotherm 7 - variable MIPA concentration, 0.1 mol dm^{-3} electrolyte

$[KNO_3]$ = 0.10 mol dm^{-3} TIME = 2.5 days T = 25°C

$[MIPA]_0$/ mol dm^{-3}	$[MIPA^+]_0$/ mol dm^{-3}	pH_0	$[MIPA]_F$/ mol dm^{-3}	$[MIPA^+]_F$/ mol dm^{-3}	Amino Loss/ μmol g^{-1}
0.0103	-	11.0	0.0105	-	0
0.0205	0.0002	11.0	0.0205	0.0012	0
0.0309	0.0010	11.0	0.0309	0.0019	0
0.0406	0.0005	11.0	0.0407	0.0017	0
0.0504	0.0018	11.0	0.0496	0.0019	41
0.0612	0.0019	11.0	0.0609	0.0026	15
0.0890	0.0026	11.0	0.0893	0.0036	0
0.101	0.0044	11.0	0.101	0.0048	0

TABLE B.3.8. Adsorption isotherm 8 - time of adsorption

T = 25°C AGITATION = $33^1/_3$ rpm

$[MIPA]_0$/ mol dm^{-3}	pH_0	Ionic Strength/ mol dm^{-3}	Time/ hour	$[MIPA]_F$/ mol dm^{-3}	Amino Loss/ μmol g^{-1}
0.0991	11.23	$1.7x10^{-3}$	19.3	0.0980	45.2
0.0991	11.23	$1.7x10^{-3}$	90.3	0.0954	152
0.0991	11.23	$1.7x10^{-3}$	235	0.0930	248
0.0991	11.23	$1.7x10^{-3}$	574	0.0872	491
0.0992	11.30	0.10	19.3	0.0984	32.5
0.0992	11.30	0.10	90.3	0.0969	93.2
0.0992	11.30	0.10	235	0.0937	218
0.0992	11.30	0.10	574	0.0927	270

TABLE B.3.9. Adsorption isotherm 9 - constant MIPA concentration, variable pH

TIME = 12.8 days T = 25°C AGITATION = $33^{1}/_{3}$ rpm $[MIPA]_0$ = 0.100 mol dm^{-3}

pH_0	$[KNO_3]$/ mol dm^{-3}	Ionic Strength/ mol dm^{-3}	$[MIPA^+]_0$/ mol dm^{-3}	$[MIPA]_F$/ mol dm^{-3}	$[MIPA^+]_F$/ mol dm^{-3}	Amino Loss/ μmol g^{-1}	$[MIPA^+]/[MIPA]$	
							Initial	Final
11.25	0.100	0.103	0.0033	0.0975	0.0036	140	0.033	0.037
10.72	0.0936	0.100	0.0065	0.0951	0.0088	238	0.065	0.093
10.07	0.0737	0.101	0.0268	0.0977	0.0279	91.6	0.27	0.29
9.51	0.0529	0.106	0.0532	0.0974	0.0576	104	0.53	0.59
9.27	0.0309	0.100	0.0693	0.0981	0.0732	77.6	0.69	0.75
8.76	0.0127	0.102	0.0888	0.0958	0.0881	208	0.89	0.92
7.85	0	0.100	0.100	0.0982	0.0982	112	1.0	1.0
3.87	0	0.100	0.100	0.101	0.100	0	1.0	0.99

TABLE B.3.10. Adsorption isotherm 10 - variable MIPA concentration, fixed pH

TIME = 24.5 days T = 25°C AGITATION = 33 rpm

$[MIPA]_0$/ mol dm^{-3}	pH_0	Ionic Strength/ mol dm^{-3}	$[MIPA]_F$/ mol dm^{-3}	Amino Loss/ μmol g^{-1}
0.0101	11.30	$2x10^{-3}$	0.00587	174
0.0202	11.30	$2x10^{-3}$	0.0144	239
0.0305	11.30	$2x10^{-3}$	0.0234	276
0.0505	11.29	$1.95x10^{-3}$	0.0434	295
0.0606	11.30	$2x10^{-3}$	0.0525	332
0.0808	11.30	$2x10^{-3}$	0.0727	327
0.0909	11.29	$1.95x10^{-3}$	0.0800	437
0.101	11.30	$2x10^{-3}$	0.0910	413
$0.4x10^{-3}$	11.30	$2x10^{-3}$	$0.152x10^{-3}$	10.2
$1.0x10^{-3}$	11.30	$2x10^{-3}$	$0.472x10^{-3}$	22.1
$2.0x10^{-3}$	11.29	$1.95x10^{-3}$	$1.17x10^{-3}$	34.7
$4.0x10^{-3}$	11.30	$2x10^{-3}$	$2.63x10^{-3}$	56.2

TABLE B.3.11. Adsorption isotherm 11 - constant MIPA concentration, variable ionic strength

TIME = 23.5 days T = 25°C AGITATION = 33 rpm
$[MIPA]_0$ = 0.101 mol dm^{-3}

$[KNO_3]$/ mol dm^{-3}	Ionic Strength/ mol dm^{-3}	$[MIPA]_F$/ mol dm^{-3}	Amino Loss/ μmol g^{-1}
-	$1.69x10^{-3}$	0.0913	397
$0.50x10^{-3}$	$2.19x10^{-3}$	0.0877	461
$2.49x10^{-3}$	$4.18x10^{-3}$	0.0879	442
$4.99x10^{-3}$	$6.68x10^{-3}$	0.0913	327

TABLE B.3.12. Adsorption isotherm 12 - variable time of adsorption

$[MIPA]_0$ = 0.100 mol dm^{-3} T = 25°C AGITATION = 15 rpm

Time/ hours	$[MIPA]_F$/ mol dm^{-3}	Amino Loss/ μmol g^{-1}
0.5	0.100	0
2	0.0994	24.3
17	0.0989	46.7
91	0.0958	179
189	0.0934	276
382	0.0893	438
600	0.0927	297
858	0.0848	623

TABLE B.3.13. Adsorption isotherm 13 - constant MIPA concentration, variable pH

TIME = 21.8 days T = 25°C AGITATION = $33^1/_3$ rpm
$[MIPA]_0$ = 0.0504 mol dm^{-3}

pH_0	$[KNO_3]$/ mol dm^{-3}	$[MIPA^+]_0$/ mol dm^{-3}	Ionic Strength/ mol dm^{-3}	$[MIPA]_F$/ mol dm^{-3}	$[MIPA^+]_F$/ mol dm^{-3}	Amino Loss/ μmol g^{-1}
11.01	0.0050	0.00119	0.0062	0.0452	0.00218	210
10.80	0.0036	0.00258	0.0062	0.0414	0.00455	371
10.75	0.0033	0.00289	0.0062	0.0424	0.00356	315
10.70	0.0029	0.00328	0.0062	0.0417	0.00582	350
10.61	0.0023	0.00388	0.0062	0.0424	0.00621	323
10.55	0.0017	0.00447	0.0062	0.0442	0.00714	247
10.46	0.0019	0.00527	0.0072	0.0447	0.00754	237
10.40	0.0010	0.00617	0.0072	0.0439	0.00843	268

TABLE B.3.14. Adsorption isotherm 14 - variable MIPA concentration, constant pH

TIME = 21 days T = 25°C AGITATION = 15 rpm
$[KNO_3]$ = 0.100 mol dm^{-3}

$[MIPA]_0$/ mol dm^{-3}	pH_0	$[MIPA]_F$/ mol dm^{-3}	Amino Loss/ μmol g^{-1}
0.0102	11.30	0.00859	66.4
0.0203	11.31	0.0177	106
0.0303	11.29	0.0279	98.8
0.0502	11.30	0.0470	129
0.0597	11.30	0.0558	155
0.0800	11.30	0.0711	349
0.0892	11.30	0.0767	496
0.0997	11.37	0.0866	530

TABLE B.3.15. Adsorption isotherm 15 - variable time of adsorption

$[MIPA]_0$ = 2.00×10^{-3} mol dm^{-3} T = 25°C AGITATION = $33^1/_3$ rpm

Time/ hour	$[MIPA]_F$/ mol dm^{-3}	Amino Loss/ μmol g^{-1}
0.5	1.83×10^{-3}	7.1
4.1	1.68×10^{-3}	12.5
21.5	1.58×10^{-3}	17.1
70.3	1.35×10^{-3}	25.6
168	1.36×10^{-3}	26.1
216	1.51×10^{-3}	19.9
384	1.41×10^{-3}	23.8
816	1.52×10^{-3}	19.4

TABLE B.3.16. Adsorption isotherm 16 - constant MIPA concentration, variable pH

TIME = 23.5 days T = 25°C AGITATION = $33^1/_3$ rpm
$[MIPA]_0 = 2.00 \times 10^{-3}$ mol dm^{-3}

pH_0	$[KNO_3]$/ mol dm^{-3}	Ionic Strength/ mol dm^{-3}	$[MIPA]_F$/ mol dm^{-3}	Amino Loss/ μmol g^{-1}
10.51	4.6×10^{-3}	4.8×10^{-3}	1.81×10^{-3}	7.7
10.07	4.4×10^{-3}	4.8×10^{-3}	1.86×10^{-3}	5.5
9.74	4.5×10^{-3}	5.2×10^{-3}	2.00×10^{-3}	0
9.46	4.4×10^{-3}	5.4×10^{-3}	2.00×10^{-3}	0
8.90	4.5×10^{-3}	6.1×10^{-3}	2.07×10^{-3}	-
8.44	3.5×10^{-3}	5.3×10^{-3}	$>2.3 \times 10^{-3}$	-
5.27	3.5×10^{-3}	5.5×10^{-3}	$>2.3 \times 10^{-3}$	-
3.09	3.0×10^{-3}	6.0×10^{-3}	2.18×10^{-3}	-

TABLE B.3.17. Adsorption isotherm - miscellaneous

T = 25°C AGITATION = 15 rpm TIME = $19^1/_2$ days

$[MIPA]_0$/ mol dm^{-3}	pH_0	Ionic Strength/ mol dm^{-3}	$[MIPA]_F$/ mol dm^{-3}	Amino Loss/ μmol g^{-1}	Remarks
0.0402	11.30	2×10^{-3}	0.0327	305	
0.0400	11.29	0.102	0.0356	176	
0.0705	11.30	2×10^{-3}	0.0628	306	
0.0705	11.30	2×10^{-3}	0.0685	81	no light
0.0700	11.30	0.102	0.0622	302	
0.0700	11.00	0.101	0.0673	110	TIME = $2^1/_2$ days

TABLE B.3.18. Adsorption isotherm 17 - constant MIPA concentration, variable ionic strength

TIME = $19^1/_2$ days T = 25°C AGITATION = $33^1/_3$ rpm
$pH_0 = 11.37$ $[MIPA]_0 = 0.100$ mol dm^{-3}

$[KNO_3]$/ mol dm^{-3}	Ionic Strength/ mol dm^{-3}	$[MIPA]_F$/ mol dm^{-3}	Amino Loss/ μmol g^{-1}
-	1.7×10^{-3}	0.0864	542
0.00603	7.7×10^{-3}	0.0923	314
0.00910	0.0108	0.0945	215
0.0993	0.101	0.0935	257

TABLE B.3.19. Amino group loss as a function of the presence or exclusion of light

TIME = 20 days T = 25°C AGITATION = 33 rpm

pH_0	$[MIPA]_0$/ mol dm^{-3}	Daylight	$[MIPA]_F$/ mol dm^{-3}	Amino Loss/ μmol g^{-1}
11.1	0.0498	Yes	0.0439	238
11.1	0.0498	No	0.0495	12.2
11.2	0.0996	Yes	0.0900	398
11.2	0.0996	No	0.0986	40.4
11.3	0.0705	Yes	0.0628	306
11.3	0.0705	No	0.0685	81

TABLE B.3.20. Adsorption isotherm 18 - variable time of adsorption (25°C)

Solution	$[MIPA]_0$/ mmol dm^{-3}	pH_0	$[KNO_3]$/ mM	Ionic Strength/ mM
A	2.11	10.44	5.14	5.42
B	2.07	9.55	5.17	6.45
C	1.99	4.60	3.68	5.99
D	1.93	11.25	-	1.78

Time/ hour	$[MIPA]_F$/mM				Amino Loss/μmol g^{-1}			
	A	B	C	D	A	B	C	D
0.67	2.05	2.07	2.10	1.93	2.4	0	-	0
4	1.91	1.92	2.08	1.73	8.1	6.0	-	8.4
21.5	1.77	1.80	2.07	1.79	13.8	11.0	-	5.6
43.5	1.54	1.83	2.00	1.48	23.3	9.8	-	17.8
77.5	1.63	2.00	2.00	0.846	19.9	2.8	-	42.9
236	1.94	2.13	2.31	1.30	7.0	-	-	26.1

TABLE B.3.21. Adsorption isotherm 19 - variable MIPA concentration, constant conjugate acid concentration

TIME = 18.7 days T = 25°C AGITATION = 33 rpm

$[MIPA]_0$/ mol dm^{-3}	pH_0	$[MIPA^+]_0$/ mol dm^{-3}	$[MIPA]_F$/ mol dm^{-3}	$[MIPA^+]_F$/ mol dm^{-3}	Amino Loss/ μmol g^{-1}
0.0200	8.09	0.0193	0.0194	0.0194	24.8
0.0302	9.45	0.0193	0.0246	0.0204	234
0.0401	9.74	0.0193	0.0319	0.0198	334
0.0500	9.90	0.0193	0.0433	0.0211	281
0.0600	10.00	0.0193	0.0517	0.0210	341
0.0698	10.10	0.0193	0.0576	0.0198	494
0.0900	10.25	0.0193	0.0807	0.0212	375
0.100	10.22	0.0140	0.0917	0.0236	338

TABLE B.3.22. Adsorption isotherm 20 - variable MIPA concentration, equilibrium pH

TIME = 19.5 days T = 25°C AGITATION = 15 rpm

$[MIPA]_0$/ mol dm^{-3}	pH	$[MIPA]_F$/ mol dm^{-3}	Amino Loss/ μmol g^{-1}
0.0202	11.01	0.0153	193
0.0303	11.11	0.0248	221
0.0403	11.15	0.0330	293
0.0501	11.21	0.0432	281
0.0602	11.25	0.0520	324
0.0702	11.30	0.0615	352
0.0898	11.35	0.0815	337
0.0998	11.37	0.0911	343

TABLE B.3.23. Adsorption isotherm 21 - variable MIPA concentration, pH 11.0

TIME = 19.5 days T = 25°C AGITATION = 33 rpm

$[MIPA]_0$/ mol dm^{-3}	pH_0	$[MIPA]_F$/ mol dm^{-3}	$[MIPA^+]_F$/ mol dm^{-3}	Amino Loss/ μmol g^{-1}
0.0202	11.01	0.0164	0.00153	151
0.0303	11.01	0.0256	0.00217	188
0.0403	11.00	0.0362	0.00221	161
0.0501	11.01	0.0455	0.00239	186
0.0602	11.01	0.0523	0.00272	316
0.0702	11.00	0.0671	0.00309	125
0.0898	11.00	0.0827	0.00462	286
0.0998	11.01	0.0930	0.00444	285

TABLE B.3.24. Adsorption isotherm 22 - effect of light colour and intensity

TIME = 22.5 days T = 25°C AGITATION = 33 rpm
$[MIPA]_0$ = 0.100 mol dm^{-3}

Light	$[MIPA]_F$/ mol dm^{-3}	Amino Loss/ μmol g^{-1}
Dark Red	0.0976	95.9
Dark Green	0.0985	61.9
Yellow	0.0989	44.8
Dark Blue	0.0988	48.5
Light Blue	0.0933	264
Rose	0.0919	322
Normal	0.0916	342
Normal (Time = 18 days)	0.0893	429
Normal + Dark (18 days 4.5 days)	0.0911	357

TABLE B.3.25. Adsorption isotherm 23 - variable time of adsorption, continuous light

T = 25°C AGITATION = 15 rpm LIGHT = 60 watt bulb

Time/ hour	$[MIPA]_F$/mol dm^{-3}		Amino Loss/μmol g^{-1}	
	A	B	A	B
0.75	0.0986	0.0499	15.7	3.9
1.5	0.0983	0.0497	24.7	12.0
3	0.0983	0.0498	24.1	8.0
6	0.0973	0.0501	62.8	-
9.7	0.0976	0.0499	50.9	4.0
18	0.0974	0.0492	60.2	31.8
210	0.0915	0.0458	299	166
346	0.0900	0.0462	360	149

A - $[MIPA]_0$ = 0.0989 mol dm^{-3}
B - $[MIPA]_0$ = 0.0500 mol dm^{-3}

TABLE B.3.26. Additional isotherm data for isotherms 20 and 21

TIME = 20.5 days T = 25°C AGITATION = 33 rpm

$[MIPA]_0$/ mol dm^{-3}	pH_0	$[MIPA]_F$/ mol dm^{-3}	Amino Loss/ $\mu mol\ g^{-1}$
9.93×10^{-4}	10.36	8.37×10^{-4}	6.3
1.99×10^{-3}	10.50	1.42×10^{-3}	22.3
4.97×10^{-3}	10.71	2.81×10^{-3}	88.6
9.93×10^{-3}	10.87	5.87×10^{-3}	164
9.93×10^{-4}	10.97	6.93×10^{-4}	12.2
1.99×10^{-3}	11.01	1.40×10^{-3}	23.8
4.97×10^{-3}	10.97	2.77×10^{-3}	86.6
9.93×10^{-3}	11.00	5.36×10^{-3}	184

TABLE B.3.27. Adsorption isotherm 24 - constant MIPA concentration, variable electrolyte concentration, continuous light

TIME = 21 days T = 25°C AGITATION = 15 rpm
$[MIPA]_0 = 0.0984$ mol dm^{-3} $pH_0 = 11.37$

$[KNO_3]$/ mol dm^{-3}	Ionic Strength/ mol dm^{-3}	$[MIPA]_F$/ mol dm^{-3}	Amino Loss/ $\mu mol\ g^{-1}$
3.96×10^{-4}	2.07×10^{-3}	0.0912	284
1.48×10^{-3}	3.15×10^{-3}	0.0913	290
5.64×10^{-3}	7.31×10^{-3}	0.0821	636
9.00×10^{-3}	1.07×10^{-2}	0.0848	541
1.54×10^{-2}	1.71×10^{-2}	0.0899	337
4.72×10^{-2}	4.89×10^{-2}	0.0925	235

TABLE B.3.28. Adsorption isotherm 25 - effect of fraction of total equilibration time in light

TIME = 144 hours T = 25°C AGITATION = 33 rpm
$[MIPA]_0 = 0.0993$ mol dm^{-3} $pH_0 = 11.37$

Time (Light) / Total Time	$[MIPA]_F$/ mol dm^{-3}	Amino Loss/ $\mu mol\ g^{-1}$
0.004	0.0987	24.0
0.016	0.0982	45.1
0.080	0.0977	66.4
0.25	0.0975	71.8
0.69	0.0950	170
1.00	0.0947	186

TABLE B.3.29. Adsorption isotherm 26 - variable time of adsorption in the absence of light (25°C)

$[MIPA]_0 = 0.101$ mol dm^{-3} $pH_0 = 11.38$

Time/ hour	$[MIPA]_F$/ mol dm^{-3}	Amino Loss/ μmol g^{-1}
1.3	0.0998	32.1
2	0.100	8.1
4	0.0999	28.7
7.7	0.0997	34.6
12.5	0.0998	34.2
48.5	0.0995	43.8
95	0.0995	43.4

TABLE B.3.30. Adsorption isotherm 27 - constant MIPA concentration, variable electrolyte concentration; dark

TIME = 70.5 hours T = 25°C AGITATION = 33 rpm
$[MIPA]_0 = 0.1007$ mol dm^{-3} $[MIPA^+]_0 = 1.86 \times 10^{-3}$ mol dm^{-3}

[LiCL]/ mol dm^{-3}	Ionic Strength/ mol dm^{-3}	$[MIPA]_F$/ mol dm^{-3}	$[MIPA^+]_F$/ mol dm^{-3}	Amino Loss/ μmol g^{-1}
0.00142	0.00310	0.1006	0.00308	4.0
0.00212	0.00380	0.0999	0.00280	30.7
0.00425	0.00593	0.0994	0.00251	52.6
0.00991	0.0116	0.1003	0.00336	15.9
0.0153	0.0170	0.1003	0.00336	15.9
0.0210	0.0227	0.0996	0.00276	43.1
0.0800	0.0817	0.1000	0.00348	27.0
0.142	0.144	0.1006	0.00387	3.9

TABLE B.3.31. Adsorption isotherm 28 - variable MIPA concentration, fixed pH; dark

TIME = 4.3 days T = 25°C AGITATION = 33 rpm

$[MIPA]_0$/ mol dm^{-3}	pH_0	$[MIPA]_F$/ mol dm^{-3}	Amino Loss/ μmol g^{-1}
0.101×10^{-3}	11.00	0.107×10^{-3}	-
0.402×10^{-3}	11.01	0.388×10^{-3}	0.6
0.604×10^{-3}	11.00	0.555×10^{-3}	2.0
1.01×10^{-3}	11.00	0.876×10^{-3}	5.1
2.01×10^{-3}	11.01	1.89×10^{-3}	4.8
3.02×10^{-3}	11.01	2.82×10^{-3}	7.8
4.02×10^{-3}	10.99	3.74×10^{-3}	11.4
5.03×10^{-3}	10.99	4.69×10^{-3}	13.6

TABLE B.3.32. Adsorption isotherm 29 - constant MIPA concentration, variable electrolyte concentration; dark

TIME = 4.3 days T = 25°C AGITATION = 33 rpm
$[MIPA]_0 = 4.98 \times 10^{-3}$ mol dm^{-3} $pH_0 = 10.95$

$[KNO_3]$/ mol dm^{-3}	Ionic Strength/ mol dm^{-3}	$[MIPA]_F$/ mol dm^{-3}	Amino Loss/ μmol g^{-1}
-	0.37×10^{-3}	4.63×10^{-3}	14
0.00227	0.00264	4.83×10^{-3}	5.9
0.00465	0.00502	4.89×10^{-3}	3.5
0.0163	0.0167	4.87×10^{-3}	4.3
0.0260	0.0264	4.94×10^{-3}	1.6
0.0451	0.0455	4.92×10^{-3}	2.4
0.0680	0.0684	5.00×10^{-3}	0
0.103	0.103	4.89×10^{-3}	3.5

TABLE B.3.33. Adsorption isotherm 30 - constant MIPA concentration, variable pH, constant ionic strength; dark

TIME = 2.75 days T = 25°C AGITATION = 33 rpm
$[MIPA]_0 = 8.05 \times 10^{-3}$ mol dm^{-3}

pH_0	$[KNO_3]$/ mol dm^{-3}	$[MIPA^+]_0$/ mol dm^{-3}	Ionic Strength/ mol dm^{-3}	$[MIPA]_F$/ mol dm^{-3}	Amino Loss/ μmol g^{-1}
10.80	0.00800	6.7×10^{-4}	0.00867	0.00793	4.8
10.10	0.00616	0.00192	0.00875	0.00793	4.8
9.86	0.00522	0.00289	0.00878	0.00771	13.8
9.62	0.00408	0.00404	0.00879	0.00784	8.2
9.45	0.00332	0.00482	0.00881	0.00768	14.6
9.20	0.00238	0.00578	0.00883	0.00763	16.9
8.16	0.00048	0.00771	0.00886	0.00769	14.4
3.80	-	0.00818	0.00885	0.00801	1.6

TABLE B.3.34. Adsorption isotherm 31 - constant MIPA concentration, variable electrolyte concentration; dark

TIME = 2.6 days T = 25°C AGITATION = 33 rpm
$[MIPA]_0 = 5.03 \times 10^{-3}$ mol dm^{-3} $pH_0 = 10.75$

[LiCL]/ mol dm^{-3}	Ionic Strength/ mol dm^{-3}	$[MIPA]_F$/ mol dm^{-3}	Amino Loss/ μmol g^{-1}
0.00401	0.00439	5.04×10^{-3}	0
0.00755	0.00793	5.08×10^{-3}	0
0.0139	0.0143	4.96×10^{-3}	2.9
0.0276	0.0280	5.02×10^{-3}	0.4

TABLE B.3.35. Adsorption isotherm 32 - variable SDS concentration, pH 3.4, low ionic strength (25°C)

TIME = 6.5 days AGITATION = 104 rpm (4 days) + 33 rpm ($2^1/_2$ days)
$[KNO_3]$ = 0.00103 mol dm^{-3}

pH_0	$[SDS]_0$/ mol dm^{-3}	$[SDS]_F$/ mol dm^{-3}	Amount Adsorbed/ μmol g^{-1}
3.38	5.98×10^{-3}	5.43×10^{-3}	27.5
3.41	7.96×10^{-3}	7.26×10^{-3}	37.1
3.40	9.94×10^{-3}	9.19×10^{-3}	37.8
3.31	20.05×10^{-3}	19.19×10^{-3}	43.2
3.43	39.06×10^{-3}	37.84×10^{-3}	60.2

TABLE B.3.36. Adsorption isotherm 33 - variable SDS concentration, pH 3.4, high ionic strength (25°C)

TIME = 4 days AGITATION = 33 rpm $[NaNO_3]$ = 0.100 mol dm^{-3}

pH_0	$[SDS]_0$/ mol dm^{-3}	$[SDS]_F$/ mol dm^{-3}	Amount Adsorbed/ μmol g^{-1}
3.40	0.974×10^{-3}	0.821×10^{-3}	7.8
3.39	1.46×10^{-3}	1.11×10^{-3}	17.4
3.40	1.96×10^{-3}	1.39×10^{-3}	29.6
3.40	2.86×10^{-3}	2.29×10^{-3}	28.6
3.41	3.90×10^{-3}	3.27×10^{-3}	30.9
3.38	4.65×10^{-3}	3.89×10^{-3}	38.2
3.40	5.84×10^{-3}	5.19×10^{-3}	33.6
3.38	6.89×10^{-3}	6.18×10^{-3}	34.4
3.38	7.81×10^{-3}	7.03×10^{-3}	38.9
3.38	9.24×10^{-3}	8.46×10^{-3}	39.9
3.41	9.66×10^{-3}	8.82×10^{-3}	41.8
3.40	11.50×10^{-3}	10.61×10^{-3}	43.4
3.39	19.43×10^{-3}	18.37×10^{-3}	52.2
3.40	23.15×10^{-3}	22.07×10^{-3}	55.4
3.41	28.48×10^{-3}	27.28×10^{-3}	59.0
3.32	38.04×10^{-3}	36.71×10^{-3}	67.8

TABLE B.4.2. Dispersibility of rutile as a function of MIPA concentration (18°C)

AGITATION = 15 rpm NO. INVERSIONS = 1650

[MIPA]/ mol dm^{-3}	pH	Time Standing/ mins	NUM No. per g $x10^{-12}$	R g MIPA per g TiO_2
0	11.61	17	0.563	0
0	2.70	35	-	0
0.036	11.00	3	1.68	8.72
0.045	11.06	8	1.88	10.6
0.072	11.11	12	2.14	20.8
0.090	11.20	22	1.65	24.1
0.18	11.32	27	1.72	54.1
0.90	11.72	33	2.05	150

TABLE B.4.3. NO. INVERSIONS = 4200

[MIPA]/ mol dm^{-3}	pH	NUM $x10^{-12}$	R
0	11.82	0.497	0
0	2.76	-	0
0.036	11.00	2.73	10.8
0.045	11.06	2.28	14.7
0.072	11.11	2.30	19.3
0.090	11.20	2.49	27.0
0.18	11.32	1.97	52.0
0.90	11.72	2.28	270

TABLE B.4.4. Maximum dispersion of rutile by ultrasonics (17°C)

NO. INVERSIONS = 6000

[MIPA]/ mol dm^{-3}	pH	NUM $x10^{-12}$	R
-	11.55	5.04	0
-	11.55	3.30	0
0.90	11.7	5.98	845
0.90	11.7	4.44	751

TABLE B.4.5. Effect of rutile mass used

[MIPA] = 0.1 mol dm^{-3} NO. INVERSIONS = 1800

Rutile mass/g	0.0004	0.0041	0.0103	0.0985
NUM $x10^{-12}$	4.35	2.12	1.79	3.02
R	188	18.3	7.29	0.76

TABLE B.4.6. Dispersibility in distilled water as a function of pH

NO. INVERSIONS = 2700

pH	NUM $x10^{-11}$
5.75	<0.07 (aggs)
6.85	<0.3 (aggs)
8.8	<0.3 (aggs)
9.44	<0.4 (aggs)
9.70	1.06 (aggs)
10.15	4.69
10.3	2.03
10.74	4.46
10.92	8.83
11.15	1.21 (aggs)
11.68	8.19
11.93	11.0
12.20	8.80
12.68	0.99

TABLE B.4.7. Effect of electrolyte concentration on the dispersibility of rutile in distilled water of various pH

NO. INVERSIONS = 2700 T = 25°C

pH	$[KNO_3]$/ mol dm^{-3}	NUM $x10^{-11}$	pH	$[KNO_3]$/ mol dm^{-3}	NUM $x10^{-11}$
11.41	0	13.0	10.96	0	17.8
	0.00297	9.97		0.00465	11.0
	0.00485	8.91		0.00880	7.94
	0.00870	7.48		0.0159	4.98
	0.0141	6.54			
	0.0170	4.03	10.64	0	11.2
	0.0216	2.03		0.00346	7.61
	0.0280	0.97		0.00940	4.97
				0.0167	2.20
11.39	0.0110	6.28			
	0.0141	4.79	10.20	0	2.01
	0.0185	3.43		0.00208	4.68
	0.0249	0.88		0.00504	4.83
				0.00851	2.73
9.63	0	0.162		0.0144	0.202
	0.00396	<0.1		0.0175	0.301
	0.00860	<<0.1		0.0236	0.184
	0.0164	<<0.1		0.0252	0.184
3.14	0	0.091			
	0.00445	<<0.01			
	0.00702	<<0.01			
	0.0177	<<0.01			

TABLE B.4.8. Effect of electrolyte concentration on the dispersibility of rutile in aqueous MIPA solutions of equilibrium pH (25°C)

NO. INVERSIONS = 2700

[MIPA]/ mol dm^{-3}	[KNO_3]/ mol dm^{-3}	NUM $x10^{-11}$	R	[MIPA]/ mol dm^{-3}	[KNO_3]/ mol dm^{-3}	NUM $x10^{-11}$	R
0.001	0.00138	9.45	0.072	0.005	0.00109	16.5	0.34
	0.00257	6.15	0.078		0.00178	16.6	0.38
	0.00356	4.30	0.076		0.00376	13.3	0.38
	0.00722	3.60	0.072		0.00851	10.1	0.35
	0.0120	1.82	0.072		0.0115	7.00	0.36
	0.0156	1.18	0.074		0.0153	4.40	0.32
	0.0198	0.687	0.076		0.0170	1.96	0.36
	0.0247	0.636	0.072		0.0233	1.53	0.38
0.010	0.00069	21.3	0.77	0.010*	0	34.4	0.099
	0.00247	17.4	0.75		0.0049	27.6	0.101
	0.00356	17.3	0.79		0.0078	15.2	0.090
	0.00841	12.9	0.78		0.0099	19.1	0.082
	0.0130	8.70	0.78				
	0.0148	7.97	0.71	0.100*	0.0051	32.3	1.08
	0.0191	3.16	0.75		0.0087	26.7	0.99
	0.0238	2.10	0.77		0.0495	0.324	0.76
					0.104	0.0537	1.00
0.0199	0.00109	17.0	1.57				
	0.00158	15.4	1.28				
	0.00336	13.5	1.45				
	0.00752	11.4	1.33				
	0.0118	11.7	1.44				
	0.0150	6.86	1.53				
	0.0194	3.88	1.56				
	0.0227	5.44	1.38				

* Dispersions allowed to settle for 10 mins before particle count.

TABLE B.4.9. Effect of conjugate acid content on the dispersing power of MIPA solutions (25°C)

NO. INVERSIONS = 2520 10 min settling
[$MIPA^+$] = 0.019 mol dm^{-3}

[MIPA]/ mol dm^{-3}	pH	$\frac{[MIPA^+]}{[MIPA]}$	NUM $x10^{-11}$	R
0.020	8.09	0.97	0.074	0.19
0.030	9.45	0.64	17.1	0.26
0.040	9.74	0.48	19.4	0.38
0.050	9.90	0.39	17.8	0.51
0.060	10.0	0.32	17.0	0.65
0.070	10.1	0.28	18.1	0.69
0.090	10.25	0.21	20.4	0.66

TABLE B.4.10. Effect of solution pH on the dispersing power of MIPA (25°C)

NO. INVERSIONS = 2700 [MIPA] = 0.0199 mol dm^{-3}

pH	$[MIPA^+]$/ mol dm^{-3}	NUM $x10^{-11}$	R
10.77	0.00096	26.9	1.45
10.59	0.00193	25.6	1.53
10.25	0.00385	21.6	1.42
9.86	0.00770	19.6	1.66
9.56	0.0116	14.4	1.56
9.15	0.0154	8.56	1.51
8.20	0.0192	<0.4	1.53
2.55	0.0231	<0.1	1.44

TABLE B.4.11. Effect of solution pH on the dispersing power of MIPA at constant ionic strength (25°C)

NO. INVERSIONS = 2700 [MIPA] = 0.010 mol dm^{-3}

$[KNO_3]$/ mol dm^{-3}	$[MIPA^+]$/ mol dm^{-3}	pH	Ionic Strength/ mol dm^{-3}	NUM $x10^{-11}$
0.00962	0.00038	10.67	0.0100	16.9
0.00924	0.00076	10.51	0.0100	16.8
0.00849	0.00151	10.29	0.0100	15.8
0.00735	0.00265	10.01	0.0100	16.0
0.00622	0.00378	9.80	0.0100	14.7
0.00432	0.00568	9.50	0.0100	12.9
0.00243	0.00757	9.10	0.0100	10.8
0.00054	0.00946	8.10	0.0100	<0.01

TABLE B.4.12. Effect of electrolyte type on the dispersing power of a MIPA solution (25°C)

NO. INVERSIONS = 2700 [MIPA] = 0.10 mol dm^{-3}

Electrolyte	[SALT]/ mol dm^{-3}	Ionic Strength/ mol dm^{-3}	NUM $x10^{-11}$
Barium Nitrate	0.00536	0.0178	-
	0.0156	0.0485	-
Lithium Chloride	0.00519	0.00687	8.72
	0.0165	0.0182	6.17
Potassium Sulphate	0.00528	0.0175	16.9
	0.0159	0.0494	0.599
Potassium Nitrate	0.00495	0.00663	14.2
	0.0164	0.0181	8.73

TABLE B.4.13. Effect of $Ba(NO_3)_2$ concentration of the dispersing power of an aqueous MIPA solution (25°C)

NO. INVERSIONS = 2700 [MIPA] = 0.020 mol dm^{-3}

[SALT]/ mol dm^{-3}	NUM $x10^{-11}$	R
0.00011	<0.4	1.49
0.00042	<0.3	1.55
0.00115	<0.3	1.37
0.00310	<0.3	1.21

TABLE B.4.14. Effect of LiCL concentration on the dispersing power of MIPA solutions (25°C)

NO. INVERSIONS = 2700

[MIPA]/ mol dm^{-3}	[SALT]/ mol dm^{-3}	NUM $x10^{-11}$	R
0.00499	0	29.3	0.37
pH = 10.78	0.00259	23.0	0.38
	0.00425	25.8	0.40
	0.0123	16.1	0.36
	0.0158	17.0	0.35
	0.0189	8.12	0.34
	0.0245	0.924	0.37
	0.0403	0.0711	0.30
0.020	0	47.8	1.34
pH = 11.12	0.00472	37.9	1.18
	0.00778	28.6	1.34
	0.00920	24.4	1.34
	0.0160	16.5	1.38
	0.0184	9.06	1.38
	0.0302	1.11	1.10
	0.0502	<<0.1	1.42

TABLE B.4.15. Effect of pH and salt concentration on the dispersing power of MIPA solution (25°C)

NO. INVERSIONS = 2700 [MIPA] = 0.0202 mol dm^{-3}

$[MIPA^+]$/ pH	$[KNO_3]$/ mol dm^{-3}	NUM $x10^{-11}$	R	$[MIPA^+]$/ pH	$[KNO_3]$/ mol dm^{-3}	NUM $x10^{-11}$	R
~0	0	27.7	1.55	0.00075	0	30.2	1.50
11.28	0.00129	25.1	1.49	11.08	0.00267	21.5	1.42
	0.00366	19.4	1.37		0.00524	21.2	1.56
	0.00821	20.4	1.50		0.00959	21.9	1.15
	0.0127	16.7	1.55		0.0146	17.3	1.58
	0.0156	14.7	1.45		0.0188	13.7	1.47
	0.0218	10.7	1.43		0.0236	12.5	1.52
	0.0271	4.92	1.55		0.0274	8.82	1.17
0.00075	0	31.2	1.46	0.00096	0	29.6	1.61
11.03	0.00287	25.4	1.26	10.79	0.00227	25.9	1.58
	0.00504	24.9	1.63		0.00534	21.0	1.52
	0.00890	19.8	1.32		0.00940	19.3	1.60
	0.0140	18.7	1.63		0.0130	17.0	1.53
	0.0181	14.5	1.46		0.0187	14.5	1.42
	0.0217	10.9	1.63		0.0224	11.3	1.53
	0.0263	8.02	1.53		0.0264	6.60	1.55
0.00193	0	31.1	1.53	0.00193	0	26.2	1.56
10.55	0.00188	23.3	1.55	10.53	0.00267	21.6	1.49
	0.00603	21.0	1.56		0.00316	22.2	1.53
	0.0104	23.1	1.39		0.00722	19.8	1.71
	0.0150	17.9	1.38		0.00880	18.5	1.60
	0.0190	15.4	1.47		0.0134	16.1	1.36
	0.0230	11.3	1.38		0.0194	14.9	1.56
	0.0273	6.07	1.50		0.0238	6.84	1.30

TABLE B.4.15. Effect of pH and salt concentration on the dispersing power of MIPA solution (25°C)

NO. INVERSIONS = 2700 [MIPA] = 0.0202 mol dm^{-3}

$[MIPA^+]$/ pH	$[KNO_3]$/ mol dm^{-3}	NUM $x10^{-11}$	R	$[MIPA^+]$/ pH	$[KNO_3]$/ mol dm^{-3}	NUM $x10^{-11}$	R
0.00385	0.00201	24.2	1.39	0.00674	0	26.4	1.60
10.27	0.00402	23.0	1.45	9.95	0.00277	21.3	1.55
	0.00804	19.9	1.37		0.00643	18.7	1.33
	0.0111	19.4	1.60		0.0105	18.1	1.61
	0.0141	14.7	1.42		0.0141	14.0	1.52
	0.0181	9.14	1.43		0.0191	11.3	1.55
	0.0221	5.90	1.34		0.0217	8.03	1.18
	0.0261	0.840	1.61		0.0281	1.71	1.55
0.00963	0	20.8	1.42	0.00963	0	29.1	1.45
9.74	0.00158	16.6	1.31	9.71	0.00297	19.1	1.60
	0.00336	14.6	1.53		0.00504	16.8	1.61
	0.00495	14.2	1.17		0.00979	15.3	1.61
	0.0105	13.8	1.53		0.0137	11.5	1.10
	0.0132	10.6	1.63		0.0185	4.39	1.50
	0.0212	6.02	1.49		0.0230	1.03	1.55
	0.0271	0.747	1.01		0.0271	0.47	1.50
0.0106	0	24.8	1.52	0.0192	0	0.574	1.43
9.65	0.00218	19.6	1.38	8.24	0.00227	0.464	1.55
	0.00425	16.4	1.58		0.00445	0.300	1.32
	0.00949	15.8	1.49		0.00544	0.224	1.55
	0.0152	8.28	1.49				
	0.0193	2.61	1.16				
	0.0237	0.742	1.42				
	0.0270	0.367	1.58				

TABLE B.4.16. Effect of pH and salt concentration on the dispersing power of MIPA solution (25°C)

NO. INVERSIONS = 2700 [MIPA] = 5.04×10^{-3} mol dm^{-3}

$[MIPA^+]$/ pH	$[KNO_3]$/ mol dm^{-3}	NUM $\times 10^{-11}$	R	$[MIPA^+]$/ pH	$[KNO_3]$/ mol dm^{-3}	NUM $\times 10^{-11}$	R
0.00038	0	30.3	0.38	0.00096	0	37.0	0.38
10.76	0.00227	21.7	0.35	10.25	0.00227	23.3	0.39
	0.00564	16.1	0.38		0.00524	19.7	0.38
	0.00940	12.7	0.38		0.00949	15.6	0.34
	0.0144	9.86	0.36		0.0151	11.9	0.38
	0.0186	5.90	0.29		0.0180	6.93	0.32
	0.0230	4.52	0.28		0.0249	2.22	0.37
	0.0274	1.56	0.37		0.0293	0.581	0.34
0.00193	0	25.1	0.36	0.00289	0	23.8	0.37
9.88	0.00227	23.2	0.26	9.51	0.00207	19.4	0.35
	0.00455	15.8	0.36		0.00445	16.7	0.35
	0.00989	11.6	0.36		0.00920	9.51	0.36
	0.0144	7.65	0.27		0.0156	6.21	0.40
	0.0186	5.02	0.35		0.0196	2.13	0.31
	0.0228	1.20	0.26		0.0239	0.622	0.36
	0.0284	0.447	0.36		0.0275	0.210	0.34
0.00385	0	22.6	0.37	0.00385	0	14.5	0.31
9.16	0.00247	15.8	0.38	9.15	0.00237	10.4	0.38
	0.00514	13.1	0.38		0.00326	10.6	0.29
	0.01038	5.93	0.39		0.00653	5.15	0.37
	0.0141	2.19	0.40		0.0107	3.36	0.37
	0.0193	0.833	0.30		0.0128	1.59	0.36
	0.0236	0.303	0.39		0.0171	0.479	0.27
	0.0281	0.107	0.37		0.0215	0.355	0.42

TABLE B.4.17. Effect of MIPA concentration at a fixed pH on the degree of dispersion of rutile (25°C)

NO. INVERSIONS = 2700 pH = 11.4

[MIPA]/ mol dm^{-3}	pH	NUM $x10^{-11}$	R
$2.0x10^{-5}$	11.40	12.8	0.0015
$2.0x10^{-4}$	11.39	14.1	0.014
$8.0x10^{-4}$	11.40	15.0	0.061
$4.0x10^{-3}$	11.40	16.8	0.30
0.010	11.40	24.4	0.75
0.020	11.40	27.9	1.58
0.050	11.39	29.9	3.58
0.100	11.38	30.4	7.44

TABLE B.4.18. Effect of electrolyte concentration on the dispersing power of MIPA at high pH (25°C)

NO. INVERSIONS = 2700

[MIPA]/ mol dm^{-3}	pH	$[KNO_3]$/ mol dm^{-3}	NUM $x10^{-11}$	R
$2x10^{-5}$	11.26	0	15.8	0.0013
		0.00475	11.5	0.0016
		0.00969	5.90	0.0014
		0.0158	3.38	0.0013
$9.98x10^{-5}$	11.20	0	15.4	0.0067
		0.00386	12.3	0.0075
		0.0102	5.77	0.0062
		0.0172	3.39	0.0074

TABLE B.4.19. Effect of electrolyte concentration on the dispersing power of low MIPA concentration solutions at equilibrium pH (25°C)

NO. INVERSIONS = 2700

[MIPA]/ pH	$[KNO_3]$/ mol dm^{-3}	NUM $x10^{-11}$	R	[MIPA]/ pH	$[KNO_3]$/ mol dm^{-3}	NUM $x10^{-11}$	R
$9.98x10^{-4}$	0	26.0	0.071	$5.99x10^{-4}$	0	27.3	0.048
10.36	0.00425	12.5	0.073	10.24	0.00405	8.27	0.040
	0.00870	6.06	0.073		0.00969	3.92	0.042
	0.0152	3.05	0.070		0.0161	2.22	0.038
$3.99x10^{-4}$	0	22.4	0.030	$2.00x10^{-4}$	0	17.4	0.015
10.10	0.00465	5.93	0.028	9.86	0.00405	4.57	0.014
	0.0102	2.78	0.028		0.01038	1.42	0.014
	0.0170	1.15	0.031		0.0159	1.08	0.013
$9.98x10^{-5}$	0	11.1	0.0073	$2.00x10^{-5}$	0	0.0143	0.0014
9.73	0.00435	2.93	0.0064	8.4	0.00415	<0.1	0.0014
	0.00890	0.843	0.0078		0.00969	<0.1	0.0015
	0.0150	0.367	0.0053		0.0137	<0.1	0.0013

TABLE B.4.20. Effect of a constant conjugate acid to MIPA concentration ratio on the dispersing power (25°C)

NO. INVERSIONS = 2700

[MIPA]/ mol dm^{-3}	$[MIPA^+]$/ mol dm^{-3}	pH	$\frac{[MIPA^+]}{[MIPA]}$	NUM $x10^{-11}$	$[KNO_3]$/ mol dm^{-3}	NUM $x10^{-11}$
$9.98x10^{-5}$	$1.93x10^{-5}$	9.39	0.193	6.35	0.0105	0.49
$9.98x10^{-4}$	$1.93x10^{-4}$	10.01	0.193	30.7	0.0103	5.28
$9.98x10^{-3}$	$1.93x10^{-3}$	10.21	0.193	37.7	0.00969	18.1
0.0499	$9.63x10^{-3}$	10.28	0.193	48.4	0.0107	24.6
$9.98x10^{-5}$	$3.85x10^{-5}$	9.05	0.386	1.46	0.0101	<<0.1
$9.98x10^{-4}$	$3.85x10^{-4}$	9.70	0.386	24.8	0.00930	3.98
$9.98x10^{-3}$	$3.85x10^{-3}$	9.84	0.386	29.5	0.00969	18.1
0.0499	0.0193	9.86	0.386	33.3	0.0104	8.46
$9.98x10^{-5}$	$5.78x10^{-5}$	8.6	0.578	0.466	0.0141	<0.1
$9.98x10^{-4}$	$5.78x10^{-4}$	9.32	0.578	23.5	0.0142	2.33
$9.98x10^{-3}$	$5.78x10^{-3}$	9.43	0.578	33.1	0.0148	9.15
0.0499	0.0289	9.46	0.578	20.3	0.0140	2.76
$9.98x10^{-5}$	0	11.29	0	14.2	0.0148	4.99
$9.98x10^{-4}$	0	11.29	0	33.3	0.0142	8.15
$9.98x10^{-3}$	0	11.28	0	43.5	0.0149	13.6
0.0499	0	11.36	0	60.1	0.0140	38.2

TABLE B.4.21. Effect of the % water content of the MIPA solution on the dispersing power (25°C)

[MIPA] = 0.0190 mol dm^{-3}

% water (v/v)	0	30	50	80
water mole fraction	0	0.64	0.80	0.94
NUM $x10^{-11}$	<0.3	<0.5	5.29	18.4

TABLE B.4.22. The dispersibility of rutile in aqueous mixtures of aminopropane and isopropanol (25°C)

NO. INVERSIONS = 2250

[Amine]/ mol dm^{-3}	[Alcohol]/ mol dm^{-3}	Mole Fraction of Amine	NUM $x10^{-11}$
0	0.262	0	-
0.0242	0.236	0.093	19.2
0.0484	0.210	0.187	16.7
0.0726	0.183	0.284	16.7
0.0968	0.157	0.381	14.3
0.121	0.131	0.480	14.7
0.145	0.105	0.580	14.0
0.169	0.0786	0.683	15.8
0.242	0	1	19.0
	NO. INVERSIONS = 2700		
0	0.262	0	-
0.0242	0.236	0.093	39.3
0.0484	0.210	0.187	29.4
0.0726	0.183	0.284	30.0
0.145	0.105	0.580	29.8
0.194	0.0524	0.787	33.0
0.218	0.0262	0.893	38.4
0.242	0	1	37.0

TABLE B.4.23. The effect of aqueous AMP on the dispersion of rutile (25°C)

NO. INVERSIONS = 2700

[AMP]/ mol dm^{-3}	pH	[KNO_3]/ mol dm^{-3}	NUM $x10^{-11}$	R
0.020	11.03	0.00099	17.4	1.78
		0.00188	14.5	1.68
		0.00425	12.9	1.63
		0.00742	13.0	1.76
		0.0122	11.4	1.65
		0.0152	11.2	1.47
		0.0189	6.19	1.60
		0.0228	7.29	1.50
0.0259	11.20	0	53.3	2.18
		0.00564	32.8	1.97
		0.00732	29.0	2.35
		0.0101	27.6	1.88
		0.0137	23.5	2.28
		0.0171	32.7	2.43
		0.0204	14.5	2.22
		0	36.4	2.14
$4.9x10^{-5}$	11.40	0	12.1	0.0045
$9.79x10^{-4}$	11.40	0	15.1	0.089
$3.92x10^{-3}$	11.39	0	22.5	0.35
0.0196	11.40	0	26.8	1.84

TABLE B.4.24. The effect of aqueous TEA on the dispersion of rutile (25°C)

NO. INVERSIONS = 2700

[TEA]/ mol dm^{-3}	pH	[KNO_3]/ mol dm^{-3}	NUM $x10^{-11}$
0.0204	10.42	0	35.4
		0.00574	23.7
		0.00880	18.9
		0.0109	21.7
		0.0134	13.6
		0.0178	9.71
		0.0206	5.86
		0	29.2
$5.26x10^{-5}$	11.41	0	10.7
$1.05x10^{-3}$	11.41	0	14.7
$2.10x10^{-3}$	11.40	0	16.9
0.0210	11.41	0	22.1

TIME OF DISPERSION STUDIES

TABLE B.4.25. Effect of the number of sample inversions on the number of rutile primary particles dispersed as a function of electrolyte (25°C)

Solution	Number Inversions	Log_{10} NI	NUM $x10^{-11}$	Solution	Number Inversions	Log_{10} NI	NUM $x10^{-11}$
water	10	1.00	0.434	10 mM	390	2.59	0.779
pH 11.10	210	2.32	1.80	KNO_3	750	2.88	1.23
	480	2.68	4.67	pH 10.93	1200	3.08	1.48
	660	2.82	3.94		2100	3.32	1.82
	900	2.95	6.78		2700	3.43	4.05
	2850	3.45	9.43		3600	3.56	4.28
10 mM	450	2.65	1.59	10.2 mM	420	2.62	1.06
LiCL	900	2.95	1.37	NaF	1110	3.05	1.38
pH 10.99	1350	3.13	1.53	pH 10.83	1800	3.26	2.10
	1800	3.26	1.88		2640	3.42	4.07
	4500	3.65	9.08		3900	3.59	6.90
	7500	3.88	12.3		6180	3.79	7.65

TABLE B.4.26. Effect of number of inversions on the dispersion of rutile in aqueous MIPA solution

[MIPA]/ mol dm^{-3}	pH	Number Inversions	Log_{10} NI	NUM $x10^{-11}$
0.0100	10.81	3.5	0.54	10.8
		6	0.78	12.3
		7.5	0.88	14.2
		10	1.00	17.6
		20	1.30	17.4
		600	2.78	21.7
		1200	3.08	21.0
		2400	3.38	22.5

TABLE B.4.27. Effect of number of inversions on the dispersion of rutile in aqueous MIPA-KNO_3 solution (25°C)

[MIPA] [KNO_3]/ mol dm^{-3}	NI	Log_{10} NI	NUM $x10^{-11}$	[MIPA] [KNO_3]/ mol dm^{-3}	NI	Log_{10} NI	NUM $x10^{-11}$
0.0091	150	2.18	5.30	0.010	3	0.48	1.96
0.0092	300	2.48	11.2	0.00992	90	1.95	2.76
pH 10.7	600	2.78	7.67	pH 10.90	270	2.43	4.91
	1350	3.13	11.0		450	2.65	7.05
	2100	3.32	16.4		750	2.88	11.1
					2250	3.35	16.0
0.010	450	2.65	1.25				
0.0152	900	2.95	1.50	0.020	5	0.70	2.63
pH 10.89	1500	3.18	1.38	0.0100	15	1.18	4.55
	2880	3.46	6.78	pH 11.11	60	1.78	5.66
	4110	3.61	8.02		450	2.65	9.75
	5490	3.74	10.9		900	2.95	16.3
					1800	3.26	10.9
0.050	7.5	0.88	2.37		2700	3.43	18.2
0.0253	30	1.48	5.10		3600	3.56	21.2
pH 11.30	150	2.18	9.20	0.050	60	1.78	1.07
	690	2.84	9.61	0.0251	150	2.18	0.709
	1350	3.13	13.2	pH 11.3	510	2.71	0.951
	2340	3.37	13.9		1470	3.17	0.795
	3000	3.48	17.7				
	3900	3.59	17.2				
0.050	15	1.18	5.24				
0.0251	60	1.78	9.28				
pH 11.32	300	2.48	11.2				
	1200	3.08	16.6				
	1500	3.18	0.772*				
	2220	3.35	17.2				

* Rutile powder moistened with distilled water prior to addition of dispersing solution.

TABLE B.4.28. Effect of number of inversions on the dispersion of rutile in aqueous MIPA-LiCL solution (25°C)

[MIPA] [LiCL]/ mol dm^{-3}	NI	Log_{10} NI	NUM $x10^{-11}$	[MIPA] [LiCL]/ mol dm^{-3}	NI	Log_{10} NI	NUM $x10^{-11}$
0.010	3	0.48	2.41	0.010	10	1.00	1.85
0.0101	90	1.95	5.92	0.0157	90	1.95	3.28
pH 10.9	240	2.38	8.97	pH 10.89	240	2.38	1.35
	360	2.56	10.6		600	2.78	3.47
	755	2.88	13.0		1530	3.18	7.67
	2250	3.35	19.5		2820	3.45	10.1
0.010	30	1.48	1.45	0.010	5	0.70	2.00
0.0148	150	2.18	1.55	0.0100	60	1.78	4.21
pH 10.85	480	2.68	1.50	pH 10.85	450	2.65	7.04
	960	2.98	2.26		810	2.91	8.39
	1500	3.18	7.55		1530	3.18	8.40
	2100	3.32	8.15		3180	3.50	14.1
	3300	3.52	10.1				
	5400	3.73	14.1				
0.020	5	0.70	5.35	0.050	15	1.18	2.50
0.0100	30	1.48	11.4	0.0251	30	1.48	4.12
pH 11.10	240	2.38	14.0	pH 11.30	135	2.13	1.26
	630	2.80	16.7		450	2.65	0.805
	1200	3.08	20.8		1050	3.02	0.818
	2250	3.35	17.1		1800	3.26	0.727
	2760	3.44	20.6		2400	3.38	0.757
	3600	3.56	20.9		3780	3.58	0.656
0.050	19	1.28	2.50	0.050	14	1.15	4.24
0.0253	60	1.78	1.61	0.0249	30	1.48	3.70
pH 11.30	270	2.43	0.721	pH 11.30	90	1.95	1.04
	660	2.82	0.674		270	2.43	0.649
					900	2.95	0.656
					1800	3.26	0.754

TABLE B.4.29. Effect of number of inversions on the dispersion of rutile in aqueous MIPA-NaF solution (25°C)

[MIPA] [NaF]/ mol dm^{-3}	NI	Log_{10} NI	NUM $x10^{-11}$	[MIPA] [NaF]/ mol dm^{-3}	NI	Log_{10} NI	NUM $x10^{-11}$
0.010	3.5	0.54	3.12	0.010	60	1.78	1.51
0.00974	15	1.18	6.79	0.0150	180	2.26	7.23
pH 10.85	30	1.48	12.6	pH 10.85	570	2.76	7.50
	90	1.95	9.48		1020	3.01	8.51
	210	2.32	11.9		1350	3.13	11.4
	450	2.65	12.7		2370	3.37	10.4
	1350	3.13	19.2				
	2700	3.43	24.6				
0.050	9	0.95	7.98	0.050	30	1.48	7.90
0.0254	16	1.20	8.75	0.0250	150	2.18	8.50
pH 11.30	45	1.65	11.8	pH 11.28	420	2.62	8.28
	150	2.18	13.8		1950	3.29	15.8
	600	2.78	19.5		2700	3.43	18.4
	1260	3.10	14.6				
	2160	3.33	20.1				
	3480	3.54	23.1				

TABLE B.4.30. Effect of number of inversions on the dispersion of rutile in aqueous MIPA-KCL solution (25°C)

[MIPA] [KCL]/ mol dm^{-3}	NI	Log_{10} NI	NUM $x10^{-11}$	[MIPA] [KCL]/ mol dm^{-3}	NI	Log_{10} NI	NUM $x10^{-11}$
0.010	7.5	0.88	1.29	0.010	90	1.95	1.10
0.0149	90	1.95	2.16	0.0100	600	2.78	2.07
pH 10.85	360	2.56	5.59	pH 10.85	1290	3.11	3.89
	600	2.78	6.95		2100	3.32	6.29
	840	2.92	9.37		3000	3.48	7.42
	2310	3.36	14.4		3600	3.56	8.13

TABLE B.4.31. Effect of number of inversions on the dispersion of rutile in aqueous MIPA-$NaNO_3$ solution (25°C)

[MIPA] = 0.010 mol dm^{-3} [$NaNO_3$] = 0.0100 mol dm^{-3}
pH = 10.84

NI	Log_{10} NI	NUM $x10^{-11}$
15	1.18	1.75
90	1.95	6.23
300	2.48	9.22
630	2.80	10.1
1050	3.02	12.4
1560	3.19	11.7
3600	3.56	17.1

TABLE B.4.32. Effect of number of inversions on the dispersion of rutile in aqueous MIPA-KNO_3-NaF solution (25°C)

[MIPA] = 0.010 mol dm^{-3} pH = 10.85
[KNO_3] = 0.00501 mol dm^{-3} [NaF] = 0.00522 mol dm^{-3}

NI	Log_{10} NI	NUM $x10^{-11}$
180	2.26	1.34
450	2.65	4.80
900	2.95	6.16
1440	3.16	6.57
2280	3.36	8.00
4620	3.66	12.5

TABLE B.5.1. Dynamic viscosity of aqueous MIPA solution as a function of concentration (25°C)

$t(H_2O)$ = 681.15 s

[MIPA]/ mol dm^{-3}	c g per 100 ml	η_r	η_{SP}	η/ centipoise	η_{SP}/c
0.0577	0.434	1.018	0.018	0.9064	0.0415
0.0635	0.477	1.019	0.019	0.9073	0.0398
0.0705	0.530	1.021	0.021	0.9091	0.0396
0.0794	0.597	1.023	0.023	0.9109	0.0385
0.0907	0.681	1.026	0.026	0.9136	0.0382
0.116	0.868	1.030	0.030	0.9171	0.0346
0.126	0.947	1.033	0.033	0.9198	0.0348
0.173	1.302	1.046	0.046	0.9314	0.0353
0.198	1.488	1.053	0.053	0.9376	0.0356
0.578	4.343	1.169	0.169	1.041	0.0389
0.630	4.733	1.186	0.186	1.056	0.0393
0.693	5.207	1.208	0.208	1.076	0.0399
0.756	5.680	1.233	0.233	1.098	0.0410
0.770	5.785	1.234	0.234	1.099	0.0404
0.866	6.506	1.268	0.268	1.129	0.0412
0.907	6.814	1.287	0.287	1.146	0.0421
0.990	7.438	1.314	0.314	1.170	0.0422

TABLE B.5.2. Dynamic viscosity of aqueous MIPA solution as a function of pH (25°C)

$t(H_2O)$ = 681.15 s

[MIPA]/ mol dm^{-3}	pH	η_r	η/ centipoise	$[MIPA^+]$/ mol dm^{-3}
1.44	11.95	1.503	1.338	0.009
1.40	10.12	1.416	1.261	0.430
1.36	9.40	1.332	1.186	0.995
1.32	7.06	1.237	1.101	1.44
1.44	0.91	1.253	1.116	1.44
water	11.90	1.002	0.8922	-
water	1.00	1.000	0.8904	-

TABLE B.5.3. Dependence of reduced viscosity on the selected value for the flow time of distilled water (25°C)

t_1 = 681.15 s t_2 = 683.3 s

[MIPA]/ mol dm^{-3}	c/ g per 100 ml	η_r		η/centipoise		η_{SP}/c	
		t_1	t_2	t_1	t_2	t_1	t_2
0.018	0.1352	1.0095	1.0063	0.8989	0.8960	0.0703	0.0466
0.020	0.1503	1.0087	1.0056	0.8981	0.8954	0.0579	0.0373
0.036	0.2705	1.0128	1.0097	0.9018	0.8990	0.0473	0.0359
0.040	0.3005	1.0151	1.0119	0.9038	0.9010	0.0502	0.0396
0.045	0.3381	1.0154	1.0122	0.9041	0.9013	0.0455	0.0361
0.050	0.3757	1.0184	1.0151	0.9068	0.9038	0.0490	0.0402
0.054	0.4057	1.0175	1.0143	0.9060	0.9031	0.0431	0.0352
0.060	0.4508	1.0203	1.0170	0.9085	0.9055	0.0450	0.0377
0.072	0.5409	1.0237	1.0205	0.9115	0.9087	0.0438	0.0379
0.080	0.6010	1.0260	1.0228	0.9136	0.9107	0.0433	0.0379
0.090	0.6762	1.0279	1.0247	0.9152	0.9124	0.0413	0.0365
0.100	0.7513	1.0308	1.0275	0.9178	0.9149	0.0410	0.0366
0.200	1.5026	1.0582	1.0549	0.9422	0.9393	0.0387	0.0365

TABLE B.5.4. Dynamic viscosity of a MIPA solution as a function of pH at a constant ionic strength (25°C)

[MIPA] = 0.500 mol dm^{-3} IS ~ 1.5 mol dm^{-3}

$t(H_2O)$ = 681.15 s

pH	[MIPA$^+$]/ mol dm^{-3}	[KNO_3]/ mol dm^{-3}	Ionic Strength/ mol dm^{-3}	η_r	η/ centipoise
11.80	0.00375	1.500	1.504	1.0363	0.9227
10.35	0.127	1.372	1.499	1.0305	0.9176
9.90	0.248	1.250	1.498	1.0242	0.9119
8.34	0.477	1.000	1.477	1.0156	0.9043
4.00	0.500	0.861	1.497	1.0117	0.9009
0.34	0.500	0.221	1.493	1.0537	0.9382

TABLE B.5.5. Dynamic viscosity of an aqueous MIPA solution as a function of ionic strength (25°C)

a) [MIPA] = 0.500 mol dm^{-3} pH = equilibrium

$[KNO_3]$/ mol dm^{-3}	Ionic Strength/ mol dm^{-3}	η_r	η/ centipoise
0	0.0038	1.1489	1.0230
0.04973	0.0535	1.1443	1.0189
0.1001	0.1039	1.1386	1.0138
0.5006	0.5044	1.0960	0.9759
1.000	1.0038	1.0595	0.9434
1.500	1.5038	1.0363	0.9227
2.000	2.0038	1.0248	0.9125

b) [MIPA] = 0.500 mol dm^{-3} pH = 9.60
[$MIPA^+$] = 0.255 mol dm^{-3}

$[KNO_3]$/ mol dm^{-3}	Ionic Strength/ mol dm^{-3}	η_r	η/ centipoise
0	0.2552	1.1097	0.9880
0.0502	0.3054	1.1045	0.9834
0.0999	0.3551	1.0986	0.9782
0.4995	0.7547	1.0601	0.9439
0.9998	1.255	1.0313	0.9183
2.000	2.256	1.001	0.8912

c) [MIPA] = 0.500 mol dm^{-3} pH = 1.60

$[KNO_3]$/ mol dm^{-3}	Ionic Strength/ mol dm^{-3}	η_r	η/ centipoise
0	0.5251	1.0792	0.9609
0.0995	0.6246	1.0706	0.9533
0.2499	0.7750	1.0573	0.9414
0.6008	1.126	1.0346	0.9212
1.201	1.726	1.0072	0.8968
2.000	2.525	0.9943	0.8853

TABLE B.5.6. Dynamic viscosity of an aqueous MIPA solution as a function of lithium chloride concentration (25°C)

[MIPA] = 0.500 mol dm^{-3} pH = equilibrium
$t(H_2O)$ = 683.05 s

[LiCL]/ mol dm^{-3}	η_r	η/ centipoise
0.0135	1.1521	1.0258
0.0501	1.1527	1.0264
0.1028	1.1654	1.0376
0.4993	1.2212	1.0874
0.9953	1.2965	1.1544
2.000	1.4679	1.3070

TABLE B.5.7. Dynamic viscosity of an aqueous MIPA solution as a function of ammonium sulphate concentration (25°C)

[MIPA] = 0.500 mol dm^{-3} pH = equilibrium
$t(H_2O)$ = 683.15 s

$[(NH_4)_2SO_4]$/ mol dm^{-3}	η_r	η/ centipoise
0.0102	1.1479	1.0221
0.0498	1.1544	1.0279
0.0998	1.1611	1.0338
0.5030	1.2242	1.0900
1.000	1.3157	1.1715
2.000	1.5864	1.4125

TABLE B.5.8. Dynamic viscosity of aqueous solutions of propylamine as a function of concentration (25°C)

$t(H_2O)$ = 682.45 s

[Amine]/ mol dm^{-3}	c/ g per 100 ml	η_r	η/ centipoise	η_{SP}/c
0.0185	0.1092	1.0083	0.8978	0.0760
0.0361	0.2131	1.0122	0.9013	0.0573
0.0725	0.4280	1.0221	0.9100	0.0516
0.0911	0.5379	1.0254	0.9130	0.0472
0.224	1.322	1.0628	0.9463	0.0475
0.370	2.184	1.1077	0.9863	0.0493
0.459	2.710	1.1336	1.0094	0.0493
0.689	4.068	1.2186	1.0851	0.0537
0.896	5.290	1.3012	1.1586	0.0569

TABLE B.5.9. Dynamic viscosity of an aqueous propylamine solution as a function of ionic strength

[Amine] = 0.591 mol dm^{-3} pH = equilibrium

$[KNO_3]$/ mol dm^{-3}	Ionic Strength/ mol dm^{-3}	η_r	η/ centipoise
0	0.0146	1.1860	1.0560
0.0400	0.0546	1.1838	1.0541
0.1200	0.1346	1.1736	1.0450
0.5203	0.5349	1.1285	1.0048
1.001	1.016	1.0902	0.9707
1.998	2.013	1.0544	0.9389

TABLE B.5.10. Dynamic viscosity of an aqueous propylamine solution at pH 2.5 as a function of ionic strength

[Amine] = 0.597 mol dm^{-3} $t(H_2O)$ = 682.9 s

pH	$[KNO_3]$/ mol dm^{-3}	Ionic Strength/ mol dm^{-3}	η_r	η/ centipoise
2.59	0	0.600	1.0986	0.9782
2.79	0.0400	0.640	1.0945	0.9745
2.56	0.1201	0.720	1.0861	0.9671
2.53	0.5203	1.120	1.0540	0.9385
2.43	0.9993	1.599	1.0291	0.9163
2.42	1.998	2.598	1.0091	0.8985

TABLE B.6.1. Calibration values for the Haake bobs and cups (25°C)

Bob & Cup	Oil Viscosity/ poise	B	K	A
MV I	10.26	1142	0.2897±0.0007	3.308
	41.33		0.2876±0.0008	3.284
MV II	10.26	441	0.8899±0.0039	3.924
	41.33		0.8435±0.0021	3.720
MV III	10.26	216	2.476±0.011	5.348
	41.33		2.487±0.009	5.372
SV I	10.26	441	2.735±0.019	12.06
	41.33		2.660±0.029	11.73
SV II	10.26	441	8.091±0.019	35.68
	41.33		7.795±0.028	34.38

TABLE B.6.2. Rutile slurries studied (25°C)

Slurry	Solids Content % w/w	Initial Milling Time/ min	Initial MIPA Content g per g TiO_2	Additional Additive Content
A	46.5	15	0	MIPA
B	44.0	20	0	MIPA
C	46.0	45	0	MIPA
D	38.6	40	0	MIPA
E	57.6	47	2.66×10^{-4}	MIPA
F	51.0	70	1.70×10^{-4}	MIPA
G	51.5	85	1.60×10^{-4}	MIPA
H	40.3	70	2.50×10^{-4}	$^1/_2$ neutral MIPA
I	43.7	70	2.33×10^{-4}	KNO_3/MIPA = 1.0
J	48.7	72	1.70×10^{-4}	KNO_3/MIPA = 1.0
K	46.0	65	1.36×10^{-4}	KNO_3/MIPA = 1.0
L	50.1	70	1.92×10^{-4}	KNO_3/MIPA = 0.040
M	48.8	70	1.78×10^{-4}	KNO_3/MIPA = 0.080
N	50.7	70	1.86×10^{-4}	KNO_3/MIPA = 0.162
O	47.9	95	1.79×10^{-4}	KNO_3/MIPA = 0.400
P	51.3	70	1.81×10^{-4}	KNO_3/MIPA = 3.20
Q	50.2	75	1.56×10^{-4}	$Ba(NO_3)_2$/MIPA = 0.022
R	44.7	75	0(pH 11.6)	MIPA then KNO_3
S	45.9	60	0(pH 10.7)	MIPA then KNO_3
T	44.5	61	0(pH 11.6)	MIPA then KNO_3
U	44.5	60	0(pH 9.4)	MIPA then KNO_3
V	36.7	60	0(pH 2.5)	MIPA then KNO_3
W	44.1	60	0(pH 4.1)	MIPA then KNO_3
X	Variable	60	0	dist. water pH 11.3
Y	Variable	60	0	dist. water pH 11.3
Z	Variable	60	1.91×10^{-4}	dist. water pH 11.3
AA	Variable	60	1.98×10^{-4}	dist. water pH 11.3
BB	Variable	62	2.32×10^{-4}	dist. water pH 11.3
CC	50.4	63	1.98×10^{-4}	KNO_3
DD	51.0	60	1.69×10^{-4}	MIPA
EE	50.9	65	1.77×10^{-4}	KNO_3/MIPA = 0.080
FF	50.9	61	1.84×10^{-4}	KNO_3/MIPA = 1.0
GG	51.0	63	1.83×10^{-4}	LiCL/MIPA = 1.0

SLURRY: A % w/w TiO_2 = 46.5

(1)			(2)		
γ/ s^{-1}	τ/ dyne cm^{-2}	η/ poise	γ/ s^{-1}	τ/ dyne cm^{-2}	η/ poise
2.722	223.4	82.1	2.722	554.9	204
5.444	312.8	57.5	5.444	659.3	121
8.167	443.5	54.3	8.167	752.0	92.1
16.33	1066	65.2	16.33	969	59.3
24.50	1437	58.7	24.50	1173	47.9
49.0	1650	33.7	49.0	1408	28.7
73.5	1812	24.7	73.5	1525	20.7
147.0	2224	15.1	147.0	1795	12.2
220.5	2482	11.3	220.5	2029	9.2
441	2819	6.4			

(3)					
γ/ s^{-1}	τ/ dyne cm^{-2}	η/ poise	γ/ s^{-1}	τ/ dyne cm^{-2}	η/ poise
7.05	180.6	25.6			
14.10	267.9	19.0			
21.15	320.5	15.2			
42.30	430.0	10.2			
63.44	499.5	7.9			
126.9	641.8	5.1			
190.3	734.4	3.9			
380.7	889.9	2.3			
571.0	992.4	1.7			

Slurry	Bob/Cup	% MIPA w/w
1	SV II	-
2	SV I	0.0116
3	MV I	0.0292

SLURRY: B % w/w TiO_2 = 44.0

(1)			(2)		
γ/ s^{-1}	τ/ dyne cm^{-2}	η/ poise	γ/ s^{-1}	τ/ dyne cm^{-2}	η/ poise
2.722	309.4	113.7	1.33	349.2	262.6
5.444	464.1	85.2	2.67	478.6	179.3
8.167	581.0	71.1	4.0	547.9	137.0
16.33	893.8	54.7	8.0	628.5	78.6
24.5	962.5	39.3	12.0	703.7	58.6
49.0	1110	22.7	24.0	891.8	37.2
73.5	1275	17.3	36.0	1010	28.1
147.0	1547	10.5	72.0	1182	16.4
220.5	1739	7.9	108.0	1273	11.8

(3)			(4)		
γ/ s^{-1}	τ/ dyne cm^{-2}	η/ poise	γ/ s^{-1}	τ/ dyne cm^{-2}	η/ poise

η < 2 poise
drying effect

Slurry	Bob/Cup	% MIPA w/w
1	SV II	0
2	MV III	0.0109
3	NV	0.0279

SLURRY: C % w/w TiO_2 = 46.0

(1)			(2)		
γ/ s^{-1}	τ/ dyne cm^{-2}	η/ poise	γ/ s^{-1}	τ/ dyne cm^{-2}	η/ poise
2.722	343.8	126.3	2.722	579.5	213
5.444	446.9	82.1	5.444	656.9	121
8.167	622.2	76.2	8.167	727.3	89.1
16.33	928.2	56.8	16.33	896.2	54.9
24.5	1169	47.7	24.5	1102	45.0
49.0	1513	30.9	49.0	1425	29.1
73.5	1688	23.0	73.5	1566	21.3
147.0	2038	13.9	147.0	1877	12.8
220.5	2200	10.0	220.5	2076	9.4

(3)			(4)		
γ/ s^{-1}	τ/ dyne cm^{-2}	η/ poise	γ/ s^{-1}	τ/ dyne cm^{-2}	η/ poise
2.7222	391.8	144	1.33	236.4	178
5.444	438.7	80.6	2.67	349.2	131
8.167	525.5	64.3	4.0	429.8	107
16.33	709.7	43.5	8.0	580.2	72.5
24.5	805.9	32.9	12.0	639.3	53.3
49.0	1009	20.6	24.0	703.7	29.3
73.5	1173	16.0	36.0	752.1	20.9
147	1414	9.6	72.0	854.1	11.9
220.5	1525	6.9	108	902.5	8.4

Slurry	Bob/Cup	% MIPA w/w
1	SV II	0
2	SV I	0.00461
3	SVI	0.0121
4	MV III	0.0175
5	MV II	0.0207
6	MV I	0.0251

SLURRY: C % w/w TiO_2 = 46.0

(5)			(6)		
γ/ s^{-1}	τ/ dyne cm^{-2}	η/ poise	γ/ s^{-1}	τ/ dyne cm^{-2}	η/ poise
2.722	184.1	67.6	7.05	148.2	21.0
5.444	311.7	57.3	14.1	203.8	14.5
8.167	363.4	44.5	21.15	257.4	12.2
16.33	450.1	27.6	42.30	352.0	8.3
24.5	517.1	21.1	63.44	425.1	6.7
49.0	625.0	12.8	126.9	565.7	4.5
73.5	677.0	9.2	190.3	661.6	3.5
147	803.5	5.5	380.7	845.2	2.2
220.5	855.6	3.9	571.0	982.5	1.7

SLURRY: D % w/w TiO_2 = 38.6

(1)			(2)		
γ/ s^{-1}	τ/ dyne cm^{-2}	η/ poise	γ/ s^{-1}	τ/ dyne cm^{-2}	η/ poise
1.33	121.9	91.7	2.722	151.0	55.5
2.67	168.1	63.0	5.444	183.0	33.6
4.0	184.8	46.2	8.167	205.3	25.1
8.0	207.9	26.0	16.33	241.4	14.8
12.0	221.3	18.4	24.5	261.9	10.7
24.0	251.4	10.5	49.0	305.0	6.2
36.0	266.5	7.4	73.5	333.3	4.5
72.0	306.2	4.3	147	398	2.7
108	322.3	3.0	220.5	409	1.9

(3)			(4)		
γ/ s^{-1}	τ/ dyne cm^{-2}	η/ poise	γ/ s^{-1}	τ/ dyne cm^{-2}	η/ poise
7.05	109.2	15.5	7.05	106.2	15.1
14.10	151.5	10.7	14.10	141.3	10.0
21.15	179.0	8.5	21.15	163.1	7.7
42.30	224.3	5.3	42.30	200.1	4.7
63.44	251.7	4.0	63.44	222.3	3.5
126.9	307.0	2.4	126.9	267.9	2.1
190.3	363.9	1.9	190.3	294.7	1.5
380.7	397.0	1.0	380.7	350.6	0.92
571.0	446.6	0.78	571.0	370.5	0.65

Slurry	Bob/Cup	% MIPA w/w
1	MV III	0
2	MV II	0.00347
3	MV I	0.00814
4	MV I	0.0115

SLURRY: E % w/w TiO_2 = 57.6

(1)			(2)		
γ/ s^{-1}	τ/ dyne cm^{-2}	η/ poise	γ/ s^{-1}	τ/ dyne cm^{-2}	η/ poise
2.722	230.3	84.6	2.722	706.2	259
5.444	412.5	75.8	5.444	764.9	140.5
8.167	670.3	82.1	8.167	856.4	104.9
16.33	1014	62.1	16.33	1208	74.0
24.5	1238	50.5	24.5	1431	58.4
49.0	1640	33.5	49.0	1748	35.7
73.5	1925	26.2	73.5	2018	27.5
147	2444	16.6	147	2628	17.9
220.5	2760	12.5	220.5	3027	13.7

(3)			(4)		
γ/ s^{-1}	τ/ dyne cm^{-2}	η/ poise	γ/ s^{-1}	τ/ dyne cm^{-2}	η/ poise
2.722	538.5	197.8	7.05	354.0	50.2
5.444	685.1	125.8	14.10	463.1	32.8
8.167	871.6	106.7	21.15	578.9	27.4
16.33	1150	70.4	42.30	866.7	20.5
24.5	1255	51.2	63.44	1121	17.7
49.0	1642	33.5	126.9	1535	12.1
73.5	1889	25.7	190.3	1823	9.6
147	2452	16.7	380.7	2408	6.3
220.5	2815	12.8	571.0	2722	4.8

Slurry	Bob/Cup	% MIPA w/w
1	SV II	0.0266
2	SV I	0.0285
3	SV I	0.0306
4	MV I	0.0351
5	MV II	0.0357
6	MV II	0.0377

SLURRY: E % w/w TiO_2 = 57.6

(5)			(6)		
γ/ s^{-1}	τ/ dyne cm^{-2}	η/ poise	γ/ s^{-1}	τ/ dyne cm^{-2}	η/ poise
2.722	343.4	126.2	2.722	279	102.5
5.444	476.2	87.5	5.444	409.2	75.2
8.167	550.6	67.4	8.167	465	56.9
16.33	706.8	43.3	16.33	629	38.5
24.5	829.6	33.9	24.5	744	30.4
49.0	1094	22.3	49.0	975	19.9
73.5	1265	17.2	73.5	1146	15.6
147	1603	10.9	147	1499	10.2
220.5	1841	8.4	220.5	1748	7.9

SLURRY: F % w/w TiO_2 = 51.0

(1)			(2)		
γ/ s^{-1}	τ/ dyne cm^{-2}	η/ poise	γ/ s^{-1}	τ/ dyne cm^{-2}	η/ poise
2.722	189.1	69.5	2.722	375.4	137.9
5.444	343.8	63.2	5.444	462.2	84.9
8.167	491.6	60.2	8.167	606.5	74.3
16.33	656.6	40.2	16.33	778.9	47.7
24.5	790.6	32.3	24.5	874.0	35.7
49.0	1038	21.2	49.0	1113	22.7
73.5	1196	16.3	73.5	1243	16.9
147	1475	10.0	147	1525	10.4
220.5	1667	7.6	220.5	1672	7.6

(3)			(4)		
γ/ s^{-1}	τ/ dyne cm^{-2}	η/ poise	γ/ s^{-1}	τ/ dyne cm^{-2}	η/ poise
2.722	256.9	94.4	1.33	281	211.3
5.444	364.8	67.0	2.67	397.5	148.9
8.167	438.7	53.7	4.0	463.1	115.8
16.33	554.9	34.0	8.0	558.7	69.8
24.5	644.0	26.3	12.0	596.3	49.7
49.0	864.6	17.6	24.0	741.3	30.9
73.5	997.1	13.6	36.0	816.5	22.7
147	1255	8.5	72.0	967.0	13.4
220.5	1384	6.3	108	1085	10.0

Slurry	Bob/Cup	% MIPA w/w
1	SV II	0.0170
2	SV I	0.0192
3	SV I	0.0215
4	MV III	0.0240
5	MV I	0.0270
6	MV I	0.0287
7	MV I	0.0319

SLURRY: F % w/w TiO_2 = 51.0

(5)			(6)		
γ/ s^{-1}	τ/ dyne cm^{-2}	η/ poise	γ/ s^{-1}	τ/ dyne cm^{-2}	η/ poise
7.05	224.3	31.8	7.05	192.2	27.3
14.10	340.7	24.2	14.10	284.2	20.2
21.15	403.6	19.1	21.15	337.4	16.0
42.3	565.7	13.4	42.3	459.8	10.9
63.4	655.0	10.3	63.4	535.8	8.4
126.9	856.8	6.8	126.9	711.2	5.6
190.3	999.0	5.2	190.3	836.9	4.4
380.7	1264	3.3	380.7	1118	2.9
571.0	1456	2.5	571.0	1307	2.3

(7)					
γ/ s^{-1}	τ/ dyne cm^{-2}	η/ poise	γ/ s^{-1}	τ/ dyne cm^{-2}	η/ poise
7.05	154.2	21.9			
14.10	226.3	16.0			
21.15	270.9	12.8			
42.3	370.5	8.8			
63.4	403.6	6.4			
126.9	542.4	4.3			
190.3	645.1	3.4			
380.7	899.8	2.4			
571.0	1092	1.9			

SLURRY: G % w/w TiO_2 = 51.5

(1)			(2)		
γ/ s^{-1}	τ/ dyne cm^{-2}	η/ poise	γ/ s^{-1}	τ/ dyne cm^{-2}	η/ poise
2.722	387.1	142.2	2.722	337.9	124.1
5.444	468.1	86.0	5.444	430.5	79.1
8.167	607.7	74.4	8.167	545.5	66.8
16.33	787.2	48.2	16.33	705.0	43.2
24.5	895.1	36.5	24.5	804.7	32.8
49.0	1129	23.0	49.0	1065	21.7
73.5	1279	17.4	73.5	1208	16.4
147	1595	10.9	147	1525	10.4
220.5	1771	8.0	220.5	1701	7.7

(3)			(4)		
γ/ s^{-1}	τ/ dyne cm^{-2}	η/ poise	γ/ s^{-1}	τ/ dyne cm^{-2}	η/ poise
2.722	256.9	94.4	2.722	230.6	84.7
5.444	397.7	73.1	5.444	316.2	58.1
8.167	483.3	59.2	8.167	375.7	46.0
16.33	605.3	37.1	16.33	479.9	29.4
24.5	700.3	28.6	24.5	554.3	22.6
49.0	929.1	19.0	49.0	703.1	14.3
73.5	1079	14.7	73.5	811.0	11.0
147	1314	8.9	147	1004	6.8
220.5	1490	6.8	220.5	1146	5.2

Slurry	Bob/Cup	% MIPA w/w
1	SV I	0.0160
2	SV I	0.0181
3	SV I	0.0203
4	MV II	0.0226
5	MV II	0.0252
6	MV I	0.0285
7	MV I	0.0420

SLURRY: G % w/w TiO_2 = 51.5

(5)			(6)		
γ/ s^{-1}	τ/ dyne cm^{-2}	η/ poise	γ/ s^{-1}	τ/ dyne cm^{-2}	η/ poise
2.722	194.9	71.6	7.05	156.8	22.2
5.444	279.0	51.2	14.10	241.5	17.1
8.167	327.4	40.1	21.15	301.7	14.3
16.33	427.8	26.2	42.3	420.1	9.93
24.5	513.4	21.0	63.4	519.4	8.19
49.0	658.4	13.4	126.9	684.8	5.40
73.5	751.4	10.2	190.3	810.5	4.26
147	941.2	6.4	380.7	1088	2.86
220.5	1053	4.8	571.0	1290	2.26

(7)					
γ/ s^{-1}	τ/ dyne cm^{-2}	η/ poise	γ/ s^{-1}	τ/ dyne cm^{-2}	η/ poise
7.05	10.3	1.46			
14.10	11.2	0.79			
21.15	13.2	0.62			
42.3	19.2	0.45			
63.4	20.8	0.33			
126.9	31.4	0.25			
190.3	40.0	0.21			
380.7	66.5	0.17			
571	90.0	0.16			

SLURRY: H % w/w TiO_2 = 40.3

(1)			(2)		
γ/ s^{-1}	τ/ dyne cm^{-2}	η/ poise	γ/ s^{-1}	τ/ dyne cm^{-2}	η/ poise
2.722	432.9	159.0	2.722	439.9	161.6
5.444	461.0	84.7	5.444	475.1	87.3
8.167	512.6	62.8	8.167	527.9	64.6
16.33	669.8	41.0	16.33	699.2	42.8
24.5	775.4	31.6	24.5	800.1	32.7
49.0	906.8	18.5	49.0	935.0	19.1
73.5	984.2	13.4	73.5	1009	13.7
147	1090	7.4	147	1127	7.7
220.5	1154	5.2	220.5	1232	5.6

(3)			(4)		
γ/ s^{-1}	τ/ dyne cm^{-2}	η/ poise	γ/ s^{-1}	τ/ dyne cm^{-2}	η/ poise
2.722	410.6	150.8	2.722	359.0	131.9
5.444	443.4	81.4	5.444	410.6	75.4
8.167	490.4	60.0	8.167	461.0	56.4
16.33	620.6	38.0	16.33	598.3	36.6
24.5	744.9	30.4	24.5	668.7	27.3
49.0	879.8	18.0	49.0	778.9	15.9
73.5	953.7	13.0	73.5	843.5	11.5
147	1070	7.3	147	940.8	6.4
220.5	1138	5.2	220.5	998.3	4.5

(5)					
γ/ s^{-1}	τ/ dyne cm^{-2}	η/ poise	γ/ s^{-1}	τ/ dyne cm^{-2}	η/ poise
2.722	225.2	82.7			
5.444	278.0	51.1			
8.167	335.5	41.1			
16.33	411.8	25.2			
24.5	448.1	18.3			
49.0	509.1	10.4			
73.5	550.2	7.5			
147	626.4	4.3			
220.5	669.8	3.0			

Slurry	Bob/Cup	% MIPA w/w
1	SV I	0.0250
2	SV I	0.0278
3	SV I	0.0339
4	SV I	0.0420
5	SV I	0.0594

SLURRY: I % w/w TiO_2 = 43.7

(1)			(2)		
γ/ s^{-1}	τ/ dyne cm^{-2}	η/ poise	γ/ s^{-1}	τ/ dyne cm^{-2}	η/ poise
2.722	178.8	65.7	2.722	518.5	190.5
5.444	278.4	51.1	5.444	592.4	108.8
8.167	433.1	53.0	8.167	622.9	76.3
16.33	642.8	39.4	16.33	798.9	48.9
24.5	759.7	31.0	24.5	946.7	38.6
49.0	931.6	19.0	49.0	1092	22.3
73.5	1042	14.2	73.5	1185	16.1
147	1220	8.3	147	1396	9.5
220.5	1289	5.8	220.5	1502	6.8

(3)			(4)		
γ/ s^{-1}	τ/ dyne cm^{-2}	η/ poise	γ/ s^{-1}	τ/ dyne cm^{-2}	η/ poise
2.722	485.7	178.4	2.722	410.6	150.8
5.444	543.1	99.8	5.444	463.4	85.1
8.167	611.2	74.8	8.167	518.5	63.5
16.33	752.0	46.1	16.33	655.8	40.2
24.5	854.0	34.9	24.5	712.1	29.1
49.0	977.2	19.9	49.0	807.1	16.5
73.5	1069	14.5	73.5	882.2	12.0
147	1255	8.5	147	1021	6.9
220.5	1337	6.1	220.5	1111	5.0

Slurry	Bob/Cup	% MIPA w/w
1	SV II	0.0233
2	SV I	0.0275
3	SV I	0.0349
4	SV I	0.0429
5	SV I	0.0516
6	MV II	0.0703
7	MV I	0.0819

SLURRY: I % w/w TiO_2 = 43.7

(5)			(6)		
γ/ s^{-1}	τ/ dyne cm^{-2}	η/ poise	γ/ s^{-1}	τ/ dyne cm^{-2}	η/ poise
2.722	207.6	72.3	2.722	152.5	56.0
5.444	298.0	54.7	5.444	186.0	34.2
8.167	350.8	43.0	8.167	200.5	24.6
16.33	475.1	29.1	16.33	225.8	13.8
24.5	513.8	21.0	24.5	241.8	9.87
49.0	598.3	12.2	49.0	274.5	5.60
73.5	649.9	8.8	73.5	294.6	4.01
147	750.8	5.1	147	337.0	2.29
220.5	808.3	3.7	220.5	359.7	1.63

(7)					
γ/ s^{-1}	τ/ dyne cm^{-2}	η/ poise	γ/ s^{-1}	τ/ dyne cm^{-2}	η/ poise
7.05	122.4	17.4			
14.10	151.2	10.7			
21.15	165.7	7.83			
42.30	188.6	4.46			
63.44	198.5	3.13			
126.9	228.6	1.80			
190.3	249.1	1.31			
380.7	304.7	0.80			
571.0	357.3	0.63			

SLURRY: J % w/w TiO_2 = 48.7

(1)			(2)		
γ/ s^{-1}	τ/ dyne cm^{-2}	η/ poise	γ/ s^{-1}	τ/ dyne cm^{-2}	η/ poise
2.722	315.6	115.9	2.722	319.1	117.2
5.444	395.3	72.6	5.444	450.5	82.8
8.167	450.5	55.2	8.167	513.8	62.9
16.33	674.5	41.3	16.33	749.6	45.9
24.5	766.0	31.3	24.5	851.7	34.8
49.0	924.4	18.9	49.0	1021	20.8
73.5	1048	14.3	73.5	1161	15.8
147	1290	8.78	147	1431	9.73
220.5	1408	6.39	220.5	1560	7.07

(3)			(4)		
γ/ s^{-1}	τ/ dyne cm^{-2}	η/ poise	γ/ s^{-1}	τ/ dyne cm^{-2}	η/ poise
2.722	363.7	133.6	2.722	281.5	103.4
5.444	411.8	75.6	5.444	488.0	89.6
8.167	485.7	59.5	8.167	530.2	64.9
16.33	715.6	43.8	16.33	750.8	46.0
24.5	891.6	36.4	24.5	892.7	36.4
49.0	1093	22.3	49.0	1068	21.8
73.5	1267	17.2	73.5	1220	16.6
147	1502	10.2	147	1502	10.2
220.5	1689	7.66	220.5	1631	7.40

Slurry	Bob/Cup	% MIPA w/w
1	SV I	0.0170
2	SV I	0.0191
3	SV I	0.0225
4	SV I	0.0286
5	SV I	0.0352
6	SV I	0.0451
7	MV I	0.0603
8	MV I	0.0649

SLURRY: J % w/w TiO_2 = 48.7

(5)			(6)		
γ/ s^{-1}	τ/ dyne cm^{-2}	η/ poise	γ/ s^{-1}	τ/ dyne cm^{-2}	η/ poise
2.722	317.9	116.8	2.722	281.5	103.4
5.444	498.6	91.6	5.444	363.7	66.8
8.167	552.5	67.7	8.167	401.2	49.1
16.33	735.5	45.0	16.33	552.5	33.8
24.5	821.2	33.5	24.5	615.9	25.1
49.0	961.9	19.6	49.0	719.1	14.7
73.5	1071	14.6	73.5	805.9	11.0
147	1302	8.86	147	974.8	6.63
220.5	1408	6.39	220.5	1082	4.91

(7)			(8)		
γ/ s^{-1}	τ/ dyne cm^{-2}	η/ poise	γ/ s^{-1}	τ/ dyne cm^{-2}	η/ poise
7.05	211.7	30.0	7.05	208.4	29.6
14.10	299.4	21.2	14.10	278.2	19.7
21.15	344.0	16.3	21.15	314.9	14.9
42.3	423.4	10.0	42.3	363.9	8.60
63.4	473.0	7.46	63.4	400.3	6.31
126.9	562.4	4.43	126.9	496.2	3.91
190.3	625.2	3.29	190.3	549.1	2.89
380.7	754.2	1.98	380.7	674.8	1.77
571.0	846.8	1.48	571.0	774.1	1.36

SLURRY: K % w/w TiO_2 = 46.0

(1)			(2)		
γ/ s^{-1}	τ/ dyne cm^{-2}	η/ poise	γ/ s^{-1}	τ/ dyne cm^{-2}	η/ poise
2.722	198.3	72.9	2.722	217.0	79.7
5.444	254.6	46.8	5.444	267.5	49.1
8.167	312.0	38.2	8.167	320.3	39.2
16.33	444.6	27.2	16.33	475.1	29.1
24.5	510.3	20.8	24.5	570.1	23.3
49.0	631.1	12.9	49.0	702.7	14.3
73.5	728.5	9.91	73.5	797.7	10.9
147	869.3	5.91	147	979.5	6.66
220.5	956.1	4.34	220.5	1089	4.94

(3)			(4)		
γ/ s^{-1}	τ/ dyne cm^{-2}	η/ poise	γ/ s^{-1}	τ/ dyne cm^{-2}	η/ poise
2.722	287.4	105.6	2.711	253.4	93.1
5.444	326.1	59.9	5.444	309.7	56.9
8.167	383.6	47.0	8.167	360.1	44.1
16.33	525.5	32.2	16.33	472.8	29.0
24.5	588.9	24.0	24.5	524.4	21.4
49.0	705.0	14.4	49.0	620.6	12.7
73.5	784.8	10.7	73.5	700.3	9.53
147	937.3	6.38	147	836.4	5.69
220.5	1031	4.68	220.5	917.4	4.16

(5)					
γ/ s^{-1}	τ/ dyne cm^{-2}	η/ poise	γ/ s^{-1}	τ/ dyne cm^{-2}	η/ poise
2.722	134.3	49.3			
5.444	234.7	43.1			
8.167	279.7	34.2			
16.33	353.0	21.6			
24.5	379.4	15.5			
49.0	435.2	8.88			
73.5	468.7	6.38			
147	535.7	3.64			
220.5	602.7	2.73			

Slurry	Bob/Cup	% MIPA w/w
1	SV I	0.0136
2	SV I	0.0173
3	SV I	0.0251
4	SV I	0.0320
5	MV II	0.0438

SLURRY: L % w/w TiO_2 = 50.1

(1)			(2)		
γ/ s^{-1}	τ/ dyne cm^{-2}	η/ poise	γ/ s^{-1}	τ/ dyne cm^{-2}	η/ poise
2.722	469.2	172.4	2.722	330.8	121.5
5.444	532.6	97.8	5.444	405.9	74.6
8.167	626.4	76.7	8.167	517.3	63.3
16.33	832.9	51.0	16.33	726.1	44.5
24.5	937.3	38.3	24.5	824.7	33.7
49.0	1112	22.7	49.0	1010	20.6
73.5	1243	16.9	73.5	1161	15.8
147	1455	9.90	147	1384	9.41
220.5	1631	7.40	220.5	1537	6.97

(3)			(4)		
γ/ s^{-1}	τ/ dyne cm^{-2}	η/ poise	γ/ s^{-1}	τ/ dyne cm^{-2}	η/ poise
2.722	288.6	106.0	2.722	215.9	79.3
5.444	382.4	70.2	5.444	340.2	62.5
8.167	481.0	58.9	8.167	400.0	49.0
16.33	632.3	38.7	16.33	482.1	29.5
24.5	713.2	29.1	34.5	545.5	22.3
49.0	864.6	17.6	49.0	685.1	14.0
73.5	996.0	13.6	73.5	783.6	10.7
147	1255	8.54	147	981.9	6.68
220.5	1373	6.23	220.5	1105	5.01

(5)			(6)		
γ/ s^{-1}	τ/ dyne cm^{-2}	η/ poise	γ/ s^{-1}	τ/ dyne cm^{-2}	η/ poise
7.05	172.7	24.5	7.05	125.7	17.8
14.10	263.10	18.7	14.10	175.0	12.4
21.15	324.2	15.3	21.15	205.8	9.73
42.3	443.3	10.5	42.3	271.6	6.42
63.4	529.3	8.34	63.4	308.0	4.85
126.9	694.7	5.47	126.9	380.4	3.00
190.3	803.8	4.22	190.3	449.9	2.36
380.7	1009	2.65	380.7	595.4	1.56
571.0	1174	2.06	571.0	737.7	1.29

Slurry	Bob/Cup	% MIPA w/w
1	SV I	0.0192
2	SV I	0.0215
3	SV I	0.0240
4	SV I	0.0280
5	MV I	0.0338
6	MV I	0.0379

SLURRY: M % w/w TiO_2 = 48.8

(1)			(2)		
γ/ s^{-1}	τ/ dyne cm^{-2}	η/ poise	γ/ s^{-1}	τ/ dyne cm^{-2}	η/ poise
2.722	349.6	128.4	2.722	335.5	123.3
5.444	408.2	75.0	5.444	398.9	73.3
8.167	522.0	63.9	8.167	519.7	63.6
16.33	692.1	42.4	16.33	681.6	41.7
24.5	774.2	31.6	24.5	761.3	31.1
49.0	945.5	19.3	49.0	915.0	18.7
73.5	1075	14.6	73.5	1043	14.2
147	1279	8.70	147	1267	8.62
220.5	1408	6.38	220.5	1408	6.38

(3)			(4)		
γ/ s^{-1}	τ/ dyne cm^{-2}	η/ poise	γ/ s^{-1}	τ/ dyne cm^{-2}	η/ poise
2.722	282.7	103.9	2.722	214.7	78.9
5.444	320.3	58.8	5.444	337.9	62.1
8.167	403.5	49.4	8.167	412.9	50.6
16.33	552.5	33.8	16.33	510.3	31.2
24.5	638.2	26.0	24.5	571.3	23.3
49.0	788.3	16.1	49.0	710.9	14.5
73.5	912.7	12.4	73.5	808.3	11.0
147	1124	7.65	147	997.1	6.78
220.5	1279	5.80	220.5	1116	5.06

Slurry	Bob/Cup	% MIPA w/w
1	SV I	0.0178
2	SV I	0.0199
3	SV I	0.0222
4	SV I	0.0246
5	SV I	0.0272
6	MV II	0.0307
7	MV II	0.0344
8	MV I	0.0404

SLURRY: M % w/w TiO_2 = 48.8

(5)			(6)		
γ/ s^{-1}	τ/ dyne cm^{-2}	η/ poise	γ/ s^{-1}	τ/ dyne cm^{-2}	η/ poise
2.722	188.9	69.4	2.722	171.9	63.2
5.444	308.5	56.7	5.444	231.0	42.4
8.167	364.8	44.7	8.167	280.9	34.4
16.33	443.4	27.2	16.33	346.3	21.2
24.5	492.7	20.1	24.5	394.3	16.1
49.0	618.2	12.6	49.0	450.1	9.19
73.5	707.4	9.62	73.5	513.4	6.99
147	879.8	5.99	147	606.4	4.13
220.5	988.9	4.48	220.5	673.3	3.05

(7)			(8)		
γ/ s^{-1}	τ/ dyne cm^{-2}	η/ poise	γ/ s^{-1}	τ/ dyne cm^{-2}	η/ poise
2.722	151.8	55.8	7.05	100.9	14.3
5.444	187.9	34.5	14.10	139.9	9.92
8.167	213.5	26.1	21.15	165.1	7.81
16.33	266.0	16.3	42.3	215.4	5.09
24.5	298.0	12.2	63.4	255.0	4.02
49.0	363.4	7.42	126.9	324.8	2.56
73.5	394.3	5.36	190.3	370.5	1.95
147	483.6	3.29	380.7	492.9	1.29
220.5	554.3	2.51	571	598.7	1.05

SLURRY: N % w/w TiO_2 = 50.7

(1)			(2)		
γ/ s^{-1}	τ/ dyne cm^{-2}	η/ poise	γ/ s^{-1}	τ/ dyne cm^{-2}	η/ poise
2.722	465.7	171.1	2.722	455.2	167.2
5.444	532.6	97.8	5.444	524.4	96.3
8.167	668.7	81.9	8.167	647.6	79.3
16.33	890.4	54.5	16.33	861.1	52.7
24.5	987.8	40.3	24.5	971.3	39.6
49.0	1152	23.5	49.0	1140	23.3
73.5	1279	17.4	73.5	1279	17.4
147	1537	10.5	147	1525	10.4
220.5	1666	7.56	220.5	1724	7.82

(3)			(4)		
γ/ s^{-1}	τ/ dyne cm^{-2}	η/ poise	γ/ s^{-1}	τ/ dyne cm^{-2}	η/ poise
2.722	398.9	146.5	2.722	275.7	101.3
5.444	466.9	85.8	5.444	384.8	70.7
8.167	601.8	73.7	8.167	483.3	59.2
16.33	786.0	48.1	16.33	608.8	37.3
24.5	876.3	35.8	24.5	672.2	27.4
49.0	1046	21.3	49.0	821.2	16.8
73.5	1220	16.6	73.5	942.0	12.8
147	1478	10.1	147	1185	8.06
220.5	1631	7.40	220.5	1326	6.01

Slurry	Bob/Cup	% MIPA w/w
1	SV I	0.0186
2	SV I	0.0208
3	SV I	0.0232
4	SV I	0.0264
5	SV I	0.0312
6	MV II	0.0357
7	MV I	0.0415

SLURRY: N % w/w TiO_2 = 50.7

(5)			(6)		
γ/ s^{-1}	τ/ dyne cm^{-2}	η/ poise	γ/ s^{-1}	τ/ dyne cm^{-2}	η/ poise
2.722	193.6	71.1	2.722	194.9	71.6
5.444	316.7	58.2	5.444	234.0	43.0
8.167	363.7	44.5	8.167	260.4	31.9
16.33	436.4	26.7	16.33	326.6	20.0
24.5	482.1	19.7	24.5	365.3	14.9
49.0	611.2	12.5	49.0	435.2	8.88
73.5	701.5	9.54	73.5	491.0	6.68
147	870.4	5.92	147	595.2	4.05
220.5	985.4	4.47	220.5	684.5	3.10

(7)					
γ/ s^{-1}	τ/ dyne cm^{-2}	η/ poise	γ/ s^{-1}	τ/ dyne cm^{-2}	η/ poise
7.05	114.1	16.2			
14.10	155.5	11.0			
21.15	180.3	8.52			
42.3	231.6	5.48			
63.4	270.3	4.26			
126.9	347.3	2.74			
190.3	403.6	2.12			
380.7	532.6	1.40			
571	635.1	1.11			

SLURRY: 0 % w/w TiO_2 = 47.9

(1)			(2)		
γ/ s^{-1}	τ/ dyne cm^{-2}	η/ poise	γ/ s^{-1}	τ/ dyne cm^{-2}	η/ poise
2.722	451.6	165.9	2.722	462.2	169.8
5.444	519.7	95.5	5.444	524.4	96.3
8.167	611.2	74.8	8.167	610.0	74.7
16.33	809.4	49.6	16.33	829.4	50.8
24.5	905.5	37.0	24.5	916.2	37.4
49.0	1068	21.8	49.0	1071	21.9
73.5	1197	16.3	73.5	1197	16.3
147	1419	9.65	147	1419	9.65
220.5	1560	7.07	220.5	1560	7.07

(3)			(4)		
γ/ s^{-1}	τ/ dyne cm^{-2}	η/ poise	γ/ s^{-1}	τ/ dyne cm^{-2}	η/ poise
2.722	414.1	152.1	2.722	310.9	114.2
5.444	470.4	86.4	5.444	375.4	69.0
8.167	567.8	69.5	8.167	469.2	57.5
16.33	739.1	45.3	16.33	595.9	36.5
24.5	820.0	33.5	24.5	667.5	27.2
49.0	969.0	19.8	49.0	800.1	16.3
73.5	1092	14.9	73.5	910.3	12.4
147	1314	8.94	147	1103	7.50
220.5	1431	6.49	220.5	1232	5.59

Slurry	Bob/Cup	% MIPA w/w
1	SV I	0.0179
2	SV I	0.0201
3	SV I	0.0230
4	SV I	0.0273
5	SV I	0.0318
6	SV I	0.0360
7	MV II	0.0405
8	MV I	0.0488

SLURRY: 0 % w/w TiO_2 = 47.9

(5)			(6)		
γ/ s^{-1}	τ/ dyne cm^{-2}	η/ poise	γ/ s^{-1}	τ/ dyne cm^{-2}	η/ poise
2.722	214.7	78.9	2.722	186.5	68.5
5.444	310.9	57.1	5.444	275.7	50.6
8.167	371.9	45.5	8.167	316.7	38.8
16.33	448.1	27.4	16.33	376.6	23.1
24.5	502.1	20.5	24.5	418.8	17.1
49.0	619.4	12.6	49.0	515.0	10.5
73.5	703.9	9.58	73.5	584.2	7.95
147	861.1	5.86	147	725.0	4.93
220.5	960.8	4.36	220.5	807.1	3.66

(7)			(8)		
γ/ s^{-1}	τ/ dyne cm^{-2}	η/ poise	γ/ s^{-1}	τ/ dyne cm^{-2}	η/ poise
2.722	206.8	76.0	7.05	112.5	16.0
5.444	267.5	49.1	14.10	151.2	10.7
8.167	301.7	36.9	21.15	173.7	8.21
16.33	364.9	22.3	42.3	219.0	5.18
24.5	405.5	16.6	63.4	248.8	3.92
49.0	450.1	9.19	126.9	317.6	2.50
73.5	502.2	6.83	190.3	360.6	1.89
147	598.9	4.07	380.7	463.1	1.22
220.5	673.3	3.05	571	552.4	0.97

SLURRY: P % w/w TiO_2 = 51.3

(1)			(2)		
γ/ s^{-1}	τ/ dyne cm^{-2}	η/ poise	γ/ s^{-1}	τ/ dyne cm^{-2}	η/ poise
2.722	512.6	188.3	2.722	281.9	103.6
5.444	578.3	106.2	5.444	433.1	79.6
8.167	695.6	85.2	8.167	615.3	75.3
16.33	974.8	59.7	16.33	1103	67.5
24.5	1092	44.6	24.5	1378	56.2
49.0	1267	25.9	49.0	1763	36.0
73.5	1384	18.8	73.5	1990	27.1
147	1631	11.1	147	2379	16.2
220.5	1771	8.03	220.5	2589	11.7

(3)			(4)		
γ/ s^{-1}	τ/ dyne cm^{-2}	η/ poise	γ/ s^{-1}	τ/ dyne cm^{-2}	η/ poise
2.722	371.3	136.4	2.722	804.7	295.6
5.444	471.0	86.5	5.444	888.0	163.1
8.167	618.8	75.8	8.167	961.9	117.8
16.33	1100	67.4	16.33	1279	78.3
24.5	1609	65.7	24.5	1419	57.9
49.0	2028	41.4	49.0	1631	33.3
73.5	2310	31.4	73.5	1748	23.8
147	2781	18.9	147	2006	13.6
220.5	3080	14.0	220.5	2205	10.0

Slurry	Bob/Cup	% MIPA w/w	% KNO_3 w/w
1	SV I	0.0181	-
2	SV II	0.0214	0.0144
3	SV II	0.0249	0.0296
4	SV I	0.0348	0.0296

SLURRY: Q % w/w TiO_2 = 50.2

(1)			(2)		
γ/ s^{-1}	τ/ dyne cm^{-2}	η/ poise	γ/ s^{-1}	τ/ dyne cm^{-2}	η/ poise
2.722	621.7	228.4	2.722	619.4	227.6
5.444	719.1	132.1	5.444	702.7	129.1
8.167	795.4	97.4	8.167	780.1	95.5
16.33	1077	66.0	16.33	1089	66.7
24.5	1255	51.2	24.5	1208	49.3
49.0	1443	29.4	49.0	1431	29.2
73.5	1631	22.2	73.5	1619	22.0
147	1947	13.2	147	1959	13.3
220.5	2123	9.63	220.5	2159	9.79

(3)			(4)		
γ/ s^{-1}	τ/ dyne cm^{-2}	η/ poise	γ/ s^{-1}	τ/ dyne cm^{-2}	η/ poise
2.722	451.6	165.9	2.722	310.9	114.2
5.444	523.2	96.1	5.444	405.9	74.6
8.167	641.7	78.6	8.167	522.0	63.9
16.33	866.9	53.1	16.33	667.5	40.9
24.5	973.7	39.7	24.5	741.4	30.3
49.0	1172	23.9	49.0	912.7	18.6
73.5	1337	18.2	73.5	1051	14.3
147	1642	11.2	147	1314	8.94
220.5	1818	8.24	220.5	1466	6.65

(5)			(6)		
γ/ s^{-1}	τ/ dyne cm^{-2}	η/ poise	γ/ s^{-1}	τ/ dyne cm^{-2}	η/ poise
7.05	246.4	35.0	7.05	149.2	21.2
14.10	340.7	24.2	14.10	225.9	16.0
21.15	403.6	19.1	21.15	282.2	13.3
42.3	565.7	13.4	42.3	380.4	8.99
63.4	661.6	10.4	63.4	463.1	7.30
126.9	870.0	6.86	126.9	631.8	4.98
190.3	995.7	5.23	190.3	727.8	3.82
380.7	1244	3.27	380.7	959.3	2.52
571.0	1396	2.44	571	1135	1.99

Slurry	Bob/Cup	% MIPA w/w
1	SV I	0.0156
2	SV I	0.0181
3	SV I	0.0215
4	SV I	0.0251
5	MV I	0.0306
6	MV I	0.0350

SLURRY: R % w/w TiO_2 = 44.7

(1)			(2)		
γ/ s^{-1}	τ/ dyne cm^{-2}	η/ poise	γ/ s^{-1}	τ/ dyne cm^{-2}	η/ poise
2.722	330.8	121.5	7.05	132.3	18.8
5.444	388.3	71.3	14.10	216.0	15.3
8.167	458.7	56.2	21.15	257.0	12.2
16.33	607.7	37.2	42.3	327.2	7.74
24.5	739.1	30.2	63.4	360.6	5.68
49.0	925.6	18.9	126.9	456.5	3.60
73.5	1046	14.2	190.3	516.0	2.71
147	1255	8.54	380.7	635.1	1.67
220.5	1384	6.28	571	721.1	1.26

(3)					
γ/ s^{-1}	τ/ dyne cm^{-2}	η/ poise	γ/ s^{-1}	τ/ dyne cm^{-2}	η/ poise
2.722	502.1	184.5			
5.444	572.5	105.2			
8.167	635.8	77.8			
16.33	796.5	48.8			
24.5	890.4	36.3			
49.0	1036	21.1			
73.5	1153	15.7			
147	1314	8.94			
220.5	1431	6.49			

Slurry	Bob/Cup	% MIPA w/w	% KNO_3 w/w
1	SV I	0	0
2	MV I	0.0144	0
3	SV I	0.0144	0.0201

SLURRY: S % w/w TiO_2 = 45.9

(1)			(2)		
γ/ s^{-1}	τ/ dyne cm^{-2}	η/ poise	γ/ s^{-1}	τ/ dyne cm^{-2}	η/ poise
2.722	493.9	181.4	2.722	201.8	74.1
5.444	591.2	108.6	5.44	281.5	51.7
8.167	695.6	85.2	8.167	341.4	41.8
16.33	904.5	55.4	16.33	435.2	26.7
24.5	1041	42.5	24.5	508.0	20.7
49.0	1267	25.9	49.0	658.1	13.4
73.5	1408	19.2	73.5	749.6	10.2
147	1666	11.3	147	903.3	6.14
220.5	1865	8.46	220.5	998.3	4.53

(3)					
γ/ s^{-1}	τ/ dyne cm^{-2}	η/ poise	γ/ s^{-1}	τ/ dyne cm^{-2}	η/ poise
2.722	462.2	169.8			
5.444	545.5	100.2			
8.167	630.0	77.1			
16.33	808.3	49.5			
24.5	904.5	36.9			
49.0	1083	22.1			
73.5	1197	16.3			
147	1431	9.73			
220.5	1595	7.23			

Slurry	Bob/Cup	% MIPA w/w	% KNO_3 w/w
1	SV I	0	0
2	SV I	0.0146	0
3	SV I	0.0146	0.0171

SLURRY: T % w/w TiO_2 = 44.5

(1)			(2)		
γ/ s^{-1}	τ/ dyne cm^{-2}	η/ poise	γ/ s^{-1}	τ/ dyne cm^{-2}	η/ poise
2.722	187.7	69.0	7.05	82.7	11.7
5.444	260.4	47.8	14.10	123.1	8.73
8.167	316.7	38.8	21.15	154.5	7.30
16.33	434.0	26.6	42.3	209.4	4.95
24.5	505.6	20.6	63.4	251.4	3.96
49.0	653.4	13.3	126.9	324.2	2.55
73.5	741.4	10.1	190.3	367.2	1.93
147	885.7	6.03	380.7	483.0	1.27
220.5	976.0	4.43	571	565.7	0.99

(3)					
γ/ s^{-1}	τ/ dyne cm^{-2}	η/ poise	γ/ s^{-1}	τ/ dyne cm^{-2}	η/ poise
2.722	125.5	46.1			
5.444	185.3	34.0			
8.167	224.1	27.4			
16.33	301.5	18.5			
24.5	355.4	14.5			
49.0	468.1	9.55			
73.5	527.9	7.18			
147	647.6	4.41			
220.5	717.9	3.26			

Slurry	Bob/Cup	% MIPA w/w	% KNO_3 w/w
1	SV I	0	0
2	MV I	0.0132	0
3	SV I	0.0132	0.0208

SLURRY: U % w/w TiO_2 = 44.5

(1)			(2)		
γ/ s^{-1}	τ/ dyne cm^{-2}	η/ poise	γ/ s^{-1}	τ/ dyne cm^{-2}	η/ poise
2.722	423.5	155.6	2.722	144.3	53.0
5.444	497.4	91.4	5.444	217.0	39.9
8.167	574.8	70.4	8.167	258.1	31.6
16.33	752.0	46.1	16.33	340.2	20.8
24.5	857.5	35.0	24.5	397.7	16.2
49.0	1055	21.5	49.0	503.3	10.3
73.5	1165	15.9	73.5	561.9	7.64
147	1326	9.02	147	672.2	4.57
220.5	1478	6.70	220.5	736.7	3.34

(3)					
γ/ s^{-1}	τ/ dyne cm^{-2}	η/ poise	γ/ s^{-1}	τ/ dyne cm^{-2}	η/ poise
2.722	339.0	124.5			
5.444	414.1	76.1			
8.167	482.1	59.0			
16.33	632.3	38.7			
24.5	701.5	28.6			
49.0	855.2	17.5			
73.5	952.6	13.0			
147	1140	7.76			
220.5	1279	5.80			

Slurry	Bob/Cup	% MIPA w/w	% KNO_3 w/w
1	SV I	0	0
2	SV I	0.0142	0
3	SV I	0.0142	0.0173

SLURRY: V % w/w TiO_2 = 36.7

(1)			(2)		
γ/ s^{-1}	τ/ dyne cm^{-2}	η/ poise	γ/ s^{-1}	τ/ dyne cm^{-2}	η/ poise
2.722	230.3	84.6	2.722	301.5	110.8
5.444	240.6	44.2	5.444	334.3	61.4
8.167	275.0	33.7	8.167	368.4	45.1
16.33	388.4	23.8	16.33	448.1	27.4
24.5	649.7	26.5	24.5	538.5	22.0
49.0	993.5	20.3	49.0	747.3	15.3
73.5	1097	14.9	73.5	817.7	11.1
147	1265	8.61	147	926.7	6.30
220.5	1299	5.89	220.5	985.4	4.47

(3)					
γ/ s^{-1}	τ/ dyne cm^{-2}	η/ poise	γ/ s^{-1}	τ/ dyne cm^{-2}	η/ poise
2.722	328.5	120.7			
5.444	351.9	64.6			
8.167	383.6	47.0			
16.33	470.4	28.8			
24.5	577.2	23.6			
49.0	821.2	16.8			
73.5	915.0	12.4			
147	1043	7.10			
220.5	1093	4.96			

Slurry	Bob/Cup	% MIPA w/w	% KNO_3 w/w
1	SV II	0	0
2	SV I	0.0171	0
3	SV I	0.0171	0.0199

SLURRY: W % w/w TiO_2 = 44.1

(1)			(2)		
γ/ s^{-1}	τ/ dyne cm^{-2}	η/ poise	γ/ s^{-1}	τ/ dyne cm^{-2}	η/ poise
2.722	409.4	150.4	2.722	140.8	51.7
5.444	477.5	87.7	5.444	208.8	38.4
8.167	547.8	67.1	8.167	244.0	29.9
16.33	733.2	44.9	16.33	317.9	19.5
24.5	839.9	34.3	24.5	373.0	15.2
49.0	1011	20.6	49.0	468.1	9.55
73.5	1114	15.2	73.5	527.9	7.18
147	1279	8.70	147	632.3	4.30
220.5	1396	6.33	220.5	689.8	3.13

(3)					
γ/ s^{-1}	τ/ dyne cm^{-2}	η/ poise	γ/ s^{-1}	τ/ dyne cm^{-2}	η/ poise
2.722	336.7	123.7			
5.444	411.8	75.6			
8.167	471.6	57.7			
16.33	610.0	37.4			
24.5	679.2	27.7			
49.0	821.2	16.8			
73.5	915.0	12.4			
147	1093	7.44			
220.5	1208	5.48			

Slurry	Bob/Cup	% MIPA w/w	% KNO_3 w/w
1	SV I	0	0
2	SV I	0.0140	0
3	SV I	0.0140	0.0160

SLURRY: X % w/w TiO_2 = variable

(1)			(2)		
γ/ s^{-1}	τ/ dyne cm^{-2}	η/ poise	γ/ s^{-1}	τ/ dyne cm^{-2}	η/ poise
2.722	658.1	241.8	2.722	217.0	79.7
5.444	766.1	140.7	5.444	286.2	52.6
8.167	858.7	105.1	8.167	344.9	42.2
16.33	1102	67.5	16.33	456.3	27.9
24.5	1314	53.6	24.5	519.7	21.2
49.0	1654	33.8	49.0	644.0	13.1
73.5	1865	25.4	73.5	716.8	9.75
147	2194	14.9	147	843.5	5.74
220.5	2440	11.1	220.5	925.6	4.20

(3)			(4)		
γ/ s^{-1}	τ/ dyne cm^{-2}	η/ poise	γ/ s^{-1}	τ/ dyne cm^{-2}	η/ poise
2.722	100.1	36.8	7.05	42.3	6.00
5.444	130.6	24.0	14.10	51.6	3.66
8.167	151.8	18.6	21.15	58.9	2.78
16.33	189.7	11.6	42.3	72.1	1.70
24.5	208.3	8.50	63.4	79.4	1.25
49.0	245.5	5.01	126.9	96.3	0.76
73.5	264.1	3.59	190.3	105.9	0.56
147	308.8	2.10	380.7	136.3	0.36
220.5	341.5	1.55	571	155.5	0.27

Slurry	Bob/Cup	% TiO_2 w/w
1	SV I	48.9
2	SV I	42.7
3	MV II	37.6
4	MV I	31.8

SLURRY: Y % w/w TiO_2 = variable

(1)			(2)		
γ/ s^{-1}	τ/ dyne cm^{-2}	η/ poise	γ/ s^{-1}	τ/ dyne cm^{-2}	η/ poise
2.722	384.8	141.4	2.722	212.3	78.0
5.444	475.1	87.3	5.444	282.7	51.9
8.167	554.9	67.9	8.167	346.1	42.4
16.33	739.1	45.3	16.33	452.8	27.7
24.5	836.4	34.1	24.5	523.2	21.4
49.0	1034	21.1	49.0	656.9	13.4
73.5	1157	15.7	73.5	734.4	9.99
147	1373	9.34	147	858.7	5.84
220.5	1502	6.81	220.5	926.7	4.20

(3)			(4)		
γ/ s^{-1}	τ/ dyne cm^{-2}	η/ poise	γ/ s^{-1}	τ/ dyne cm^{-2}	η/ poise
2.722	184.2	67.7	2.722	127.9	47.0
5.444	240.5	44.2	5.444	183.0	33.6
8.167	295.6	36.2	8.167	224.1	27.4
16.33	397.7	24.4	16.33	302.7	18.5
24.5	459.9	18.8	24.5	348.4	14.2
49.0	576.0	11.8	49.0	432.9	8.83
73.5	645.2	8.78	73.5	482.1	6.56
147	754.3	5.13	147	570.1	3.88
220.5	820.0	3.72	220.5	619.4	2.81

(5)			(6)		
γ/ s^{-1}	τ/ dyne cm^{-2}	η/ poise	γ/ s^{-1}	τ/ dyne cm^{-2}	η/ poise
2.722	138.0	50.7	7.05	73.1	10.4
5.444	186.4	34.2	14.10	100.2	7.11
8.167	218.0	26.7	21.15	117.1	5.54
16.33	271.6	16.6	42.30	147.5	3.49
24.5	305.0	12.4	63.4	166.4	2.62
49.0	364.6	7.44	126.9	201.5	1.59
73.5	390.6	5.31	190.3	225.3	1.18
147	446.4	3.04	380.7	283.5	0.74
220.5	491.0	2.23	571	321.2	0.56

Slurry	Bob/Cup	% TiO_2 w/w
1	SV I	46.7
2	SV I	43.4
3	SV I	42.3
4	SV I	40.6
5	MV II	39.1
6	MV I	35.3

SLURRY: Z % w/w TiO_2 = variable

(1)			(2)		
γ/ s^{-1}	τ/ dyne cm^{-2}	η/ poise	γ/ s^{-1}	τ/ dyne cm^{-2}	η/ poise
2.722	432.9	159.0	2.722	153.7	56.5
5.444	532.6	97.8	5.444	231.1	42.5
8.167	654.6	80.2	8.167	263.9	32.3
16.33	859.9	52.7	16.33	366.0	22.4
24.5	950.2	38.8	24.5	443.4	18.1
49.0	1197	24.4	49.0	580.7	11.9
73.5	1384	18.8	73.5	660.5	8.99
147	1642	11.2	147	810.6	5.51
220.5	1807	8.20	220.5	891.6	4.04

(3)			(4)		
γ/ s^{-1}	τ/ dyne cm^{-2}	η/ poise	γ/ s^{-1}	τ/ dyne cm^{-2}	η/ poise
2.722	130.9	48.1	2.722	85.9	31.6
5.444	185.3	34.0	5.444	119.8	22.0
8.167	220.2	27.0	8.167	145.1	17.8
16.33	290.5	17.8	16.33	197.5	12.1
24.5	336.3	13.7	24.5	223.6	9.13
49.0	405.5	8.28	49.0	276.0	5.63
73.5	446.4	6.07	73.5	311.0	4.23
147	550.6	3.75	147	379.4	2.58
220.5	610.1	2.77	220.5	420.4	1.91

(5)					
γ/ s^{-1}	τ/ dyne cm^{-2}	η/ poise	γ/ s^{-1}	τ/ dyne cm^{-2}	η/ poise
7.05	75.8	10.8			
14.10	111.5	7.91			
21.15	131.7	6.23			
42.3	191.9	4.54			
63.4	233.9	3.69			
126.9	301.7	2.38			
190.3	340.7	1.79			
380.7	423.4	1.11			
571	469.7	0.82			

Slurry	Bob/Cup	% TiO_2 w/w	% MIPA w/w
1	SV I	53.7	0.0191
2	SV I	49.8	0.0191
3	MV II	48.5	0.0191
4	MV II	47.3	0.0191
5	MV I	44.3	0.0191

SLURRY: AA % w/w TiO_2 = variable

(1)			(2)		
γ/ s^{-1}	τ/ dyne cm^{-2}	η/ poise	γ/ s^{-1}	τ/ dyne cm^{-2}	η/ poise
2.722	168.1	61.8	2.722	142.5	52.4
5.444	237.3	43.6	5.444	201.6	37.0
8.167	282.0	34.5	8.167	240.3	29.4
16.33	368.3	22.6	16.33	324.4	19.9
24.5	405.5	16.6	24.5	375.7	15.3
49.0	487.3	9.94	49.0	450.1	9.19
73.5	550.6	7.49	73.5	491.0	6.68
147	647.3	4.40	147	591.5	4.02
220.5	736.6	3.34	220.5	665.9	3.02

(3)			(4)		
γ/ s^{-1}	τ/ dyne cm^{-2}	η/ poise	γ/ s^{-1}	τ/ dyne cm^{-2}	η/ poise
2.722	149.2	54.8	2.722	75.1	27.6
5.444	212.0	38.9	5.444	110.1	20.2
8.167	250.7	30.7	8.167	130.6	16.0
16.33	333.7	20.4	16.33	176.0	10.8
24.5	375.7	15.3	24.5	203.9	8.32
49.0	457.6	9.34	49.0	251.5	5.13
73.5	517.1	7.04	73.5	280.5	3.82
147	617.5	4.20	147	356.4	2.42
220.5	684.5	3.10	220.5	390.6	1.77

Slurry	Bob/Cup	% TiO_2 w/w	% MIPA w/w
1	MV II	50.6	0.0198
2	MV II	49.8	0.0198
3	MV II	49.1	0.0198
4	MV II	46.9	0.0198
5	MV I	45.2	0.0198
6	MV I	44.4	0.0198
7	MV I	41.6	0.0198

SLURRY: AA % w/w TiO_2 = variable

(5)			(6)		
γ/ s^{-1}	τ/ dyne cm^{-2}	η/ poise	γ/ s^{-1}	τ/ dyne cm^{-2}	η/ poise
7.05	79.1	11.2	7.05	77.7	11.0
14.10	115.8	8.21	14.10	117.1	8.30
21.15	145.9	6.90	21.15	142.9	6.76
42.3	204.1	4.83	42.3	190.5	4.50
63.4	241.8	3.81	63.4	222.0	3.50
126.9	310.6	2.45	126.9	275.9	2.17
190.3	340.7	1.79	190.3	317.6	1.67
380.7	456.5	1.20	380.7	400.3	1.05
571	552.4	0.97	571	459.8	0.81

(7)					
γ/ s^{-1}	τ/ dyne cm^{-2}	η/ poise	γ/ s^{-1}	τ/ dyne cm^{-2}	η/ poise
7.05	2.32	0.33			
14.10	3.31	0.23			
21.15	4.63	0.22			
42.3	8.93	0.21			
63.4	10.25	0.16			
126.9	19.5	0.15			
190.3	25.1	0.13			
380.7	58.9	0.15			
571	105.9	0.19			

SLURRY: BB % w/w TiO_2 = variable

(1)			(2)		
γ/ s^{-1}	τ/ dyne cm^{-2}	η/ poise	γ/ s^{-1}	τ/ dyne cm^{-2}	η/ poise
2.722	225.2	82.7	2.722	191.2	70.2
5.444	369.5	67.9	5.444	303.8	55.8
8.167	442.3	54.2	8.167	353.1	43.2
16.33	559.6	34.3	16.33	455.2	27.9
24.5	656.9	26.8	24.5	549.0	22.4
49.0	857.5	17.5	49.0	716.8	14.6
73.5	984.2	13.4	73.5	822.3	11.2
147	1208	8.22	147	1019	6.93
220.5	1314	5.96	220.5	1117	5.07

(3)			(4)		
γ/ s^{-1}	τ/ dyne cm^{-2}	η/ poise	γ/ s^{-1}	τ/ dyne cm^{-2}	η/ poise
2.722	152.5	56.0	2.722	117.2	43.1
5.444	215.9	39.7	5.444	169.6	31.2
8.167	261.6	32.0	8.167	205.3	25.1
16.33	375.4	23.0	16.33	282.0	17.3
24.5	457.5	18.7	24.5	324.8	13.3
49.0	597.1	12.2	49.0	405.5	8.28
73.5	680.4	9.26	73.5	457.6	6.23
147	832.9	5.67	147	569.2	3.87
220.5	938.5	4.26	220.5	654.7	2.97

Slurry	Bob/Cup	% TiO_2 w/w	% MIPA w/w
1	SV I	54.0	0.0232
2	SV I	52.7	0.0232
3	SV I	51.8	0.0232
4	MV II	49.8	0.0232
5	MV II	48.6	0.0232
6	MV I	47.6	0.0232
7	MV I	45.9	0.0232

SLURRY: BB % w/w TiO_2 = variable

(5)			(6)		
γ/ s^{-1}	τ/ dyne cm^{-2}	η/ poise	γ/ s^{-1}	τ/ dyne cm^{-2}	η/ poise
2.722	74.8	27.5	7.05	95.6	13.6
5.444	111.6	20.5	14.10	142.9	10.1
8.167	133.9	16.4	21.15	179.3	8.48
16.33	180.0	11.0	42.3	245.8	5.81
24.5	218.4	8.91	63.4	285.1	4.49
49.0	274.9	5.61	126.9	357.3	2.82
73.5	306.5	4.17	190.3	416.8	2.19
147	401.8	2.73	380.7	529.3	1.39
220.5	472.4	2.14	571	628.5	1.10

(7)					
γ/ s^{-1}	τ/ dyne cm^{-2}	η/ poise	γ/ s^{-1}	τ/ dyne cm^{-2}	η/ poise
7.05	79.7	11.3			
14.10	119.1	8.45			
21.15	142.2	6.72			
42.3	195.2	4.61			
63.4	234.9	3.70			
126.9	299.0	2.36			
190.3	337.4	1.77			
380.7	433.3	1.14			
571	519.4	0.91			

SLURRY: CC % w/w TiO_2 = 50.4

(1)			(2)		
γ/ s^{-1}	τ/ dyne cm^{-2}	η/ poise	γ/ s^{-1}	τ/ dyne cm^{-2}	η/ poise
2.722	144.3	53.0	2.722	181.8	66.8
5.444	210.0	38.6	5.444	292.1	53.7
8.167	244.0	29.9	8.167	350.8	43.0
16.33	341.4	20.9	16.33	444.6	27.2
24.5	410.6	16.8	24.5	529.1	21.6
49.0	526.7	10.7	49.0	702.7	14.3
73.5	598.3	8.14	73.5	801.2	10.9
147	726.1	4.94	147	974.8	6.63
220.5	811.8	3.68	220.5	1068	4.84

(3)			(4)		
γ/ s^{-1}	τ/ dyne cm^{-2}	η/ poise	γ/ s^{-1}	τ/ dyne cm^{-2}	η/ poise
2.722	259.3	95.3	2.722	366.0	134.5
5.444	356.6	65.5	5.444	449.3	82.5
8.167	445.8	54.6	8.167	558.4	68.4
16.33	560.7	34.3	16.33	706.2	43.2
24.5	644.0	26.3	24.5	786.0	32.1
49.0	855.2	17.5	49.0	1011	20.6
73.5	985.4	13.4	73.5	1171	15.9
147	1197	8.14	147	1419	9.65
220.5	1314	5.96	220.5	1548	7.02

Slurry	Bob/Cup	% MIPA w/w	% KNO_3 w/w
1	SV I	0.0198	0
2	SV I	0.0198	0.00170
3	SV I	0.0198	0.00354
4	SV I	0.0198	0.00553
5	SV I	0.0230	0.00553
6	SV I	0.0230	0.00791
7	SV I	0.0230	0.0107

SLURRY: CC % w/w TiO_2 = 50.4

(5)			(6)		
γ/ s^{-1}	τ/ dyne cm^{-2}	η/ poise	γ/ s^{-1}	τ/ dyne cm^{-2}	η/ poise
2.722	259.3	95.3	2.722	362.5	133.2
5.444	371.9	68.3	5.444	449.3	82.5
8.167	452.8	55.4	8.167	543.1	66.5
16.33	571.3	35.0	16.33	705.0	43.2
24.5	645.2	26.3	24.5	782.5	31.9
49.0	847.0	17.3	49.0	999.5	20.4
73.5	976.0	13.3	73.5	1152	15.7
147	1197	8.14	147	1408	9.58
220.5	1314	5.96	220.5	1560	7.07

(7)					
γ/ s^{-1}	τ/ dyne cm^{-2}	η/ poise	γ/ s^{-1}	τ/ dyne cm^{-2}	η/ poise
2.722	422.3	155.1			
5.444	511.5	94.0			
8.167	604.1	74.0			
16.33	793.0	48.6			
24.5	877.5	35.8			
49.0	1093	22.3			
73.5	1279	17.4			
147	1548	10.5			
220.5	1736	7.87			

SLURRY: DD % w/w TiO_2 = 51.0

(1)			(2)		
γ/ s^{-1}	τ/ dyne cm^{-2}	η/ poise	γ/ s^{-1}	τ/ dyne cm^{-2}	η/ poise
2.722	354.3	130.2	2.722	385.9	141.8
5.444	449.3	82.5	5.444	475.1	87.3
8.167	556.0	68.1	8.167	576.0	70.5
16.33	714.4	43.7	16.33	754.3	46.2
24.5	801.2	32.7	24.5	836.4	34.1
49.0	1032	21.1	49.0	1077	22.0
73.5	1185	16.1	73.5	1197	16.3
147	1361	9.26	147	1443	9.82
220.5	1513	6.86	220.5	1631	7.40

(3)			(4)		
γ/ s^{-1}	τ/ dyne cm^{-2}	η/ poise	γ/ s^{-1}	τ/ dyne cm^{-2}	η/ poise
2.722	289.8	106.5	2.722	194.9	71.6
5.444	383.6	70.5	5.444	258.2	47.4
8.167	472.8	57.9	8.167	309.5	37.9
16.33	605.3	37.1	16.33	409.2	25.1
24.5	688.6	28.1	24.5	468.7	19.1
49.0	916.2	18.7	49.0	598.9	12.2
73.5	1058	14.4	73.5	669.6	9.11
147	1232	8.38	147	814.7	5.54
220.5	1408	6.39	220.5	922.7	4.18

Slurry	Bob/Cup	% MIPA w/w
1	SV I	0.0169
2	SV I	0.0180
3	SV I	0.0212
4	MV II	0.0266
5	MV II	0.0311
6	MV I	0.0343
7	MV I	0.0389

SLURRY: DD % w/w TiO_2 = 51.0

(5)			(6)		
γ/ s^{-1}	τ/ dyne cm^{-2}	η/ poise	γ/ s^{-1}	τ/ dyne cm^{-2}	η/ poise
2.722	70.3	25.8	7.05	110.8	15.7
5.444	99.0	18.2	14.10	153.8	10.9
8.167	119.0	14.6	21.15	191.9	9.07
16.33	158.5	9.71	42.3	258.4	6.11
24.5	180.8	7.38	63.4	299.7	4.72
49.0	228.0	4.65	126.9	370.5	2.92
73.5	267.1	3.63	190.3	453.2	2.38
147	372.0	2.53	380.7	602.1	1.58
220.5	439.0	1.99	571	737.7	1.29

(7)					
γ/ s^{-1}	τ/ dyne cm^{-2}	η/ poise	γ/ s^{-1}	τ/ dyne cm^{-2}	η/ poise
7.05	6.29	0.89			
14.10	8.27	0.59			
21.15	10.3	0.49			
42.3	18.5	0.44			
63.4	27.1	0.43			
126.9	43.7	0.34			
190.3	57.2	0.30			
380.7	105.9	0.28			
571	165.4	0.29			

SLURRY: EE % w/w TiO_2 = 50.9

(1)			(2)		
γ/ s^{-1}	τ/ dyne cm^{-2}	η/ poise	γ/ s^{-1}	τ/ dyne cm^{-2}	η/ poise
2.722	315.6	115.9	2.722	271.0	99.6
5.444	416.5	76.5	5.444	364.8	67.0
8.167	511.5	62.6	8.167	450.5	55.2
16.33	669.8	41.0	16.33	579.5	35.5
24.5	752.0	30.7	24.5	669.8	27.3
49.0	985.4	20.1	49.0	893.9	18.2
73.5	1136	15.5	73.5	1041	14.2
147	1314	8.94	147	1267	8.62
220.5	1490	6.76	220.5	1408	6.39

(3)			(4)		
γ/ s^{-1}	τ/ dyne cm^{-2}	η/ poise	γ/ s^{-1}	τ/ dyne cm^{-2}	η/ poise
2.722	201.8	74.1	2.722	153.7	56.5
5.444	287.4	52.8	5.444	234.6	43.1
8.167	357.8	43.8	8.167	282.7	34.6
16.33	459.9	28.2	16.33	370.7	22.7
24.5	544.3	22.2	24.5	450.5	18.4
49.0	749.6	15.3	49.0	610.0	12.4
73.5	871.6	11.9	73.5	701.5	9.54
147	1087	7.39	147	877.5	5.97
220.5	1197	5.43	220.5	988.9	4.48

Slurry	Bob/Cup	% MIPA w/w	% KNO_3 w/w
1	SV I	0.0177	0
2	SV I	0.0201	2.56×10^{-4}
3	SV I	0.0227	5.32×10^{-4}
4	SV I	0.0261	9.01×10^{-4}
5	MV II	0.0298	1.30×10^{-3}
6	MV II	0.0330	1.63×10^{-3}
7	MV I	0.0363	1.99×10^{-3}

SLURRY: EE % w/w TiO_2 = 50.9

(5)			(6)		
γ/ s^{-1}	τ/ dyne cm^{-2}	η/ poise	γ/ s^{-1}	τ/ dyne cm^{-2}	η/ poise
2.722	97.8	35.9	2.722	81.5	29.9
5.444	138.4	25.4	5.444	113.5	20.8
8.167	165.5	20.3	8.167	136.2	16.7
16.33	229.5	14.1	16.33	183.0	11.2
24.5	267.8	10.9	24.5	222.5	9.08
49.0	343.0	7.0	49.0	278.3	5.68
73.5	405.5	5.52	73.5	326.2	4.44
147	505.9	3.44	147	405.5	2.76
220.5	591.5	2.68	220.5	479.9	2.18

(7)		
γ/ s^{-1}	τ/ dyne cm^{-2}	η/ poise
7.05	6.95	0.99
14.10	9.26	0.66
21.15	10.6	0.50
42.3	17.2	0.41
63.4	245.1	3.86
126.9	330.8	2.61
190.3	426.7	2.24
380.7	569.0	1.49
571	694.7	1.22

SLURRY: FF % w/w TiO_2 = 50.9

(1)			(2)		
γ/ s^{-1}	τ/ dyne cm^{-2}	η/ poise	γ/ s^{-1}	τ/ dyne cm^{-2}	η/ poise
2.722	187.7	69.0	2.722	235.8	86.6
5.444	305.0	56.0	5.444	344.9	63.4
8.167	367.2	45.0	8.167	423.5	51.9
16.33	469.2	28.7	16.33	534.9	32.8
24.5	560.7	22.9	24.5	612.4	25.0
49.0	730.8	14.9	49.0	816.5	16.7
73.5	831.7	11.3	73.5	929.1	12.6
147	1004	6.83	147	1127	7.67
220.5	1114	5.05	220.5	1232	5.59

(3)			(4)		
γ/ s^{-1}	τ/ dyne cm^{-2}	η/ poise	γ/ s^{-1}	τ/ dyne cm^{-2}	η/ poise
2.722	258.1	94.8	2.722	241.7	88.8
5.444	353.1	64.9	5.444	349.6	64.2
8.167	443.4	54.3	8.167	417.6	51.1
16.33	560.0	34.3	16.33	518.5	31.8
24.5	633.5	25.9	24.5	588.9	24.0
49.0	832.9	17.0	49.0	774.2	15.8
73.5	950.2	12.9	73.5	882.2	12.0
147	1147	7.80	147	1071	7.29
220.5	1279	5.80	220.5	1197	5.43

Slurry	Bob/Cup	% MIPA w/w	% KNO_3 w/w
1	SV I	0.0184	0
2	SV I	0.0209	0.00335
3	SV I	0.0242	0.00777
4	SV I	0.0284	0.0134
5	SV I	0.0322	0.0185
6	SV I	0.0404	0.0295
7	MV II	0.0493	0.0415
8	MV II	0.0603	0.0563

SLURRY: FF % w/w TiO_2 = 50.9

(5)			(6)		
γ/ s^{-1}	τ/ dyne cm^{-2}	η/ poise	γ/ s^{-1}	τ/ dyne cm^{-2}	η/ poise
2.722	235.8	86.6	2.722	208.8	76.7
5.444	335.5	61.6	5.444	298.0	54.7
8.167	398.9	48.8	8.167	348.4	42.7
16.33	490.4	30.0	16.33	422.3	25.9
24.5	560.7	22.9	24.5	479.8	19.6
49.0	735.5	15.0	49.0	620.6	12.7
73.5	834.1	11.3	73.5	699.2	9.51
147	1014	6.90	147	856.4	5.83
220.5	1126	5.11	220.5	954.9	4.33

(7)			(8)		
γ/ s^{-1}	τ/ dyne cm^{-2}	η/ poise	γ/ s^{-1}	τ/ dyne cm^{-2}	η/ poise
2.722	241.8	88.8	2.722	130.6	48.0
5.444	294.6	54.1	5.444	158.8	29.2
8.167	327.4	40.1	8.167	177.4	21.7
16.33	409.2	25.1	16.33	222.8	13.6
24.5	461.3	18.8	24.5	249.6	10.2
49.0	569.2	11.6	49.0	298.7	6.10
73.5	636.1	8.65	73.5	337.8	4.60
147	747.7	5.09	147	409.2	2.78
220.5	833.3	3.78	220.5	465.0	2.11

SLURRY: GG % w/w TiO_2 = 51.0

(1)			(2)		
γ/ s^{-1}	τ/ dyne cm^{-2}	η/ poise	γ/ s^{-1}	τ/ dyne cm^{-2}	η/ poise
2.722	210.0	77.1	2.722	251.0	92.2
5.444	315.6	58.0	5.444	353.1	64.9
8.167	384.8	47.1	8.167	441.1	54.0
16.33	493.9	30.2	16.33	550.2	33.7
24.5	577.2	23.6	24.5	633.5	25.9
49.0	757.8	15.5	49.0	836.4	17.1
73.5	856.4	11.7	73.5	959.6	13.1
147	1031	7.01	147	1148	7.81
220.5	1150	5.22	220.5	1267	5.75

(3)			(4)		
γ/ s^{-1}	τ/ dyne cm^{-2}	η/ poise	γ/ s^{-1}	τ/ dyne cm^{-2}	η/ poise
2.722	224.1	82.3	2.722	202.9	74.5
5.444	322.6	59.3	5.444	301.5	55.4
8.167	391.8	48.0	8.167	368.4	45.1
16.33	493.9	30.2	16.33	450.5	27.6
24.5	571.3	23.3	24.5	532.6	21.7
49.0	760.2	15.5	49.0	701.5	14.3
73.5	869.3	11.8	73.5	796.5	10.8
147	1068	7.27	147	979.5	6.66
220.5	1232	5.59	220.5	1082	4.91

Slurry	Bob/Cup	% MIPA w/w	% LiCL w/w
1	SV I	0.0183	0
2	SV I	0.0208	0.00140
3	SV I	0.0241	0.00327
4	SV I	0.0269	0.00487
5	SV I	0.0315	0.00745
6	MV II	0.0355	0.00973
7	MV II	0.0399	0.0122
8	MV I	0.0454	0.0153

SLURRY: GG % w/w TiO_2 = 51.0

(5)			(6)		
γ/ s^{-1}	τ/ dyne cm^{-2}	η/ poise	γ/ s^{-1}	τ/ dyne cm^{-2}	η/ poise
2.722	165.4	60.8	2.722	149.2	54.8
5.444	252.2	46.3	5.444	192.0	35.3
8.167	288.6	35.3	8.167	227.7	27.9
16.33	368.4	22.6	16.33	299.1	18.3
24.5	435.2	17.8	24.5	340.0	13.9
49.0	572.5	11.7	49.0	416.6	8.50
73.5	648.7	8.83	73.5	472.4	6.43
147	791.8	5.39	147	561.7	3.82
220.5	891.6	4.04	220.5	643.6	2.92

(7)			(8)		
γ/ s^{-1}	τ/ dyne cm^{-2}	η/ poise	γ/ s^{-1}	τ/ dyne cm^{-2}	η/ poise
2.722	81.5	29.9	7.05	95.9	13.6
5.444	109.0	20.0	14.10	128.4	9.11
8.167	126.1	15.4	21.15	152.8	7.22
16.33	161.1	9.87	42.3	195.5	4.62
24.5	183.4	7.49	63.4	224.9	3.55
49.0	234.7	4.79	126.9	294.4	2.32
73.5	267.8	3.64	190.3	344.0	1.81
147	340.8	2.32	380.7	459.8	1.21
220.5	405.5	1.84	571	552.4	0.97

TABLE B.7.1. Fraction redispersion for rutile in aqueous MIPA solution as a function of centrifuge speed

Rotor = angle t_c = 30 mins

[MIPA]/ mol dm^{-3}	ω/ rad s^{-1}	C_0 $\times 10^{-14}$	C $\times 10^{-14}$	F
2.0×10^{-4}	524	12.6	10.7	0.849
	3142		3.10	0.246
0.010	524	3.86	3.55	0.920
	3142		2.00	0.518
0.030	524	3.93	3.60	0.916
	3142		1.49	0.379
0.100	524	5.79	5.26	0.908
	3142		1.52	0.263

TABLE B.7.2. Fraction redispersion as a function of ionic strength for 0.1 M MIPA

Rotor = angle t_c = 30 mins

[KNO_3]/ mol dm^{-3}	ω/ rad s^{-1}	C_0 $\times 10^{-14}$	C $\times 10^{-14}$	F
8.0×10^{-4}	115	5.47	1.93	0.353
	262		2.22	0.406
	367		1.45	0.265
1.0×10^{-3}	524	9.68	1.52	0.157
	1571		0.882	0.091
1.9×10^{-3}	115	4.67	0.790	0.169
	262		0.779	0.167
	367		0.551	0.118
4.1×10^{-3}	115	4.38	0.632	0.144
	262		<0.29	<0.066
	367		<0.26	<0.059
7.0×10^{-3}	524	19.2	1.45	0.076
	1571		0.294	0.015
0.0109	115	5.76	0.544	0.094
	262		<0.22	<0.038
	367		<0.14	<0.024

TABLE B.7.3. Fraction redispersed as a function of t_c for 0.1 M MIPA

ω = 262 rad s^{-1} Rotor = angle

$[KNO_3]$/ mol dm^{-3}	t_c/ min	C_0 $x10^{-14}$	C $x10^{-14}$	F
$0.8x10^{-3}$	10	5.47	3.47	0.634
	30		2.22	0.406
$1.9x10^{-3}$	10	4.67	1.48	0.317
	30		0.779	0.167
$4.1x10^{-3}$	10	4.38	0.514	0.117
	30		<0.29	<0.066
0.0109	10	5.76	0.239	0.041
	30		<0.22	<0.038

TABLE B.7.4. Fraction redispersed as a function of pH for 0.1 M MIPA

Rotor = angle t_c = 30 mins

$[MIPA^+]$/ mol dm^{-3}	$\frac{[MIPA^+]}{[MIPA]}$	ω/ rad s^{-1}	C_0 $x10^{-14}$	C $x10^{-14}$	F
0.00193	0.0193	157	10.9	4.85	0.445
		314		2.57	0.236
0.00385	0.0385	157	12.0	11.2	0.933
		314		5.58	0.465
0.00963	0.0963	157	4.52	0.735	0.163
		314		0.162	0.036
0.0193	0.193	157	3.36	-	-
		314		-	-

TABLE B.7.5. Effect of initial particle number on the fraction redispersed

Rotor = angle t_c = 30 mins [MIPA] = 0.1 mol dm^{-3}

ω/ rad s^{-1}	C_0 $\times 10^{-14}$	C $\times 10^{-14}$	F
440	2.48	0.882	0.356
1047		1.30	(0.524)
440	9.28	3.53	0.380
1047		1.98	0.213
440	14.5	7.49	0.517
1047		4.20	0.290
440	26.5	17.9	0.675
1047		6.83	0.258

Rotor = swing-out t_c = 35 mins [MIPA] = 0.010 mol dm^{-3}
ω = 1246 rad s^{-1}

C_0 $\times 10^{-14}$	C $\times 10^{-14}$	F
2.48	1.45	0.585
7.85	2.20	0.280
24.9	7.83	0.314
30.5	7.41	0.243
39.2	10.2	0.260
73.8	58.7	0.795

TABLE B.7.6. Effect of ω and ionic strength on fraction redispersed (25°C)

[MIPA] = 5×10^{-3} mol dm^{-3}

$[KNO_3]$/ mol dm^{-3}	ω/ rad s^{-1}	t_c/ min	C_0 $\times 10^{-14}$	C $\times 10^{-14}$	F
0	524	36	3.71	3.67	0.989
	1058	36	3.71	3.56	0.960
	1319	37	4.19	2.27	0.542
	1571	35	5.14	3.81	(0.741)
	1812	41	4.04	1.92	0.475
	2105	39	5.14	2.07	0.403
0.001	524	36	4.00	3.64	0.910
	1058	36	4.00	2.23	0.558
	1319	37	4.40	1.63	0.370
	1571	35	4.50	1.40	0.311
	1812	41	4.05	1.33	0.328
	2105	39	4.50	1.04	0.231
0.002	524	36	3.78	2.94	0.778
	1058	36	3.78	1.59	0.421
	1319	37	4.31	1.51	0.350
	1571	35	4.79	1.04	0.217
	1812	41	4.05	1.09	0.269
	2105	39	3.79	0.997	0.208
0.004	115	36	4.25	3.75	0.882
	209	35	5.75	4.08	0.710
	325	35	4.60	2.07	0.450
	429	35	5.78	2.87	0.497
	534	36	4.35	1.67	0.384
	628	36	4.46	1.62	0.363
0.006	115	36	4.31	1.41	0.327
	209	35	4.25	2.61	0.614
	325	35	4.55	0.794	0.175
	429	35	4.34	1.42	0.327
	534	36	4.37	1.20	0.275
	628	36	4.40	0.566	0.129
0.0100	115	36	4.25	0.836	0.197
	209	35	4.43	0.718	0.162
	325	35	4.19	0.338	0.081
	429	35	4.60	0.528	0.115
	534	36	4.44	0.499	0.112
	628	36	4.31	0.514	0.119

TABLE B.7.7. Check for reproducibility with respect to choice of polypropylene centrifuge tube

[MIPA] = 0.010 mol dm^{-3} ω = 419 rad s^{-1} [KNO_3] = 0.005 mol dm^{-3} t_c = 30 mins

Tube	1	2	3
C $x10^{-14}$	4.16	4.21	4.18

TABLE B.7.8. Effect of ω and ionic strength on the fraction redispersed (25°C)
[MIPA] = 0.020 mol dm^{-3} t_c = 35 mins

$[KNO_3]$/ mol dm^{-3}	ω/ rad s^{-1}	C_0 x10^{-14}	C x10^{-14}	F
0	230	8.87	8.14	0.918
	335	9.46	7.92	0.837
		9.97	9.60	0.963
	(534	8.98	5.78)	
	545	9.82	8.14	0.829
	806	10.5	8.94	0.851
		7.99	7.77	0.972
	1058	8.21	7.48	0.911
	(1079	9.53	5.59)	
	1309	8.58	7.70	0.897
	1330	9.90	8.28	0.836
	1581	10.7	7.99	0.747
	1602	7.99	7.70	0.964
	1843	9.16	7.11	0.776
	1916	9.68	7.92	0.818
	2094	8.80	6.22	0.707
0.00372	335	10.0	7.77	0.777
	534	9.82	5.01	0.510
	545	9.90	1.63	0.165
	806	8.43	3.14	0.372
	1330	9.97	0.982	0.098
	1581	10.2	1.50	0.147
	1916	9.75	1.48	0.152
0.00520	230	8.43	7.44	0.883
	335	8.36	6.74	0.806
	534	7.92	5.83	0.736
	806	10.85	6.89	0.635
	1058	7.92	3.62	0.457
	1309	10.63	6.96	0.655
	1602	8.50	1.81	0.213
	1843	8.58	1.55	0.181
	2094	10.48	1.77	0.169
0.00743	230	7.70	1.59	0.206
	335	8.28	1.20	0.145
	534	9.24	3.12	0.338
	806	9.24	1.86	0.201
	1058	8.94	2.26	0.253
	1309	9.68	0.938	0.097
	1602	8.36	1.20	0.144
	1843	8.14	1.26	0.155
	2094	9.60	0.909	0.095
0.0149	335	9.09	1.10	0.121
	534	9.60	0.880	0.092
	545	8.36	0.997	0.119
	806	8.72	0.953	0.109
	1079	8.87	0.513	0.058
	1330	8.28	0.557	0.067
	1581	9.09	0.279	0.031
	1916	7.33	0.455	0.062

TABLE B.7.9. Effect of ω on the fraction redispersed in high pH water

t_c = 35 mins distilled water

pH	ω/ rad s^{-1}	C_0 $x10^{-14}$	C $x10^{-14}$	F
10.56	524	9.38	8.87	0.946
	1068	9.68	6.22	0.643
	1351	9.75	3.61	0.370
	1592	9.38	3.39	0.361
	1801	10.26	3.55	0.346
	2105	10.41	3.23	0.310
11.01	524	9.75	8.28	0.849
	1068	9.60	7.55	0.786
	1351	10.19	6.62	0.650
	1592	9.53	5.85	0.614
	1801	11.22	5.66	0.504
	2105	10.63	2.80	0.263
11.50	524	9.24	8.72	0.944
	1068	9.68	4.89	0.505
	1351	9.42	4.14	0.439
	1592	9.82	3.98	0.405
	1801	10.19	3.23	0.317
	2105	10.12	1.96	0.194

TABLE B.7.10. Fraction redispersed as a function of MIPA concentration at a fixed pH (25°C)

t_c = 35 mins pH = 10.95

[MIPA]/ mol dm^{-3}	ω/ rad s^{-1}	C_0 $\times 10^{-14}$	C $\times 10^{-14}$	$^{\circ}F$
1.01×10^{-4}	534	10.41	6.38	0.613
	942	10.04	2.78	0.277
	1340	9.92	1.70	0.171
	1592	8.67	2.79	0.322
	1854	8.89	2.19	0.246
	2094	9.11	2.04	0.224
5.04×10^{-4}	534	9.77	8.21	0.840
	942	10.12	6.58	0.650
	1340	9.63	4.40	0.457
	1592	10.41	5.29	0.508
	1854	9.92	3.64	0.367
	2094	9.99	4.63	0.463
2.02×10^{-3}	534	9.92	9.85	0.993
	942	10.56	7.97	0.755
	1340	10.56	8.43	0.798
	1592	9.18	5.03	0.548
	1854	8.89	3.95	0.444
	2094	9.11	5.14	0.564

TABLE B.7.11. Fraction redispersed as a function of MIPA concentration at a fixed pH (25°C)

t_c = 35 mins

[MIPA]/ mol dm^{-3}	pH	ω/ rad s^{-1}	C_0 $x10^{-14}$	C $x10^{-14}$	F
$2.02x10^{-5}$	10.95	440	10.41	8.51	0.817
		754	10.48	9.02	0.861
		1131	9.97	7.05	0.707
		1299	10.48	6.96	0.664
		1581	10.52	6.84	0.650
		2094	10.85	4.62	0.426
$3.02x10^{-4}$	10.97	440	10.26	5.37	0.523
		754	9.97	5.41	0.543
		1131	10.63	4.86	0.457
		1299	10.04	2.90	0.289
		1581	11.29	3.61	0.320
		2094	10.34	2.26	0.219
0.0101	11.12	440	10.45	9.75	0.933
		754	9.90	9.24	0.933
		1131	10.34	9.09	0.879
		1299	10.19	8.28	0.813
		1581	10.78	8.94	0.829
		2094	10.78	8.50	0.788

TABLE B.7.12. Fraction redispersed as a function of MIPA concentration at pH 11 (25°C)

t_c = 35 mins

[MIPA]/ mol dm^{-3}	pH	ω/ rad s^{-1}	C_0 $x10^{-14}$	C $x10^{-14}$	F
$5.03x10^{-5}$	11.07	230	9.97	10.19	1.02
		325	9.31	8.80	0.945
		806	9.16	6.71	0.733
		1288	9.09	5.78	0.636
		1613	10.70	7.69	0.719
		2094	10.41	4.79	0.460
$2.01x10^{-4}$	10.93	230	10.19	10.04	0.985
		325	8.94	7.27	0.813
		806	8.06	6.16	0.764
		1288	8.36	4.93	0.590
		1613	10.78	5.21	0.483
		2094	10.26	2.96	0.288
$1.01x10^{-3}$	10.95	230	11.95	11.51	0.963
		325	9.53	8.87	0.931
		806	8.87	7.48	0.843
		1288	8.87	6.42	0.724
		1613	10.19	8.13	0.798
		2094	9.97	4.99	0.501
$3.02x10^{-5}$	10.95	555	10.12	8.87	0.876
		2094	9.97	3.54	0.355
$9.03x10^{-5}$	10.92	555	8.28	8.14	0.983
		2094	8.65	3.70	0.428
$4.02x10^{-3}$	10.94	555	10.04	9.16	0.912
		2094	10.04	7.18	0.715

TABLE B.7.13. Fraction redispersed as a function of MIPA concentration in the presence of electrolyte (25°C)
t_c = 35 mins $[KNO_3]$ = 0.005 mol dm^{-3}

[MIPA]/ mol dm^{-3}	pH	ω/ rad s^{-1}	C_0 $\times 10^{-14}$	C $\times 10^{-14}$	F
2.00×10^{-5}	10.95	440	8.36	1.74	0.208
		1068	8.50	1.60	0.188
		1916	8.58	1.03	0.120
1.00×10^{-4}	10.97	450	9.02	4.82	0.534
		1068	9.75	1.19	0.122
		1927	9.82	1.45	0.148
5.00×10^{-4}	10.93	440	10.34	6.79	0.657
		1068	10.48	3.80	0.363
		1916	10.41	0.821	0.079
8.00×10^{-4}	10.95	450	8.65	5.81	0.672
		1068	8.94	2.04	0.228
		1927	9.09	1.52	0.167
2.00×10^{-3}	10.95	440	8.65	5.01	0.579
		1068	8.72	3.58	0.411
		1916	8.87	1.96	0.221
5.00×10^{-3}	10.92	450	8.72	5.48	0.628
		1068	8.94	3.34	0.374
		1927	9.09	2.28	0.251

TABLE B.7.14. Fraction redispersed as a function of MIPA concentration and ionic strength (25°C)

t_c = 35 mins

[MIPA]/ mol dm^{-3}	[KNO_3]/ mol dm^{-3}	pH	ω/ rad s^{-1}	C_0 x10^{-14}	C x10^{-14}	F
2.0×10^{-5}	2.0×10^{-4}	10.95	450	8.80	8.50	0.966
			1079	8.58	6.93	0.808
			1906	8.58	4.38	0.510
2.0×10^{-5}	2.0×10^{-3}	10.96	450	10.12	8.28	0.818
			1089	10.34	4.47	0.432
			1906	9.82	4.94	0.503
6.0×10^{-4}	2.0×10^{-4}	10.95	450	9.16	8.69	0.949
			1079	8.98	7.92	0.882
			1906	9.24	4.70	0.509
6.0×10^{-4}	2.0×10^{-3}	10.95	450	10.19	8.06	0.791
			1089	10.19	5.62	0.552
			1906	9.60	4.06	0.423
0.020	2.0×10^{-4}	11.02	450	8.72	8.83	1.01
			1079	8.80	8.65	0.983
			1906	9.60	7.70	0.802
0.020	2.0×10^{-3}	11.03	450	11.44	10.34	0.904
			1089	10.26	8.28	0.807
			1906	10.12	3.70	0.366
0.0499	5.0×10^{-3}	11.58	450	9.79	6.74	0.688
			1068	9.53	6.38	0.669
			1916	9.24	1.58	0.171
0.150	5.0×10^{-3}	11.58	450	9.38	6.52	0.695
			1068	9.75	7.40	0.759
			1916	9.82	8.06	0.821
0.250	5.0×10^{-3}	11.59	450	8.80	7.33	0.833
			1068	9.38	6.45	0.688
			1916	9.75	5.72	0.587

TABLE B.7.15. Fraction redispersed as a function of pH at constant ionic strength (25°C)

t_c = 35 mins [MIPA] = 0.020 mol dm^{-3}

pH	[$MIPA^+$]/ mol dm^{-3}	[KNO_3]/ mol dm^{-3}	Ionic Strength/ mol dm^{-3}	ω/ rad s^{-1}	C_0 x10^{-14}	C x10^{-14}	F
10.72	0.95×10^{-3}	9.05×10^{-3}	0.0100	199	9.38	1.67	0.178
				639	9.24	0.990	0.107
				1319	8.58	1.36	0.159
10.50	1.89×10^{-3}	8.11×10^{-3}	0.0100	199	10.26	4.18	0.407
				639	10.63	3.74	0.352
				1319	10.56	1.54	0.146
10.20	3.78×10^{-3}	6.22×10^{-3}	0.0100	199	11.95	1.39	0.116
				639	10.04	2.75	0.274
				1319	9.90	1.23	0.124
9.95	5.68×10^{-3}	4.32×10^{-3}	0.0100	94	9.38	4.49	0.479
				199	10.19	3.34	0.328
				440	10.78	2.95	0.274
9.74	7.57×10^{-3}	2.43×10^{-3}	0.0100	94	9.82	5.21	0.531
				199	9.82	4.06	0.413
				440	9.82	3.02	0.308
9.55	9.46×10^{-3}	0.54×10^{-3}	0.0100	94	8.72	5.81	0.666
				199	8.94	5.02	0.562
				440	8.65	4.18	0.483

TABLE B.7.16. Fraction dispersed as a function of pH at constant ionic strength (25°C)

t_c = 35 mins [MIPA] = 0.010 mol dm^{-3}

pH	[$MIPA^+$]/ mol dm^{-3}	[KNO_3]/ mol dm^{-3}	Ionic Strength/ mol dm^{-3}	ω/ rad s^{-1}	C_0 x10^{-14}	C x10^{-14}	F
10.60	4.73×10^{-4}	4.53×10^{-3}	0.005	209	10.41	7.26	0.697
				429	10.04	6.05	0.603
				607	10.26	4.02	0.392
10.20	1.89×10^{-3}	3.11×10^{-3}	0.005	209	9.90	6.86	0.693
				429	9.68	5.66	0.585
				607	10.04	3.74	0.373
9.60	4.73×10^{-3}	2.70×10^{-3}	0.005	209	9.68	8.54	0.882
				429	9.90	6.85	0.692
				607	10.34	5.13	0.496

TABLE B.7.17. Fraction dispersed as a function of MIPA concentration at constant pH (25°C)

t_c = 35 mins pH = 10.95

[MIPA]/ mol dm^{-3}	ω/ rad s^{-1}	C_0 $x10^{-14}$	C $x10^{-14}$	F
$2.0x10^{-4}$	963	10.41	6.62	0.636
	1990	10.70	4.65	0.435
$8.0x10^{-5}$	963	10.70	9.16	0.856
	1990	11.80	4.88	0.414
$2.0x10^{-4}$	963	10.12	7.99	0.790
	1990	10.26	3.90	0.380
$6.0x10^{-4}$	1990	10.04	1.98	0.197
$1.0x10^{-3}$	1990	9.24	3.78	0.409
$4.0x10^{-3}$	1990	8.80	3.48	0.395

TABLE B.7.18. Fraction redispersed as a function of distilled water pH

t_c = 35 mins ω = 2030 rad s^{-1}

pH	Ionic Strength/ mol dm^{-3}	C_0 $x10^{-14}$	C $x10^{-14}$	F
10.90	$0.8x10^{-3}$	8.94	2.97	0.332
9.45	$0.3x10^{-4}$	8.80	1.01	0.115
3.51	$0.3x10^{-3}$	7.92	<0.07	<0.01

TABLE B.7.19. The effect of aqueous solutions of AMP, TEA and propylamine on the fraction redispersed (25°C)

t_c = 35 mins

Solution	pH	ω/ rad s^{-1}	C_0 $\times 10^{-14}$	C $\times 10^{-14}$	F
0.0108 M AMP	10.92	1487	10.26	9.53	0.929
		2094	10.26	11.00	1.07
		2587	10.12	9.09	0.898
0.0105 M TEA	10.98	1487	12.39	7.70	0.621
		2094	13.01	8.14	0.626
		2587	12.24	1.48	0.121
0.0104 M PROPYLAMINE	11.39	1487	10.34	9.13	0.883
		2094	10.78	8.94	0.829
		2587	10.41	8.76	0.841

TABLE B.7.20. Effect of MIPA concentration on the fraction redispersed at high pH (25°C)

t_c = 35 mins ω = 1257 rad s^{-1}

[MIPA]/ mol dm^{-3}	pH	C_0 $\times 10^{-14}$	C $\times 10^{-14}$	F
4.0×10^{-5}	11.42	11.44	6.41	0.560
1.0×10^{-4}	11.35	10.56	5.58	0.528
2.0×10^{-4}	11.40	11.36	5.27	0.464
6.0×10^{-4}	11.37	11.36	5.99	0.527
2.0×10^{-3}	11.39	10.48	4.82	0.460
3.0×10^{-3}	11.40	10.63	6.73	0.633
4.0×10^{-3}	11.34	11.00	5.67	0.515
0.010	11.31	11.07	6.67	0.603
0.499	11.77	10.92	10.15	0.929

TABLE B.7.21. Fraction redispersed as a function of pH and electrolyte

[MIPA]/ mol dm^{-3}	pH	Electrolyte	ω/ rad s^{-1}	C_0 $\times 10^{-14}$	C $\times 10^{-14}$	F
0.0100	10.7	-	555	11.07	10.04	0.907
		5.26 mM KNO_3	555	13.56	6.31	0.465
		5.57 mM LiCL	555	11.58	7.64	0.660
0.0200	11.29	-	545	13.34	10.85	0.813
		4.02 mM KNO_3	545	12.83	8.31	0.648
		4.03 mM LiCL	545	12.02	7.13	0.593
0.0200	9.79	9.6 mM $MIPA^+$	545	12.68	5.83	0.460
		4.02 mM KNO_3	545	10.63	1.51	0.142
		4.03 mM LiCL	545	11.88	1.23	0.104

APPENDIX C

THE METAL OXIDE-SOLUTION INTERFACE

APPENDIX C. - The Metal Oxide-Solution Interface

Direct measurement of the surface potential of oxides, such as rutile, silica, and alumina, is not possible and so electrokinetic studies complemented by material balance measurements are used to investigate the electrical double layer structure of the oxide-solution interface. Early electrokinetic and potentiometric studies confirmed the importance of hydrogen ions in establishing the double layer at the oxide-aqueous solution interface[C2,C3]. Davis et al[C1] have reviewed the studies of oxides up to 1977. The establishment of the surface charge is generally taken to occur through either of two distinct but basically similar mechanisms:

a) the adsorption or desorption of hydrogen ions at an amphoteric surface site

$$MOH + H^+ = MOH^+_2 \qquad (A)$$

$$MOH = MO^- + H^+ \qquad (B)$$

(the latter could also be written as the reaction of an hydroxyl anion with the surface site to give the negative site plus water);

b) the formation of hydroxylated metal complexes in solution which readsorb onto the particle surface

$$M^{y+} + x\ OH^- \rightarrow M(OH)_x^{(y-x)+}$$

The metal complexes on the surface can then interact with both hydrogen and hydroxyl ions to give changes in σ_o:

$$M(OH)_x^{(y-x)+} + OH^- \rightarrow M(OH)_{x+1}^{(y-x-1)+}$$

and

$$M(OH)_x^{(y-x)+} + H^+ \rightarrow M(OH)_{x-1}^{(y-x+1)+} + H_2O$$

Alternatively the metal hydroxyl species can be considered to be directly created on the particle surface[C3,C4].

However, the equilibrium σ_o-ψ_o relationships do not depend upon the precise charge acquisition mechanism. The site dissociation models generally assume the first mechanism.

The inorganic oxides often exhibit a slow approach to equilibrium with an aqueous electrolyte solution. This is to be anticipated since the process involves the wetting of a partially or completely dehydrated, or dehydroxylated dry solid by an electrolyte solution. In some instances the process may involve the penetration of water and ions into the surface structure e.g. as in the slow rehydration of the titanium dioxide surface after calcining. A general view is that the oxide dissolves until the composition of the solution corresponds to the appropriate solubility condition. However, leached rutile dissolves so slowly that for most purposes it can be regarded as insoluble. It should be noted that silicas, including Pyrex, exhibit appreciable solubility and ageing effects[C5]. But a standard method of pretreating a silica surface has been suggested which enables reproducible electrokinetic data to be obtained[C6]. Figure C1 shows the zeta potential variation with both pH and indifferent electrolyte concentration for silica dispersions.

A typical set of electrokinetic data for an oxide-aqueous solution system exhibit a symmetric shape in the regions above and below the isoelectric point. This is a characteristic of these dispersions and reflects the importance of the hydrogen and hydroxyl ions in determining the surface charge. One of the most significant general features of the oxide systems is that compared to the mercury or silver iodide-solution interfaces the values of σ_o are larger at comparable values of ψ_o i.e. the electrical double layer capacitance values are higher. Other features include the observation that σ_o-pH curves are convex to the pH axis and that large σ_o values are associated with relatively small values of the zeta potential. The initial detailed evidence for the unusual behaviour of the oxide-solution interface was summarised by Hunter and Wright[C19], and by Lyklema[C7]. Prior to this time it was thought that the GCSG model of the double layer was flexible enough to

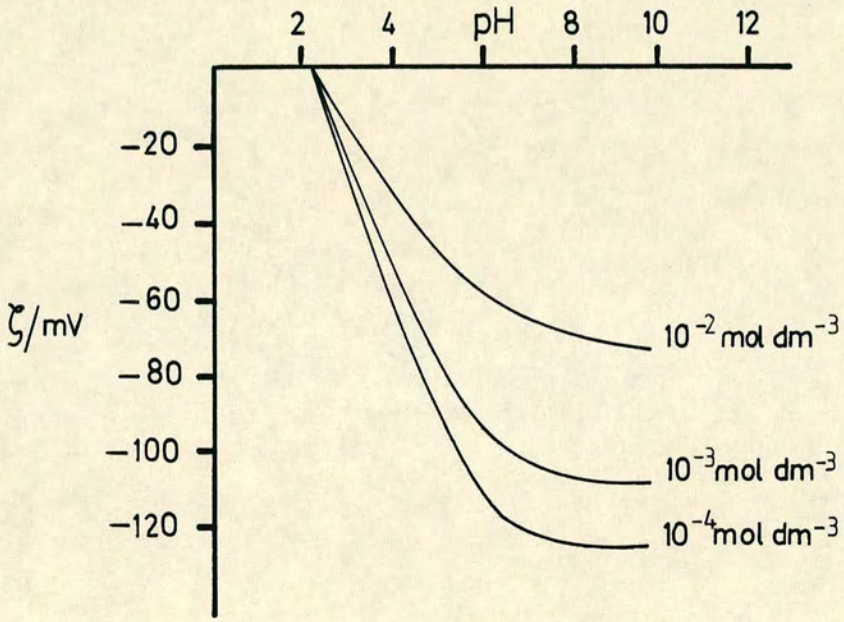

FIGURE C.1 The variation of the zeta potential of silica as a function of the pH in aqueous solutions of KNO_3

describe the σ_o-ψ_o relationship for any interface. In fact it was often found that even if zeta potential values could be predicted the predicted surface charge densities were underestimated[C8]. The extremely high values of surface charge (obtained from titration data) for oxides were taken as evidence of a porous layer, at least for some oxides[C7]. These σ_o values often come close to or may even exceed the accepted maximum surface site density for hydroxyl groups on the oxide surface, 0.2 nm^2 per site corresponding to ~80 $\mu C\ cm^{-2}$. Both the porous interface and site dissociation models were instigated in order to understand these features.

C.1 The Porous Gel Model

The model was originally suggested by Lyklema[C9] as a possible explanation for the large double layer capacitance of some oxide interfaces. The oxide surface was assumed to be porous and thereby capable of absorbing indifferent and potential determining electrolyte ions. The gel layer consisted of hydrolysed metal oxide due to the interaction of hydrogen and hydroxyl ions with the surface layers of the oxide. In this fashion large values of surface charge could exist whilst maintaining a reasonable distance between the charged groups. In addition since the counterions could also penetrate the layer the net electrical potential at the outer edge of the porous layer would be considerably reduced in value. In this way the high titratable surface charges could be reconciled with the modest electrokinetic potential values and the modest stability, with respect to coagulation, of such systems.

Various workers have attempted to quantify the treatment, but the most complete analysis has been given by Perram et al[C10], who give the model for the most general case (unsymmetric electrolyte).

The concentrations of all ions within the gel were taken to be related to the bulk concentrations by expressions of the type

$$c_i = c_i^0 \exp\left(-\frac{ze\,\psi + \mu_i}{kT}\right) \qquad (C1)$$

in which ψ is the local potential within the gel relative to the value in the bulk solution, and μ_i represents the specific adsorption potential of the ith ion species.

Poisson's equation was used to give a unique solution given the appropriate boundary conditions for both the bulk solution and the solid surface-gel layer junction. The solution even for the relatively simple case of a 1:1 electrolyte cannot be written explicitly but requires the solving of two simultaneous transcendental equations in order to obtain the appropriate values of titratable charge and zeta potential. The former was taken to be equal to the sum of the diffuse layer charge and the gel layer charge due to the presence of indifferent ions. The latter was identified as the potential at the gel-electrolyte solution boundary. Although no Stern layer per se was postulated the gel layer could be taken as a limiting case where the solid surface is significantly disordered. The model contains several adjustable parameters -

i) the thickness of the gel layer;

ii) the adsorption potentials of the indifferent electrolyte ions;

iii) the dielectric permittivity of the gel layer;

iv) the dissociation constants of the surface groups.

Perram et al calculated values of σ_o and zeta potential for various oxides, including titanium dioxide, using tabulated values of the dissociation constants and adsorption potentials. However, the authors state that the model can only be applied to those systems for which high titratable surface charges have been measured.

The values of the adsorption potential were assumed to be equal in line with the observation that the properties of the oxides are reasonably symmetric about the i.e.p. The dielectric constant of the gel layer was taken to be 40, although the predictions of the model are fairly insensitive to its value for values >20. The value of the gel layer thickness is the most crucial parameter and values between 1 and 30 nm have been suggested. For titanium dioxide a value of -kT for the

adsorption potentials and of 4 nm for the gel layer thickness gave good agreement with experiment. The total gel layer charge for a 1:1 electrolyte was given by -

$$\Sigma = -L \left(\frac{S_o}{K\ h}\right)^{0.5} (c^0)^{0.5} \exp\left(-\frac{\mu}{2kT}\right) \qquad (C2)$$

where L is the gel layer thickness, S_o is the total concentration of ionisable groups within the gel layer, K is the dissociation constant for the acidic dissociation of one of the groups, h is the bulk concentration of hydrogen ions, and c^0 is the bulk indifferent electrolyte concentration.

The predicted values for various combinations of μ and L are shown in figure C2 (data for titanium dioxide in aqueous sodium chloride is included for comparison).

Perram et al[C10] found that the model could account for the experimental data on various oxides if values of L between 2 and 4 nm and values of μ between -2kT and 0 were used to characterise the gel layer. The authors concluded that the agreement between theory and experiment supported the view that a thin surface layer, made gel-like by the penetration of electrolyte solution, was a general feature of the oxide-solution interface.

However, the experimental zeta potential data is somewhat limited (when used as a function of indifferent electrolyte concentration) which limits the truly critical assessment of the model predictions. In fact, although the model predicts the correct order of magnitude for the zeta potentials, the experimental data do not exhibit the strong dependence on electrolyte concentration as predicted.

It should be noted that there is no experimental evidence of a porous layer on the titanium dioxide surface, in fact certain studies indicate the contrary. Titania is probably not typical of oxides in that it possesses semiconductor properties and may have multivalent metal cation surface sites in addition to the hydroxyls. However, some silica systems[C11] may be best analysed by the porous gel model.

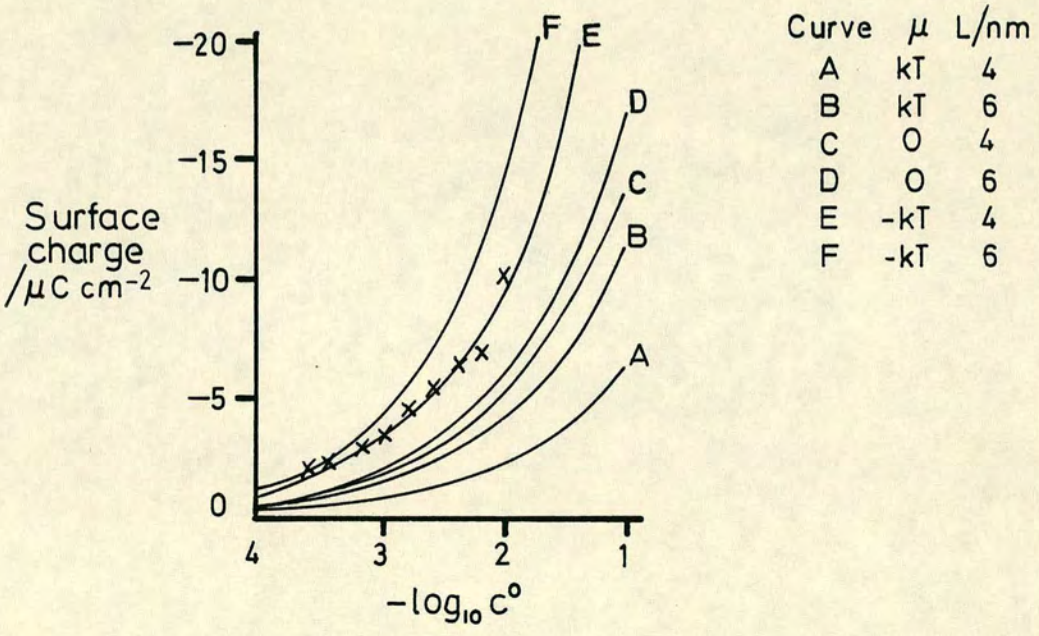

FIGURE C.2 The variation of the titratable surface charge as a function of the indifferent electrolyte concentration for TiO_2 at pH8 according to the porous gel model. The experimental data of Wright for rutile in NaCl, at pH8.8, are included for comparison.

C.2 Electrical Double Layer Models

As previously stated the various models predicting the σ_o-ψ_o behaviour of the interface utilise a picture of the double layer. The simple site dissociation models assume a classical Gouy-Chapman diffuse layer model. However, various workers have included a detailed description of the inner, compact region of the double layer. Depending on the sophistication of the model describing σ_o in terms of the ionisation and complexation constants various levels of double layer pictures are used:

i) the zeroth Order Stern model in which an inner region of thickness, β, is devoid of ions and represents the distance of closest approach to the plane of surface charge. The thickness is taken to be the distance of closest approach of the counterions. The β plane is taken to represent the start of the diffuse layer i.e. $\psi_\beta = \psi_d$, and since no layer of adsorbed ions is postulated then $\sigma_\beta = 0$ and $\sigma_o = -\sigma_d$. The zeroth Order model takes account of the finite size of ions, but by making $\sigma_\beta = 0$ the restriction that the lateral size of the counterions places on the occupation of the β plane is ignored. Within this plane the potential-distance profile is linear

$$\psi(x) = \psi_o - \frac{x}{\beta}(\psi_o - \psi_d) \qquad (C3)$$

for $$0 \leqslant x \leqslant \beta$$

and $$\sigma_o = K_I(\psi_o - \psi_d) \qquad (C4)$$

with $$K_I = \varepsilon_I \varepsilon_o/\beta \qquad (C5)$$

The inner layer capacitance, K_I, is treated as an adjustable parameter.

ii) the Stern model which expands on the zeroth Order model and makes allowance for a Langmuir type adsorption of counterions.

iii) the Site Binding Stern model in which the lateral occupancy of the β plane is governed by the requirement that the counterions must be coupled to specific surface sites.

The Zeroth Order Stern model has been used instead of the classical Gouy-Chapman picture in the simple site dissociation models[C12]. The values of K_I which must be chosen to make the predictions fit experimental data are very large, typically 200 μF cm^{-2}. Such high values can be interpreted as implying a large value of ε_I or a small value of β. The oft quoted figures of ~30 μF cm^{-2} for K_I refer to the mercury-water interface which bears an interfacial water structure vastly different to that for the oxide-solution system. In addition the nature of the surface of oxides makes the interpretation of the distance of closest approach more ambiguous than for the mercury surface and so it is not difficult to understand the vast difference in the K_I values. Some workers interpret the need to introduce a high value for this parameter in order to correctly predict the σ_o-pH relation for surfaces possessing ionisable groups as evidence for a porous gel surface region, while others assume a value of 80 and 0.3 nm for the inner region dielectric constant and thickness, respectively[C20].

Westall and Hohl[C13] have looked at five electrostatic models of the oxide-solution interface and classify each depending on the double layer picture used. They considered two general pictures of the double layer - the Basic Stern model and the Extended Stern model. The former assumes that the capacitance between the IHP and OHP could be neglected so that $\psi_I=\psi_d$ (this is akin to the Zeroth Order Stern model). The latter allows for the existence of the two Helmholtz planes. The Basic Stern model can be further split into two limiting cases. At low ionic strengths and relatively low potentials the diffuse layer capacitance dominates the total double layer capacitance, whereas at high ionic strengths the compact layer dominates the total capacitance. With regard to the assignment of the ions to planes of mean electrical potential within the interface the authors compared the oxide interface with the two limiting cases; the mercury-solution and silver iodide-solution interfaces. Stern derived his model with the mercury electrode in mind and hence σ_o refers to the electronic charge on the mercury surface, σ_I refers to the charge associated with the electrostatically and/or

chemically bound ions at the IHP, and σ_d refers to the diffuse layer charge. For the silver iodide interface σ_o refers to the adsorbed potential determining ions while σ_I and σ_d are as defined for the mercury system. The norm has been to regard the oxide surfaces as being similar to the silver halide surface with the adsorbed potential determining ions, hydrogen and hydroxyl, forming the surface charge. However, since the p.d.i. for oxides do not form part of the solid lattice and are not therefore adsorbed in the same manner as the silver and halide ions, the oxide surface can be treated as being similar to mercury, with $\sigma_o = 0$ since the oxide itself has zero charge. The IHP would contain both the chemically adsorbed potential-determining ions and the electrostatically bound counterions. This "mercury" model for the oxide-solution interface is thus a strict interpretation of Stern's model.

The "silver halide" and "mercury" models for the location of ions at the oxide-solution interface represent the extremes between which the true situation exists.

It is the choice of description of the electrical double layer both in terms of the assignment of the ions to mean planes of adsorption and the equations used to relate ψ_o to σ_o which distinguish many of the site dissociation or complexation models of the oxide-solution interface.

C.3 Simple Site Dissociation Model

The most appropriate form of site dissociation model for the oxides considers the surface to be composed ofamphoteric sites which can be negatively or positively charged, depending on the pH[C21]. The method involves analysing the manner in which the chemical ionisation behaviour affects the surface charging process and hence the resulting surface potential as a function of pH. Both Levine and Smith[C21], and Healy and White[C20] have devised similar versions of the model. The parameter ΔpK is probably the single most important factor since it determines the extent to which the system departs from Nernst type behaviour. Its value expresses the relative strengths of the two surface acidic groups i.e. MOH^+_2 and MOH. Figure C3 shows the effect of ΔpK. For oxides its value normally lies in the range +3 to +6 (the former value being typical for

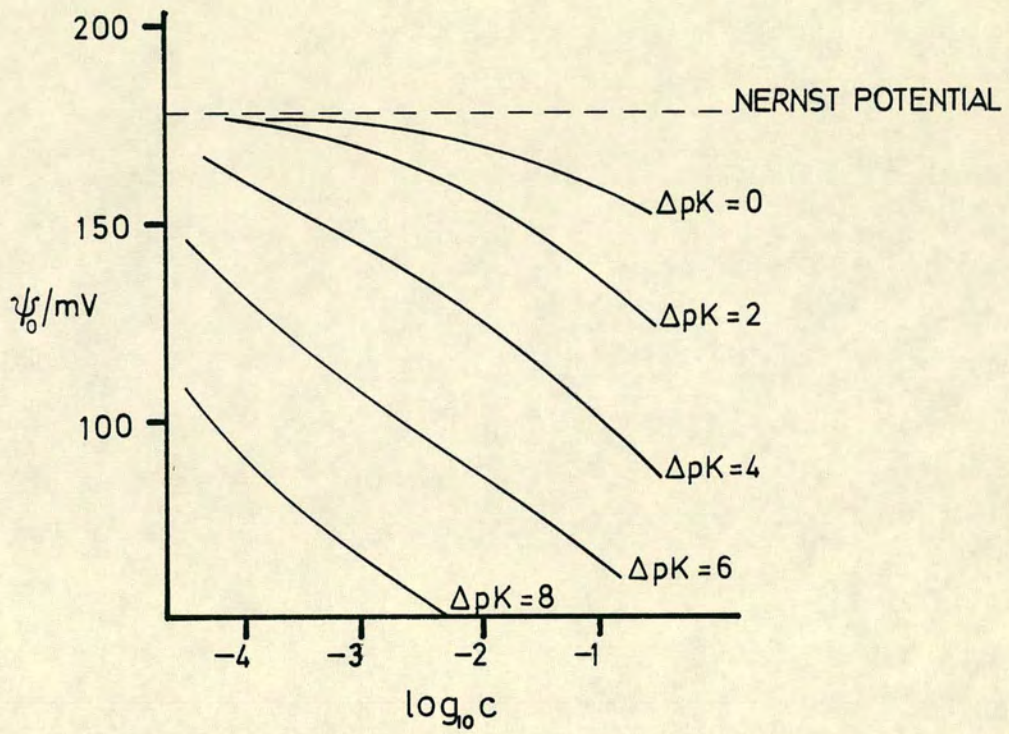

FIGURE C.3 The variation of the surface potential as a function of the indifferent electrolyte concentration for an ionisable surface at a pH 3 units away from the i.e.p.

rutile). The larger the ΔpK the greater the deviation from Nernstian behaviour and the greater the ionic strength the more pronounced the deviation. A more extensive discussion of the effect of ΔpK can be found in the original papers. Comparison of the predicted σ_o-pH and zeta potential-pH relationships with experiment has been carried out[C20]. The plane of shear was assumed to be located at 2 nm from the surface. The model is able to reproduce the broad features of the charge-pH data, see figure C4. The theoretical curves assume a value of 5×10^{14} sites per cm^2 and an indifferent electrolyte concentration of 0.1 mol dm^{-3}. The figure shows that silica exhibits anomalous behaviour compared to the other oxides at least with respect to the surface charge data. In contrast, the zeta potential-pH behaviour of all the oxides is similar[C14]. Although a ΔpK value of 10 gives a reasonable theoretical fit to the surface charge data, a simultaneous fit with the electrokinetic data is not obtained. The electrokinetic data can be predicted if a value ΔpK = 6 is used but a poor fit to the surface charge data results. Simple shifts in ΔpK alone do not produce agreement between theory and experiment. The discrepancy could be partially removed by using a Stern layer model but the addition of such a compact region causes an increase in the magnitude of σ_o and a decrease in the magnitude of the potential[C14], the opposite to what is required. Alternatively, fixing the ΔpK value to fit the electrokinetic data and reducing the assumed number density of surface groups has the effect of giving reasonable simultaneous fit to both charge and potential data[C20].

A better agreement is found for titanium dioxide using the simple Gouy-Chapman site dissociation model. Figure C5 illustrates the extent of agreement between theory and experiment. Using a ΔpK value in the range 3-4 and a site density of 5×10^{14} cm^{-2} gives good agreement over the range 0-4 ΔpH units. However, theory overestimates the double layer potential especially at low ionic strengths. The fit of the predicted surface charge could be improved by assuming a lower value of the site density. It is a general feature of the Gouy-Chapman based models that the predicted variation of zeta potential with the electrolyte concentration is overestimated especially at pH values distant from the isoelectric point. At the same time, such models successfully predict the surface charge at all ionic strengths and the zeta potential for ionic strengths in the 0.01-0.1 mol dm^{-3} range. A notable observation is

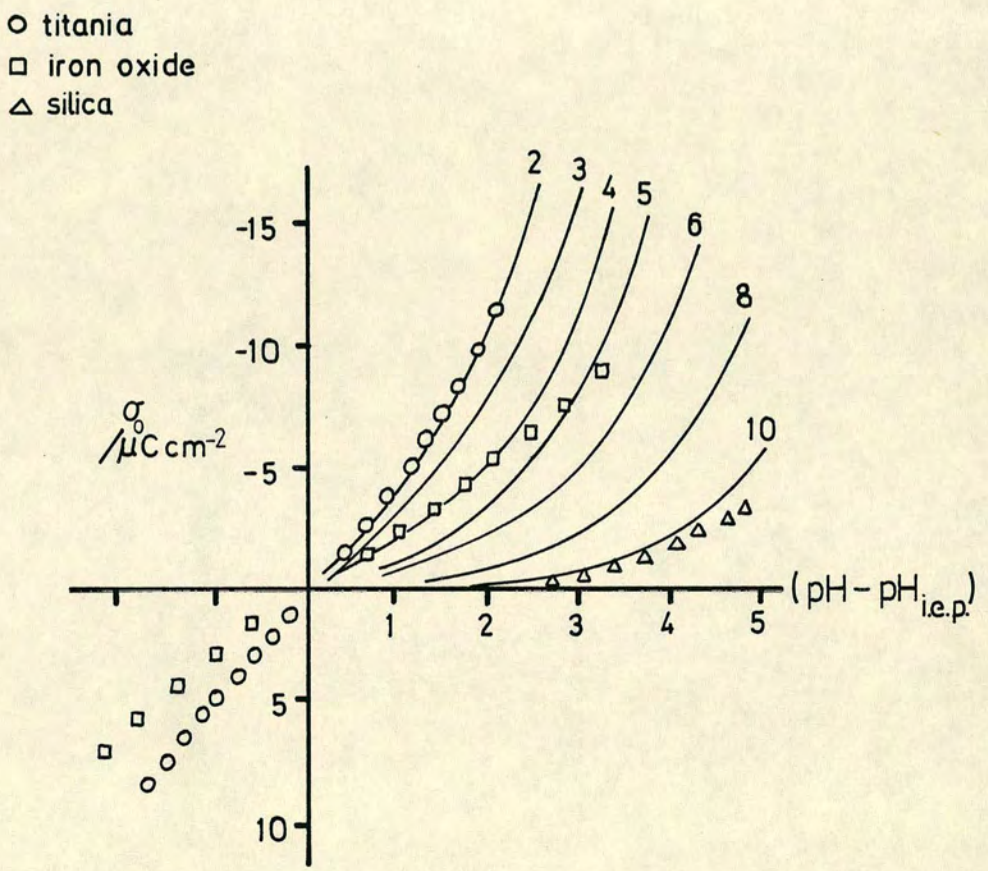

FIGURE C.4 Comparison of experimental data for three oxides with the predictions of a simple site dissociation model.(The numbers refer to the assumed pK_a value)

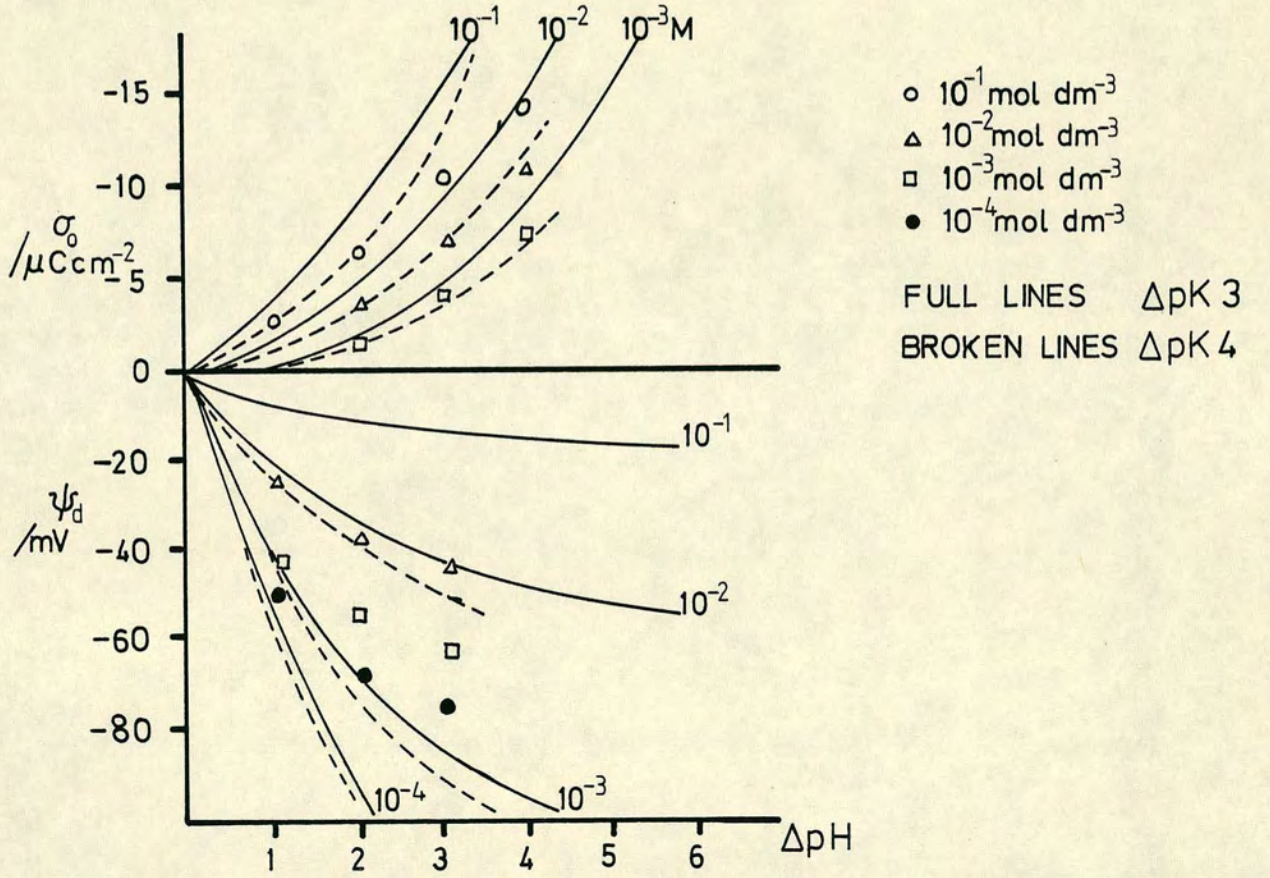

FIGURE C.5 Comparison of experimental data[2.115,2.155] for TiO_2 with theoretical predictions using a[2] site dissociation model

that the values of the adjustable parameters of the model needed to give reasonable agreement with experiment do not agree with independent analysis e.g. the measured surface group density is greater than the value required by the model[C16]. This shortcoming is due to the neglect of electrolyte binding to the surface groups.

C.4 Electrolyte Binding-Dissociation Models

An alternative method of explaining the high surface charge densities and low zeta potentials of oxides involves the postulation of direct binding of the counterions to the surface charge sites. Such a procedure clouds the distinction between indifferent ions and specifically adsorbed ions, but the adoption of such a postulate reaps good rewards. Yates et al[C23] introduced the first site binding-site dissociation model which was a natural extension of the studies due to Stumm and co-workers[C16], and Posner and Quirk[C17] on chemical dissociation processes in solution. The basic idea is that the negative and positive sites formed by the surface ionisation reactions can, in effect, be neutralised by cations and anions from the bulk solution binding to the particular surface site. The protons involved in these equilibrium reactions are normally assumed to lie in the surface plane and the electrolyte ions are assumed to lie in the compact layer at a distance β from the surface, i.e. at the IHP. The thermodynamic activity of an ion is modified by the electrical work required to bring it from bulk solution to the plane of adsorption and is given by an equation similar to that for the hydrogen ion. Thus for an ion at the IHP the activity is given by

$$[i_s] = [i] \exp\left(\frac{-ze\,\psi_I}{kT}\right) \qquad (C6)$$

The total surface charge density for an oxide, MOH, in the presence of a simple electrolyte, AX, can be given as

$$\sigma_o = e\,N_A\left(\Gamma_{MOH_2} + \Gamma_{MOH_2X} - \Gamma_{MO} - \Gamma_{MOA}\right) \qquad (C7)$$

whereas the compact layer charge is given by

$$\sigma_I = e\ N_A \left(\Gamma_{MOA} - \Gamma_{MOH_2X}\right) \qquad (C8)$$

Using the various stoichiometric, thermodynamic, and electroneutrality constraints the set of governing equations can be solved for unique values of the solution pH and electrolyte concentration, given values for the equilibrium constants of the various ionic reactions at the surface, the surface site density, and the integral capacities of the compact layer. The determination of the intrinsic ionisation and complexation constants is carried out by the adoption of reasonable approximations and graphical extrapolations. Davis et al[C1] were able to solve the set of equations using generalised chemical equilibrium computer programs.

The original treatment of Yates et al[C23] considered the bound conterion and surface group to be a small dipole but in order to obtain a usable final expression were forced to assume that the total electrostatic energy of the dipole was $-e\left(\psi_o - \psi_I\right)$ which corresponds to a classical Stern description. The analysis also assumes, in addition to the normal practice of neglecting the discreteness of charge effect, that both electrolyte ions have the same approach distance to the surface when undergoing association and that the number of sites in the IHP equals the net number of charged surface sites. The equation relating the surface potential to the bulk solution can be written as

$$\psi_o = \frac{2.303\ kT}{e}\left(pH_{p.z.c.} - pH\right) - \frac{kT}{2e}\ln\left(\frac{[MOH_2]}{[MO]}\right) \qquad (C9)$$

so that ψ_o depends upon the electrolyte concentration at constant pH; the last term being dependent upon the ionic strength.

For a simple Gouy-Chapman double layer the diffuse layer charge is given by

$$\sigma_d = \frac{-e\ N_s}{B} \sinh\left(z\ e\ \psi_d/2kT\right) \qquad (C10)$$

where $B\left(= N_s\ \kappa/4N_A\ n_\infty\right)$ is a dimensionless factor combining site density and electrolyte concentration effects. N_s includes all the charged,

neutral, and ion-paired surface groups.

Both the inner and outer layer capacitances are introduced to define the potential drops within the compact layer and are given by equations (3.32) and (3.33). The model therefore requires for its solution estimates of N_s, K_I, K_o, and the four ionisation- complexation equilibrium constants. The model was found to give reasonable agreement with the experimental surface charge and potential data of oxides but suffers from similar shortcomings as the simpler site dissociation models. To achieve the fit values for N_s of 5×10^{14} cm^{-2} and for ΔpK of 3 or 6 were used. The adsorption potentials for the ions within the Stern layer were several kT larger than for the analogous adsorption at either the mercury or silver iodide-solution interfaces. The inner and outer Helmholtz plane capacitances were taken to be 140 μF cm^{-2} and 20 μF cm^{-2}, respectively. Yates et al[C23] consider several possible explanations for the high K_I and low K_o values. To explain the former the following were suggested -

i) the potential-determining and counterions are located in almost the same plane; so that the distance β in equation (3.32) becomes small; and

ii) the existence of partial charge transfer within the bound ion-surface group unit as the result of proton resonance between the surface group and the water molecule separating the adsorbed ion from the surface. Such charge transfer effectively raising the potential at the adsorption plane thereby raising the capacitance.

The first suggestion would require the dipole moments of the ion pairs to lie parallel to the surface. The second suggestion requires that the ion adsorption occurs at the OHP instead of the IHP.

To explain the low value of the outer plane capacitance Yates et al proposed another couple of explanations -

i) the dielectric constant of the outer layer could be low, e.g. between 6 and 15, and/or two or more layers of water molecules separate the OHP from the IHP; and

ii) the electrokinetic shear plane is located further out from the oxide surface than the OHP; so that the OHP potential, ψ_d, exceeds the zeta potential and hence K_o is larger than calculated assuming the identity of ψ_d and ζ.

The former suggestion implies that the water between the two Helmholtz planes is significantly oriented by the oxide surface resulting in a structured solvent layer between the diffuse layer ions and the IHP. The authors also put forward the additional view that the high inner and low outer capacitances could be due to the presence of a porous hydrated oxide surface region, although their calculations were unable to support or dismiss the idea.

The approach of Yates et al has been criticised by Davis et al[C1], particularly the method used to evaluate the ionisation and complexation constants. They proposed a modified approach which gives these constants a non-dependence upon the electrolyte concentration. The model assumes a value of 20 $\mu F\ cm^{-2}$ for K_o, as before, but treats the inner layer capacitance as an adjustable parameter. All the other unknowns can be determined from experimental data using the extrapolation procedures of James et al[C18]. An important new concept in this model is the introduction of the single ionisation-complexation reaction such as

$$MOH + A^+ = MO^- A^+ + H^+_s$$

whose equilibrium constant can be quoted as the product of the ionisation equilibrium constant and complexation equilibrium constant. A schematic of the compact layer believed to exist is givcen in figure C6. The chemisorbed water layer can adsorb or release hydrogen ions to form the charged surface sites. The centres of these molecules represent the σ_o plane, while the IHP represents the distance of closest approach of the complexing ions. As the result of the chemisorbed water layer an adsorbed ion may possess one of these water molecules as part of its solvation sheath. This picture allows a close approach of the electrolyte ions to the surface charge plane, to within 0.1 nm, that is consistent with the experimental observations of large inner layer capacitance.

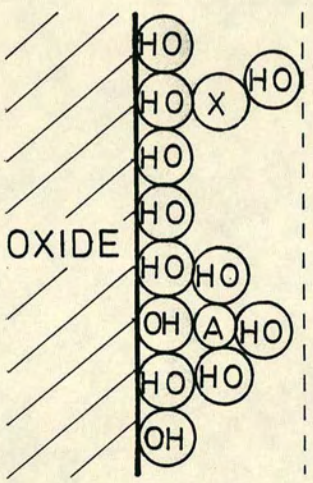

FIGURE C.6 Schematic view of the oxide-solution interface showing the locations of the ionic species and the planes of charge[2.141]

Before assessing the validity of these models, with particular regard to titanium dioxide, there are a few more site dissociation-site binding models worthy of comment. Westall and Hohl have reviewed and compared these models[C13], which differ in the choice of the double layer structure.

The constant capacitance model of Stumm et al[C24] can be regarded as the high ionic strength limiting case of the basic Stern model. The model can be formulated using either i) a linear relationship between the surface charge and potential, and incorporating the latter into the dissociation equilibrium constants; or ii) an empirical correction term to the intrinsic surface ionisation constants such that the pK value becomes a function of the surface charge and hence surface potential. According to the model all specifically adsorbed ions contribute to σ_o and experience the potential ψ_o. However, the capacitance values are only valid for a given cation and anion, and for a particular ionic strength.

The diffuse layer model of Stumm, Huang, and Jenkins[C16] can be regarded as the low ionic strength, low potential limiting case of the basic Stern model. The double layer charge-potential equation takes the same form as the simple Gouy-Chapman expression but the fixed number of surface sites implicit in the dissociation-complexation model is not a part of the classical theory. The capacitance of the double layer is fixed by theory and hence cannot be used as an adjustable parameter, unlike the previous model. As in the latter all specifically adsorbed ions are assumed to contribute to σ_o.

The picture of the double layer used by Bowden et al[C25] is a version of the basic Stern model (i.e. IHP and OHP taken to be coincident) applicable at all ionic strengths. The assignment of ions to the various planes of constant charge follows that for the silver halide-solution interface. The potential-determining ions are assigned to the oxide surface and the other specifically adsorbed ions are assigned to the IHP. All non-adsorbing ions are excluded from the Stern layer and reside exclusively in the diffuse layer. Between the surface and the IHP there is a region of capacitance $K_I = K_s$ since the potential at the OHP is assumed to be equal to that at the IHP. The method given by the authors

for solving the equations is non-iterative whereas an iterative technique is in fact required in order to achieve reasonable agreement with experimental data.

The so-called triple layer model[C1,C26] is a version of the complete Stern model applicable at all ionic strengths. The term "triple layer" is used to emphasize the fact that the surface plane, IHP, and OHP are assumed to exist. This is in fact the picture used by Yates et al[C23] for their original complexation model. The potential- determining ions are assigned to the oxide surface, the site binding electrolyte ions are assigned to the IHP, and the other ions are assigned to the OHP and diffuse layer. This model has several advantages over the simpler models including the ability to give an estimate of the zeta potential.

An adaptation of the original Stern model can be used in which the assignment of ions follows that at the mercury-solution interface. The potential-determining and the adsorbing ions are both assigned to the IHP so that the actual oxide surface has zero charge. The surface charge is therefore considered to reside at the IHP. The diffuse layer can be taken to be separated from the IHP by a Helmholtz capacitance corresponding to an OHP. The charge and potential values given by this model are lower than predicted by the other models because the specifically adsorbed and potential-determining ions are taken to be located in the same plane.

All the models suffer from the same difficulty of finding unique and acceptable values for the adjustable parameters. In fact it is found that a wide range of these parameter values can yield the optimum fit of a model to experimental data. It is clearly difficult to unambiguously divide the adsorption energies into the electrical and chemical components. The models can represent the data adequately using physically acceptable values of the adjustable parameters but the values of analogous parameters have different values in different models. Thus each model is of the correct mathematical form but does not necessarily give the correct physical picture of the interface.

The application of the Davis et al[C1] model to experimental data for titanium dioxide in potassium nitrate solution has been carried out by

James and Parks[C30]. They used revised values of the reaction constants calculated from a double extrapolation method. The inner layer capacitance was taken to be an adjustable parameter and used as such in order to optimise the fit to experimental data over the widest possible ionic strength and pH range. Figure C7 shows the model description and the experimental data of Yates[C27] (surface charge densities) and Wiese[C28] (zeta potentials). The theoretical curves were calculated assuming the following values for the model parameters - K_I = 110 $\mu F\ cm^{-2}$, pK_a for the acidic dissociation of the MOH_2^+ surface group = 2.7, pK_a for the acidic dissociation of the MOH group = 9.1, pK value for the nitrate ion complexation = 4.2, and pK value for the potassium ion complexation = 7.2. The agreement both with σ_o and zeta potential is good and is an improvement on the predictions of the simple site dissociation model. The points of interest include

a) the use of a larger ΔpK_a value for describing the relative acidities of the surface groups; and

b) the large value assigned to the intrinsic dissociation constants of the bound electrolyte ions, approx. -8kT.

The latter leads to the conclusion that these simple inorganic ions are strongly adsorbed in equal amounts under all conditions. Although this proposition is suspect the model has the advantage of being able to distinguish between possible competing modes of adsorption for multivalent ions[C1].

Similar agreement between experiment and this electrolyte complexation triple layer model has been obtained with the rutile data of Bérubé and de Bruyn[C12]. Once again the double extrapolation method was used to obtain values for the ionisation and complexation constants[C30]. However, a larger value for the inner capacitance was necessary, namely K_I = 250 $\mu F\ cm^{-2}$, which leads to a separation of 0.05 nm between the planes of surface charge and bound electrolyte ions. This high capacitance value may indicate that there was some penetration of counterions into the surface.

Westall and Hohl[C13] found that both the constant capacitance model and the triple layer model were able to give excellent fit to the

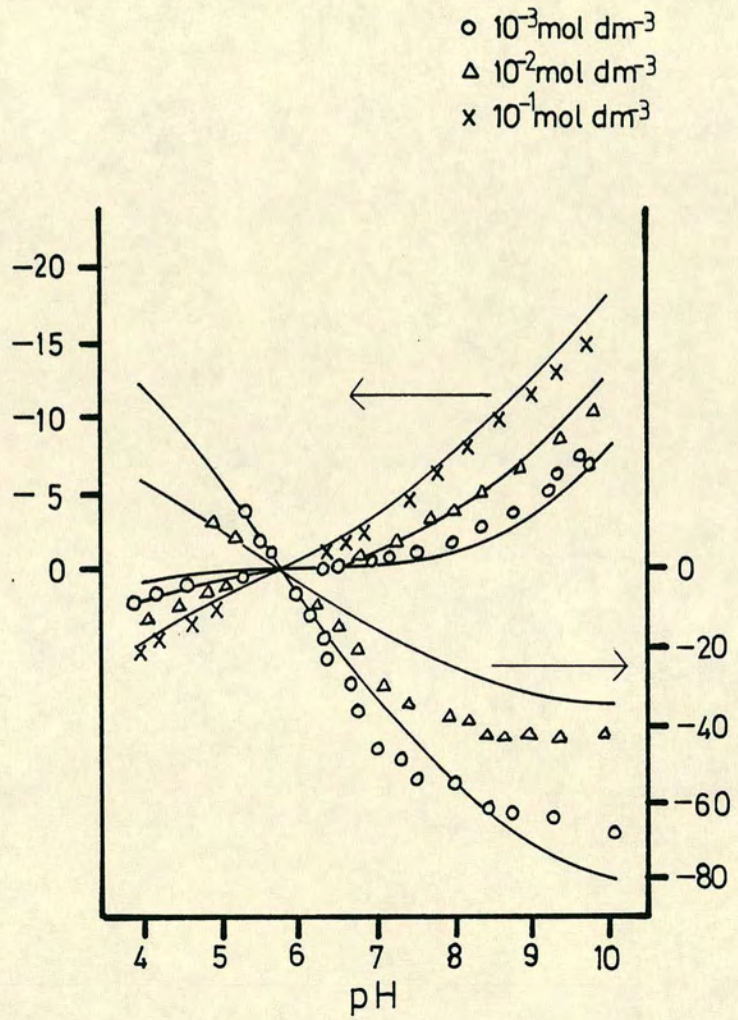

FIGURE C.7 The surface charge density and zeta potential for TiO_2 in aqueous dispersion as a function of pH and KNO_3 concentration (25^0C)

experimental surface titration data of Yates[C27] on dispersions of rutile in potassium nitrate solutions.

However, for many models several combinations of values for the adjustable parameters can be used to represent the experimental data so that there is no unique description of the chemical and electrostatic contributions to the oxide-solution interface. In addition, the models can be made to give reasonable agreement with experimental data although with widely differing values of equivalent parameters. As Westall and Hohl have stated, until a universally agreed model for the surface-solution interface at a given oxide exists it is necessary to report the chemical reaction constants along with the complete description of the model. The evaluation of the various model parameters could be carried out more realistically if methods which are not dependent upon the explicit and implicit assumptions of a particular model were available.

C.5 Summary

By integrating the various theories for the electrical double layer with the mechanism of specific chemical interaction between solutes and the oxide surface it is possible to develop a model accounting for the surface charge density-surface potential relationship of oxides in the presence of electrolyte solutions. The polymer lattices appear to be the ideal examples of the surface ionisation and complexation double layer models. On the other hand solids, such as silver halides, involved in the formation of electrochemically reversible electrodes are examples of colloidal systems in which ψ_o is determined by the relative activities of the ionic components in both the solid and aqueous phases. As a rule the behaviour of colloidal dispersions of oxides falls somewhere between these two extremes. Presumably the reversible oxide electrodes, e.g. silver/silver oxide, are best described by the latter model, whereas the insoluble insulating oxides such as alumina and silica would behave more akin to the ideally ionisable colloids. Titanium dioxide being a semiconductor is probably intermediate in its behaviour. This property of being a semiconductor may also give rise to perturbation of the electrical double layer as the result of the formation of space charge layers within the oxide[C29].

C1 Davis, J.A., James, R.O. and Leckie, J.O. J. Colloid Interface Sci., (1978), 63, 480.

C2 Bolt, G.H. J. Phys. Chem., (1957), 61, 1166.

C3 Parks, G.A. and de Bruyn, P.L. J. Phys. Chem., (1962), 66, 967.

C4 Boehm, H.P. Disc. Farad. Soc., (1971), 52, 264.

C5 van Lier, J.A., de Bruyn, P.L. and Overbeek, J.Th.G. J. Phys. Chem., (1960), 64, 1675.

C6 Wiese, G.R., James, R.O. and Healy, T.W. Disc. Farad. Soc., (1971), 52, 302.

C7 Lyklema, J. Croatica Chem. Acta., (1971), 43, 249.

C8 Wright, J.J.L. and Hunter, R.J. Aust. J. Chem., (1973), 26, 1191.

C9 Lyklema, J. J. Electroanal. Chem., (1968), 18, 341.

C10 Perram, J.W., Hunter, R.J. and Wright, H.J.L. Aust. J. Chem., (1974), 27, 461.

C11 Smit, W., Holten, C.L.M., Stein, H.N., de Goeij, J.J.M. and Theelen, H.M.J. J. Coll. Int. Sci., (1978), 67, 397.

C12 Bérubé, Y.G. and de Bruyn, P.L. J. Coll. Int. Sci., (1968), 28, 92.

C13 Westall, J. and Hohl, H. Adv. Coll. Int. Sci., (1980), 12, 265.

C14 Yates, D.E. and Healy, T.W. J. Coll. Int. Sci., (1976), 55, 9.

C15 Yates, D.E. and Healy, T.W. J. Chem. Soc. Farad. I, (1980), 76, 9.

C16 Huang, C.P. and Stumm, W. J. Colloid Interface Sci., (1973), 43, 409.

C17 Bar-Yosef, B., Posner, A.M. and Quirk, J.P. J. Soil. Sci., (1975), 26, 1.

C18 James, R.O., Davis, J.A. and Leckie, J.O. J. Colloid Interface Sci., (1978), 65, 331.

C19 Hunter, R.J. and Wright, H.J.L. J. Colloid Interface Sci., (1971), 37, 564.

C20 Healy, T.W. and White, L.R. Adv. Colloid Interface Sci., (1978), 9, 303.

C21 Levine, S. and Smith, A.L. Disc. Faraday Soc., (1971), 52, 290.

C22 Wiese, G.R. and Healy, T.W. J. Colloid Interface Sci., (1975), 51, 427.

C23 Yates, D.E., Levine, S. and Healy, T.W. J. Chem. Soc. Faraday Trans. I, (1974), 70, 1807.

C24 Hohl, H. and Stumm, W. J. Colloid Interface Sci., (1976), 55, 281.

C25 Bowden, J.W., Posner, J.P. and Quirk, J.P. Aust. J. Soil Res., (1977), 15, 121.

C26 Davis, J.A. and Leckie, J.O. J. Colloid Interface Sci., (1978), 67, 90.

C27 Yates, D.E. Ph.D. Thesis, University of Melbourne, (1975).

C28 Wiese, G.R. Ph.D. Thesis, University of Melbourne, (1973).

C29 Bérubé, Y.G., Onoda, G.Y. and de Bruyn, P.L. Surf. Sci., (1967), 8, 448.

C30 James, R.O. and Parks, G.A. "Surface and Colloid Science", vol. 12, ed. E. Matijevic, Plenum Press (1982).